

IMPACT OF MATERIAL DETERIORATION ON TORNADIC VULNERABILITY IN BUILT
INFRASTRUCTURE

by

Pauline Wanjiku Karanja

A dissertation submitted to the faculty of
The University of North Carolina at Charlotte
in partial fulfillment of the requirements
for the degree of Doctor of Philosophy in
Infrastructure and Environmental Systems

Charlotte

2024

Approved by:

Dr. Stephanie Pilkington

Dr. Erik Nielsen

Dr. Omid Shoghli

Dr. Jake Smithwick

Dr. Deborah Thomas

ABSTRACT

PAULINE WANJIKU KARANJA. Impact of Material Deterioration on Tornadoic Vulnerability in Built Infrastructure. (Under the direction of DR. STEPHANIE PILKINGTON)

Tornadoes are among the most destructive natural disasters, posing significant risks to communities and infrastructure, underlining the need for robust methodologies to assess building vulnerability and enhance structural resilience. This research addresses the gap in current tornado vulnerability studies by investigating the impact of material deterioration on building fragility, focusing on commercial and government buildings at the end of their useful life. The overarching goal is to comprehensively quantify the effects of material deterioration on tornado vulnerability, including its implications for EF-scale ranking and associated wind-speed thresholds for Damage Indicators (DIs) and Degree of Damage (DOD) classifications. As a secondary goal, the research seeks to understand the critical components prioritized during condition assessments to facilitate comparisons with National Weather Service (NWS) post-event storm surveys.

The research employs a multifaceted methodology to achieve its objectives. Firstly, a Qualtrics survey of architects, engineers, facility managers, construction managers, and building owners reveals critical components prioritized during facility condition assessments of commercial and government buildings, facilitating comparisons with post-event storm surveys. The analysis shows that while built environment professionals often focus on operational and maintenance concerns, NWS post-event storm surveys prioritize structural integrity and safety. This misalignment underscores the importance of harmonizing pre- and post-event storm surveys.

Secondly, predictive models are developed to forecast deterioration trends for various building components, such as roofs, walls, doors, and windows. These models provide valuable insights into the dynamics of material degradation over time, leading to the analysis of deterioration rates under different maintenance scenarios, ranging from poor to excellent practices. Focusing on deterioration rates for poorly maintained buildings at the end of their useful life and using probabilistic modeling approaches, the research develops time-dependent deterioration fragility curves to quantify the changing vulnerability of materials used in commercial and government buildings over time.

The results reveal decreased wind speed thresholds for EF-scale ranking, indicating notable changes in tornado-induced damage potential due to material deterioration. These findings highlight the importance of considering time-dependent deterioration fragilities in tornado vulnerability assessments and the observed leftward shifts in fragility curves.

Additionally, changes in EF-scale ranking and DOD wind speed thresholds underscore the probable inadequacy of existing evaluation protocols that do not account for material deterioration. Post-event storm surveys may now consider the impact of aging and degradation on building resilience to assess structural integrity and accurately prioritize repair and reconstruction efforts.

This research enhances resilience and promotes sustainable development in tornado-prone regions by illuminating the dynamic nature of tornado vulnerability.

ACKNOWLEDGEMENTS

I would like to express my sincere gratitude to all those who have contributed to completing this dissertation. First and foremost, I am deeply thankful to my supervisor, Dr. Stephanie Pilkington, for their invaluable support, guidance, and mentorship throughout the research process. Their expertise, encouragement, and constructive feedback have been instrumental in molding the direction and quality of this research.

I am also grateful to the members of my dissertation committee, Dr. Jake Smithwick, Dr. Omid Shoghli, Dr. Erik Nielsen, and Dr. Deborah Thomas, for their insightful comments, suggestions, and encouragement at various stages of the research. Their expertise and diverse perspectives have enriched the scholarly content of this dissertation.

I extend my appreciation to the participants who generously shared their insights and expertise during the data collection phase of the Facility Condition Assessment study. Their contributions have been integral to developing and validating the research findings.

I would like to acknowledge the University of North Carolina at Charlotte, the Department of Engineering Technology and Construction Management, and the Infrastructure and Environmental Systems program director, Dr. Jay Wu, for providing the necessary resources, facilities, and support for conducting this research. Their commitment to academic excellence and research innovation has fostered an environment conducive to scholarly inquiry and intellectual growth.

I am indebted to my colleagues, especially the Smith Girls Club, friends, and family members for their unwavering encouragement, understanding, and support throughout this academic journey. Their encouragement and support have been a source of motivation.

DEDICATION

This dissertation is dedicated to the memory of my late father, Eng. Charles Waithaka Karanja. Though he is no longer with us, his unwavering belief in my potential and enduring encouragement inspire me daily. I promised him that I would pursue my academic aspirations to the highest level, and though he left us in 2011 and did not live to see this come to fruition, I am grateful for the opportunity to fulfill that promise. To my mother, Mrs. Ruth Karanja, for calling me every Friday without fail with words of love and encouragement. I dedicate this work to my lovely sisters Stella, Joan, and Mumbi, whose love, support, and encouragement have been my guiding light throughout this journey. Your unwavering belief in me, endless calls, laughter, and encouragement have been the foundation upon which I have built my academic pursuits.

TABLE OF CONTENTS

LIST OF TABLES	xi
LIST OF FIGURES	xiv
LIST OF ABBREVIATIONS.....	xx
CHAPTER 1: INTRODUCTION	1
1.1 Problem Statement.....	1
1.2 Objectives and Scope of Research.....	3
1.3 Dissertation Outline	5
CHAPTER 2: BACKGROUND.....	7
2.1 Introduction to Extreme Weather and Tornadoes	7
2.2 National Weather Service Post-event Storm Surveys of Extreme Wind Events and the Enhanced Fujita Scale	10
2.3 Damage Characterization and Limit States.....	14
2.4 Review of the Current State of Building Tornado Modeling Failure of Structural Components Using Fragilities	17
2.5 Limitation of Current Approaches.....	23
2.6 Deterioration.....	25
2.6.1 Service Life of Materials.....	26
2.6.2 Facility Condition Rating.....	27
2.6.3 Deterioration Modeling.....	31

2.6.4	Markovian Models	32
2.6.5	Deterioration Rates	35
CHAPTER 3: RESEARCH METHODOLOGY		40
3.1	Facility Condition Assessments	40
3.1.1	Introduction	40
3.1.2	Data collection and cleaning	42
3.1.3	Questionnaire.....	44
3.1.4	Comparative Analysis	45
3.1.5	Integration with Post-Tornado Surveys	48
3.2	Deterioration Prediction and Deterioration Rates	48
3.2.1	Introduction	48
3.2.2	Deterioration Prediction Model.....	49
3.2.3	Data Collection	50
3.2.4	Markov Process Application	51
3.3	Summary	63
3.4	Deterioration Rates	64
3.4.1	Introduction	64
3.4.2	Materials Selection for Commercial and Government Buildings	64
3.4.3	Data Collection	67
3.4.4	Formulation of Deterioration Models	69

3.5	Summary	71
3.6	Building Materials Fragilities.....	71
3.6.1	Introduction	71
3.6.2	Tornado fragility curves methodology and intensity measures.....	73
3.7	Summary	85
CHAPTER 4: RESULTS AND DISCUSSION		87
4.1	Facility Condition Assessment.....	87
4.1.1	Respondents and Characteristics	88
4.1.2	Inferential Statistics Summary	90
4.1.3	Discussion regarding Research Question 1	91
4.2	Building Material Deterioration Impacts to Fragility Curves	93
4.2.1	Deterioration Prediction Results.....	93
4.2.2	Resulting Deterioration Rates.....	98
4.2.3	Time-dependent Materials Fragilities	102
4.2.4	Fragility Curves	103
4.3	EF Scale Analysis.....	110
4.3.1	Discussion on EF Scale Analysis	123
4.4	Summary	125
4.5	Assumptions and Limitations.....	127

CHAPTER 5: KEY FINDINGS, CONTRIBUTIONS, AND FUTURE RESEARCH

RECOMMENDATIONS	129
5.1 Key Findings	129
5.2 Contributions	132
5.3 Future Research Recommendations	134
REFERENCES	138
APPENDICES	149
7.1 APPENDIX A: DETERIORATION PREDICTION – TRANSITION MATRICES AND PROBABILITIES	149
7.2 APPENDIX B: DETERIORATION RATES	154
7.3 APPENDIX C: TIME-DEPENDENT FRAGILITY CURVES – PRISTINE VS DETERIORATING BUILDINGS	157
7.4 APPENDIX D: TIME-DEPENDENT FRAGILITY CURVES – PRISTINE VS DETERIORATING BUILDINGS EF SCALE	168

LIST OF TABLES

Table 2.1: Enhanced Fujita Scale for rating tornado magnitude (Adapted from Texas Tech University, 2006).	11
Table 2.2: NWS damage indicators (commercial structures). (Adapted from Texas Tech University 2006).	12
Table 2.3: Strip Mall Degree of Damage and Wind Bounds	13
Table 2.4: FEMA Damage States (Adapted from FEMA, 2010)	15
Table 2.5: Wind damage rating criteria for components.	17
Table 2.6: Condition States following FCA	28
Table 2.7: Example of Building Systems and their Elements: Unifomat II Format	29
Table 2.8: formulae to determine deterioration (Adapted from Konior et al., 2018)	36
Table 3.1: Research Variables under the Condition Assessment Section of the Research	44
Table 3.2: Critical building components during NWS post-event storm survey (Adapted from Jain et al. 2020)	45
Table 3.3: Condition Rating Scale	54
Table 3.4: Building Component Inventory	68
Table 3.5: Deterioration Models	69
Table 3.6: Damage states for commercial building Memari et al. (2018)	73
Table 3.7: Tornado Pressure Adjustments (Adapted from ASCE 7-22, 2022)	80
Table 3.8: Wind Load Statistics (Adapted from ASCE 7-22, 2022)	81
Table 3.9: Component and Materials Structural Resistance Data	82
Table 3.10: Quantitative guidelines for assigning overall wind damage rating.	83
Table 4.1: Assets for Which Condition Assessments Table 4.2: Building Components	90

Table 4.3: Assets for Which Condition Assessments Should be Carried Out When Vacating a Building – United States Respondents Only	90
Table 4.4: Association Between Respondent’s Current Role and Research Variables and Their Strength.....	91
Table 4.5: Individual Deterioration Rates of Materials	99
Table 4.6: Individual Deterioration Rates of Materials (cont.).	100
Table 4.7: Upper and Lower Bound wind speed thresholds for pristine (non-deteriorated) and deteriorated asphalt shingles.....	112
Table 4.8: Probabilities of Exceedance for Asphalt Shingles (boxed area corresponds to Figure 4.10).....	114
Table 4.9: Probabilities of Exceedance for Walls.....	115
Table 4.10: Probabilities of Exceedance for H2.5 clips.....	116
Table 4.11: Percentage Change in Fragility Parameter Lambda and the Upper and Lower bound wind speed thresholds for materials in pristine (non-deteriorated) and deteriorated Small Retail Buildings (SRB) and Large Isolated Retail Building (LIRB)	121
Table 7.1: Transition matrices for doors, windows, and walls.....	149
Table 7.2: Condition State 1 Matric and Deterioration Trends for all Components	149
Table 7.3: Condition State 2 Matric and Deterioration Trends for all Components	150
Table 7.4: Condition State 3 Matric and Deterioration Trends for all Components	150
Table 7.5: Condition State 4 Matric and Deterioration Trends for all Components	151
Table 7.6: Condition State 5 Matric and Deterioration Trends for all Components	151
Table 7.7: Expected Deterioration Matrix and Trends for all Components	152

Table 7.8: Observed Deterioration Data	152
Table 7.9: Expected Deterioration Data	153
Table 7.10: Chi-Square Test Results.....	153
Table 7.11: All Deterioration Rates across all Maintenance Conditions	154

LIST OF FIGURES

Figure 2.1: Tornado-prone region (Adapted from ASCE 7, 2022)	9
Figure 2.2: Flowchart showing methodology to develop tornado fragility of components. (Adapted from Mehmari et al. 2018).....	22
Figure 2.3: Example of fragility curves for doors and windows. (Adapted from Memari et al. 2018).....	23
Figure 2.4: Deterioration Prediction	33
Figure 2.5: Example of a Markov chain deterioration model - Transition relations	34
Figure 3.1: Transition Matrix	56
Figure 3.2: Critical values of Chi-Square distribution for v degrees (NIST 2012)	63
Figure 3.3: Hurricane clips	68
Figure 3.4: Flowchart for Developing Time-dependent Fragility Curves	78
Figure 4.1: Distribution of Responses.....	88
Figure 4.2: Characteristics of Respondents	89
Figure 4.3: Condition State 2 Deterioration Trends for all Components	94
Figure 4.4: Condition State 3 Deterioration Trends for all Components	95
Figure 4.5: Condition State 4 Deterioration Trends for all Components	95
Figure 4.6: Condition State 5 Deterioration Trends for all Components	96
Figure 4.7: Exponential Regression Line Y_n	97
Figure 4.8: Critical values of Chi-Square distribution for v degrees	98
Figure 4.9: Best Fit Model for Monte Carlo Simulation.....	104
Figure 11.10: Lognormal best-fitted asphalt shingles fragilities at (a) 10-year interval, (b) 30-year interval, and (c) 50-year interval.....	105

Figure 4.11: Fragilities for asphalt shingles at a 30-year time interval – Poor

Maintenance 107

Figure 4.12: Fragilities for asphalt shingles at a 30-year time interval – Average

Maintenance 107

Figure 4.13: Fragilities for walls at a 40-year time interval – Poor Maintenance 108

Figure 4.14: Fragilities for walls at a 40-year time interval – Average Maintenance 108

Figure 4.15: Fragilities for two H2.5 clips at a 30-year time interval – Poor

Maintenance 109

Figure 4.16: Fragilities for two H2.5 clips at a 30-year time interval – Average

Maintenance 109

Figure 4.17: Leftward shift of EF scale wind speed thresholds for asphalt shingles..... 111

Figure 4.18: Fragilities for Asphalt Shingles with DOD 4 bounds for a Small Retail

Building..... 118

Figure 4.19: Fragilities for Walls with DOD 7 wind speed bounds for a Small Retail

Building..... 119

Figure 4.20: Fragilities for Asphalt Shingles with DOD 2 and 3 wind speed bounds for a

Large Isolated Retail Building..... 119

Figure 4.21: Fragilities for Walls with DOD 6 wind speed bounds for a Large Isolated

Retail Building..... 120

Figure 4.22: Leftward shift of DOD threshold wind speeds for roof covering to a Large

Isolated Retail Building at 0-50-year intervals. Year 0 and year 50 thresholds

are boxed. 123

Figure 7.1: Lognormal best-fitted asphalt shingles fragilities at 0 and 10-year intervals..... 157

Figure 7.2: Lognormal best-fitted asphalt shingles fragilities at 20 and 30-year intervals.....	157
Figure 7.3: Lognormal best-fitted asphalt shingles fragilities at 40 and 50-year intervals.....	158
Figure 7.4: Lognormal best-fitted clay tile fragilities at 0 and 10-year intervals.....	158
Figure 7.5: Lognormal best-fitted clay tiles fragilities at 20 and 30-year intervals.....	158
Figure 7.6: Lognormal best-fitted clay tiles fragilities at 40 and 50-year intervals.....	159
Figure 7.7: Lognormal best-fitted wall fragilities at 0 and 10-year intervals.....	159
Figure 7.8: Lognormal best-fitted wall fragilities at 20 and 30-year intervals.....	159
Figure 7.9: Lognormal best-fitted wall fragilities at 40 and 50-year intervals.....	160
Figure 7.10: Lognormal best-fitted door fragilities at 0 and 10-year intervals	160
Figure 7.11: Lognormal best-fitted door fragilities at 20 and 30-year intervals	160
Figure 7.12: Lognormal best-fitted door fragilities at 40 and 50-year intervals	161
Figure 7.13: Lognormal best-fitted window fragilities at 0 and 10-year intervals.....	161
Figure 7.14: Lognormal best-fitted window fragilities at 20 and 30-year intervals	161
Figure 7.15: Lognormal best-fitted window fragilities at 40 and 50-year intervals.....	162
Figure 7.16: Lognormal best-fitted aluminum siding fragilities at 0 and 10-year intervals	162
Figure 7.17: Lognormal best-fitted aluminum siding fragilities at 20 and 30-year intervals	162
Figure 7.18: Lognormal best-fitted aluminum siding fragilities at 40 and 50-year intervals	163
Figure 7.19: Lognormal best-fitted steel roof joists fragilities at 0 and 10-year intervals.....	163
Figure 7.20: Lognormal best-fitted steel roof joists fragilities at 20 and 30-year intervals.....	163
Figure 7.21: Lognormal best-fitted steel roof joists at 40 and 50-year intervals.....	164
Figure 7.22: Lognormal best-fitted two 16d toenail fragilities at 0 and 10-year intervals	164
Figure 7.23: Lognormal best-fitted two 16d toenail fragilities at 20 and 30-year intervals	164
Figure 7.24: Lognormal best-fitted two 16d toenail fragilities at 40 and 50-year intervals	165

Figure 7.25: Lognormal best-fitted one H2.5 clip fragilities at 0 and 10-year intervals.....	165
Figure 7.26: Lognormal best-fitted one H2.5 clip fragilities at 20 and 30-year intervals.....	165
Figure 7.27: Lognormal best-fitted one H2.5 clip fragilities at 40 and 50-year intervals.....	166
Figure 7.28: Lognormal best-fitted two H2.5 clip fragilities at 0 and 10-year intervals	166
Figure 7.29: Lognormal best-fitted two H2.5 clip fragilities at 20 and 30-year intervals	166
Figure 7.30: Lognormal best-fitted two H2.5 clip fragilities at 40 and 50-year intervals	167
Figure 7.31: Time-dependent asphalt shingles fragilities with EF-Scale overlay at 0 and 10- year intervals	168
Figure 7.32: Time-dependent asphalt shingles fragilities with EF-Scale overlay at 20 and 30-year intervals	169
Figure 7.33: Time-dependent asphalt shingles fragilities with EF-Scale overlay at 40 and 50-year intervals	169
Figure 7.34: Time-dependent clay tile fragilities with EF-Scale overlay at 00 and 10-year intervals	169
Figure 7.35: Time-dependent clay tile fragilities with EF-Scale overlay at 20 and 30-year intervals	169
Figure 7.36: Time-dependent clay tile fragilities with EF-Scale overlay at 40 and 50-year intervals	170
Figure 7.37: Time-dependent wall fragilities with EF-Scale overlay at 0 and 10-year intervals	170
Figure 7.38: Time-dependent wall fragilities with EF-Scale overlay at 40 and 50-year intervals	171

Figure 7.39: Time-dependent wall fragilities with EF-Scale overlay at 40 and 50-year intervals	171
Figure 7.40: Time-dependent door fragilities with EF-Scale overlay at 0 and 10-year intervals	171
Figure 7.41: Time-dependent door fragilities with EF-Scale overlay at 20 and 30-year intervals	172
Figure 7.42: Time-dependent asphalt door with EF-Scale overlay at 40 and 50- year intervals	172
Figure 7.43: Time-dependent windows fragilities with EF-Scale overlay at 0 and 10-year intervals	172
Figure 7.44: Time-dependent windows fragilities with EF-Scale overlay at 20 and 30-year intervals	173
Figure 7.45: Time-dependent windows fragilities with EF-Scale overlay at 40 and 50-year intervals	173
Figure 7.46: Time-dependent aluminum siding fragilities with EF-Scale overlay at 0 and 10-year intervals	173
Figure 7.47: Time-dependent aluminum siding fragilities with EF-Scale overlay at 10 and 20-year intervals	174
Figure 7.48: Time-dependent aluminum siding fragilities with EF-Scale overlay at 40 and 50-year intervals	174
Figure 7.49: Time-dependent steel roof joists fragilities with EF-Scale overlay at 0 and 10-year intervals	175

Figure 7.50: Time-dependent steel roof joists fragilities with EF-Scale overlay at 20 and 30-year intervals	175
Figure 7.51: Time-dependent steel roof joists fragilities with EF-Scale overlay at 40 and 50-year intervals	175
Figure 7.52: Time-dependent 16d toenail fragilities with EF-Scale overlay at 0 and 10-year intervals	176
Figure 7.53: Time-dependent 16d toenail fragilities with EF-Scale overlay at 20 and 30-year intervals	176
Figure 7.54: Time-dependent 16d toenail fragilities with EF-Scale overlay at 40 and 50-year intervals	176
Figure 7.55: Time-dependent one H2.5 clip fragilities with EF-Scale overlay at 0 and 10-year intervals	177
Figure 7.56: Time-dependent one H2.5 clip fragilities with EF-Scale overlay at 20 and 30-year intervals	177
Figure 7.57: Time-dependent one H2.5 clip fragilities with EF-Scale overlay at 40 and 50-year intervals	177
Figure 7.58: Time-dependent two H2.5 clip fragilities with EF-Scale overlay at 0 and 10-year intervals	178
Figure 7.59: Time-dependent two H2.5 clip fragilities with EF-Scale overlay at 20 and 30-year intervals	178
Figure 7.60: Time-dependent two H2.5 clip fragilities with EF-Scale overlay at 40 and 50-year intervals	179

LIST OF ABBREVIATIONS

λ_R	Logarithmic median of capacity
ξ_R	Logarithmic standard deviation of capacity
AIA	American Institute of Architects
AMS	American Meteorological Society
ASCE	American Society of Civil Engineers
C&C	Cladding and Connections
CDF	Cumulative Distribution Function
CMU	Concrete Masonry Units
DI	Damage Indicator
DOD	Degree of Damage
DS	Damage State
EF Scale	Enhanced Fujita Scale
FCA	Facility Condition Assessment
IFMA	International Facilities Management Association
IIMM	International Infrastructure Management Manual
LS	Limit State
MWFRS	Main Wind-resisting Systems
NIST	National Institute of Science and Technology
NOAA	National Oceanic and Atmospheric Administration
NSSL	National Severe Storms Laboratory
NWS	National Weather Service

PGA	Peak Ground Acceleration
SPSS	Statistical Package for Social Sciences

CHAPTER 1: INTRODUCTION

1.1 Problem Statement

Tornadoes are among the most devastating natural disasters in the United States and other countries, especially for smaller communities. Tornado risk reduction has not benefited from research as much as risk reduction for earthquakes, hurricanes, or flood hazards, even though more than 1,200 tornadoes are reported each year in the U.S. (NOAA, 2019), and tornadoes have produced the highest annualized fatalities for decades (NIST, 2014). Most tornado research in the structural engineering discipline has been on post-tornado field investigations.

The Enhanced Fujita Scale is used to assign a tornado a rating based on estimated wind speeds and related damage. When surveyed, tornado-related damage is compared to a list of Damage Indicators (DIs) and Degrees of Damage (DODs) for various building types, which help estimate the range of wind speeds the tornado likely produced. From the survey, a rating between EF0 and EF5 is assigned. When assigning wind damage ratings, a visual assessment of the damaged building is conducted by evaluating the state and condition of the main wind force-resisting systems (MWFRS) and components & cladding (C&C) (Attary et al., 2018). The state these damaged buildings are in can depend on the hazard's strength, building materials, construction quality, and potential state of deterioration based on continuous maintenance.

Continuous maintenance implies that the facility has not run down or deteriorated over time. However, buildings deteriorate for various reasons, including age, overloading, and lack of preventative maintenance and planning, more so when they are left unoccupied when they reach the end of their useful life. Facility condition assessments (FCASs) are used to measure this deterioration to collect data to determine the requirement and timing of preventative or remedial

action to assess and maintain a level of service (Aktan et al., 1997; Mayo & Karanja, 2018).

Deteriorating buildings are likely to be more vulnerable to extreme wind hazards compared to pristine buildings.

Vulnerability is a fundamental component of risk, and understanding it is essential for determining the reliability of infrastructure assets and systems and mitigating risk. Vulnerability analysis of buildings exposed to natural hazards has become a significant area of research due to infrastructure's critical role in society. This topic has also been the subject of significant advances from new data and insights (Argyroudis et al., 2019). Previous studies of post-event storm surveys have documented common failure modes of residential and commercial buildings using fragility curves. Tornado fragility curves, defined as conditional probability curves that give the likelihood of damage for a given windspeed, have been found to be a valuable tool for assessing potential damages to structures. They are also an essential component of tornadic wind risk assessment procedures.

Methods of modeling failure of structural components using fragilities have been widely employed for tornadic vulnerability assessment for non-deteriorating structures (e.g., Unanwa et al., 2000; Rosowsky et al., 2002; Ellingwood et al., 2004; Hwang et al., 2007; Koliou et al., 2014; Amini et al., 2014; Masoomi et al., 2016; Koliou et al., 2017; Masoomi et al., 2018b; Memari et al., 2018), while traditionally ignoring the impact of deterioration that affect buildings. Further research is required to evaluate the effect of deterioration on material response and fragility. This research discussed herein aims to address this need.

1.2 Objectives and Scope of Research

This research aims to provide a greater understanding of the impact of deterioration on the structural vulnerability of building materials, which may have been neglected in the literature. The primary objective is to develop efficient time-evolving fragility functions for poorly maintained buildings and assess how this may affect its tornado ranking with respect to DOD definitions. The creation of these fragility focuses on the materials used in building components; in this case, roofs, walls, windows, doors, and those used for roof-to-wall connections; to statistically compute the tornadic wind vulnerability of deteriorated buildings' materials along their service lives, more so at the end of their useful lives. These fragility functions are used to create time-dependent fragility curves, which are then compared to those for materials in pristine or non-deteriorated, well-maintained buildings.

This research is motivated by the need to address the following pivotal questions:

1. During facility condition assessments (FCAs), are building managers prioritizing the same components as NWS evaluators conducting post-event storm surveys?
2. Does deterioration have an effect on the tornadic wind-loading response of building materials? How significant are the shifts in material tornadic fragilities of deteriorating buildings when compared to non-deteriorating (pristine) buildings?
3. Would a structure's age and material deterioration ultimately impact how tornadoes are ranked on the EF scale?

The tasks designed to answer the research questions are as follows:

1. Conducting a comprehensive literature review.

2. Surveying professionals involved in building decommissioning who are aware of standard FCA procedures for FCAs.
3. Comparing the focus of facility managers' FCAs with NWS' post-event storm surveys to address the alignment between pre- and post-tornado facility/building assessments/surveys, shedding light on potential discrepancies.
4. Researching and characterizing the rates of material deterioration in poorly maintained and averagely maintained buildings, impacting the structural performance of critical components.
5. Developing capacity models for structural resistance based on material deterioration rates.
6. Creating fragility models for deteriorated building materials and conducting a comparative analysis with pristine building material behavior.
7. Developing time-dependent fragility curves at the building material level to quantify the detrimental effects of deterioration on the tornadic fragilities of those materials.
8. Assessing how the effects of deterioration impact the Enhanced Fujita Scale.
9. Evaluating the impact of deterioration on degrees of damage (DODs) for commercial buildings, specifically small professional buildings, strip malls, large shopping malls, and large industrial retail buildings.

The focus of this research is to address these questions using probabilistic methods. This research holds significant importance as it not only bridges critical gaps in current literature by exploring the relationship between building material deterioration and tornado fragility but also offers practical insights that can directly impact real-world scenarios. By advancing methodologies in tornado modeling failure of structural components using fragilities, this

research contributes to academic conversations. The research has the potential to inform procedures in classifying tornadic events and enhance the overall understanding of structural tornado vulnerabilities, ultimately striving toward a safer and more prepared society in tornado-prone regions. The findings of this research challenge current wind speed bounds relating to DODs, providing an opportunity to consider both structural integrity and how a building is used and maintained when examining the effects of wind on buildings.

1.3 Dissertation Outline

Time-dependent tornadic fragility functions with specific consideration to the deterioration of building materials are investigated in this dissertation. The full probabilistic analysis evaluating materials' time-dependent tornadic fragility curves, given uncertainty in building, wind speed, and deterioration parameters, reveals a notable increase in the individual materials' vulnerability over time due to deterioration. This dissertation is arranged into five chapters with the following content:

Chapter 1 presents a brief introduction to the problem being assessed, tornadic fragility functions, with consideration of the effects of deterioration, and describes the objectives of this dissertation.

Chapter 2 provides a comprehensive background to contextualize the subsequent discussions on tornado modeling failure of structural components using fragilities. It presents an overview of existing literature on tornado modeling failure of structural components using fragilities of buildings while highlighting methodologies and existing deficiencies that will be addressed in this research. The chapter critically examines the limitations identified in current studies, paving the way for a focused exploration of these gaps and challenges in the following chapters. Chapter

2 also gives an overview of deterioration, discusses deterioration prediction modeling, and introduces deterioration rating methodologies.

Chapter 3 presents the research methodology used in the research. The research questions and the methods utilized to address the questions are detailed in this chapter. It encompasses a conceptual framework for research integrating insights from the literature review, evaluates current methodologies, and conducts a gap analysis to identify research needs. The chapter also presents the methodology for deterioration prediction and outcomes for building components using the Markov chain and presents deterioration rates for the individual materials within these components. Deterioration of materials is unavoidable since they are exposed to the impact of natural environmental factors on a continuous basis.

Chapter 4 presents the results and discussion of the research. It includes a detailed fragility functions model for building materials' time-dependent tornado fragility curves. Fragility curves for pristine and deteriorated materials are presented, and comparisons are made.

Finally, Chapter 5 gives the overall conclusions, research implications, and future research opportunities.

The following section summarizes past research on tornado fragility while highlighting the existing deficiencies, which will be extensively addressed in this research.

CHAPTER 2: BACKGROUND

2.1 Introduction to Extreme Weather and Tornadoes

Before considering the body of literature on tornadic wind damage and fragilities, it is essential to understand extreme weather and how extreme wind events form. Extreme weather encompasses thunderstorms with damaging winds, tornadoes, large hail, flooding, and flash flooding. The American Meteorological Society (AMS) defines extreme weather as any weather phenomenon relating to extreme thunderstorms (AMS, 2013). Extreme thunderstorms can be categorized and evaluated as "approaching severe," "severe," and "significantly severe."

"Approaching severe" is defined as hail less than half an inch in diameter or winds between 50 and 58 mph. Such storms will usually warrant a Significant Weather Alert. "Severe" is defined as hail 1 to 2 inches in diameter, winds between 58 and 75 mph, or an EF1 tornado. In contrast, "significantly severe" is defined as hail 2 inches in diameter or larger, winds 75 mph or more, or a tornado EF2 or stronger (NWS, 2014). Severe weather generally requires atmospheric moisture, a mechanism to lift air and condense moisture, and instability. An added ingredient necessary for the formation of rotating thunderstorms is wind shear, which aids in displacing updraft from downdraft, thus tilting the storm. It also allows the updraft to prolong itself, makes the development of a mesocyclone possible, and allows rotating air to merge into the updraft, thus tornadogenesis (Houser et al., 2015).

The most destructive tornadoes occur from supercells, rotating thunderstorms with a well-defined radar circulation called a mesocyclone; however, not all tornadoes result from supercells. According to the National Severe Storms Laboratory (NSSL), close to 20% of all tornadoes are associated with lines of strong thunderstorms called "quasi-linear convective

systems" (QLCS). QLCSs include squall lines (a linearly oriented zone of convection, i.e., thunderstorms) common across the United States east of the Rockies (NOAA NSSL, 2017), bow echoes, an arched/bowed outline of thunderstorms, sometimes embedded within a squall line. Bow echoes are usually associated with straight-line wind damage at the surface. In fact, bow-echo-induced winds or downbursts account for most structural damage resulting from convective, non-tornadic winds (Houser et al., 2015). Brief tornadoes can also occur in squall lines, especially with bow echoes, but are weaker and short-lived on average than those associated with supercell thunderstorms.

The occurrence rate of tornadoes is higher in the United States than in any other country. More than 1200 tornadoes touch down annually in the United States (NOAA, 2019), approximately four times the amount reported in Europe (Houser and Bluestein, 2015). Tornado reports have become more frequent in recent years due partly to the invention of Doppler radar and the increased population. Heavy damage and loss of life have been observed in previous tornado outbreaks in heavily populated areas. Although the number of injuries and fatalities caused by tornadoes has decreased in the last few decades, mainly due to improvements in warning technologies (Standohar-Alfano et al., 2017), the cost of damage, repair, and reconstruction has considerably increased (Amini and van de Lindt, 2014).

According to Boruff et al. (2003), many states throughout the United States, especially those east of the Rocky Mountains, are susceptible to tornadoes (Figure 2.1). Still, the probability of a tornado striking any particular community in any given year is relatively low. In the past, this low probability of occurrence of tornadoes has prevented accounting for these events in modern building codes, but this has changed over the last years due to deadly and damaging

tornadoes in recent years. For example, Tuscaloosa, Alabama (2011), Joplin, Missouri (2011), and Moore, Oklahoma (2013). Following the catastrophic tornadoes in Moore, Oklahoma (i.e., an EF5 tornado in 1999, an EF4 tornado in 2003, and an EF5 tornado in 2013), building code was revised so that residential buildings in their community could withstand EF2 tornadic winds (i.e., 135 mph) (Masoomi et al., 2018a). EF2 intensity for the design process was considered because more than 97% of recorded tornadoes are historically rated EF2 or lower (FEMA, 2011). Moreover, even in higher-intensity tornadoes, most affected areas are associated with EF2 level intensity or less (Standohar-Alfano and Van de Lindt, 2014).

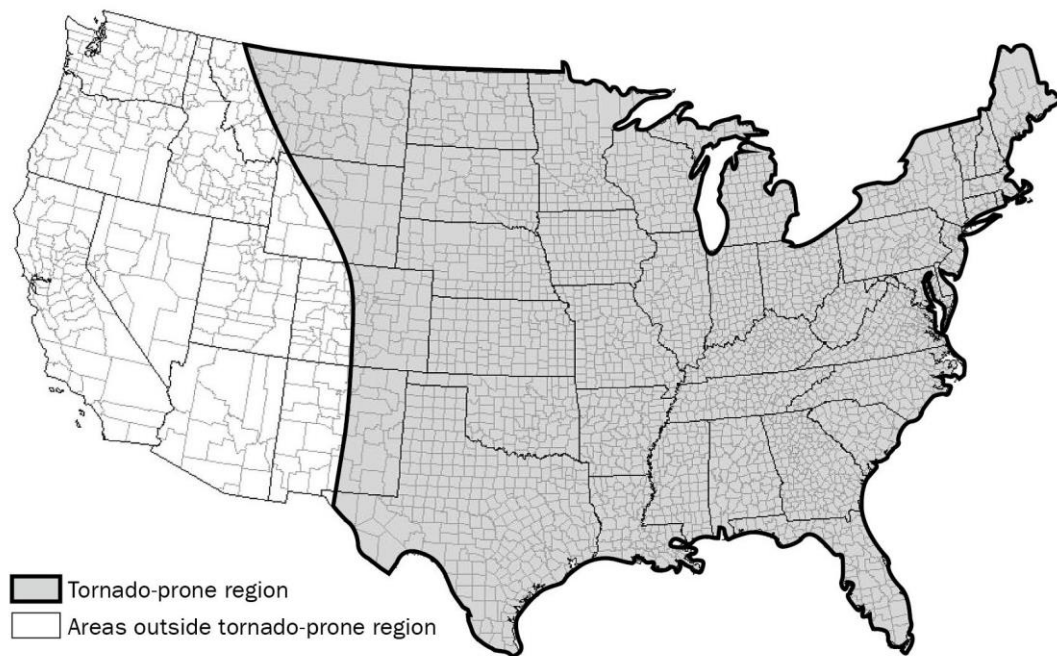


Figure 2.1: Tornado-prone region (Adapted from ASCE 7, 2022)

Following the 2011 Joplin tornado disaster, the deadliest and costliest tornado in the U.S. since 1950, tornado load provisions have been added to ASCE 7 (ASCE, 2022). With the publication of ASCE 7-22 (ASCE 2022), According to the FEMA/NIST guide (2023), “tornado load requirements are now considered a minimum design load in conventional building design

when buildings are in tornado-prone areas. The ASCE 7 load requirements will be included in the 2024 International Building Code (IBC), the 2024 National Fire Protection Association (NFPA), the 50000 Building Construction and Safety Code, and the 2023 Florida Building Code. The adoption of the ASCE 7 tornado load provisions by the State of Florida is an example of local authorities having jurisdiction incorporating the most current design guidance prior to their inclusion in the model building codes”.

2.2 National Weather Service Post-event Storm Surveys of Extreme Wind Events and the Enhanced Fujita Scale

Because of the locational variability and the small coverage area, recording wind speed inside tornadoes is not considered feasible (Wurman et al., 2010). Hence, the intensity of a tornado in terms of wind speed is estimated indirectly by using damage to buildings, structures, and trees. The intensity and severity of extreme wind events are typically determined post-event through damage surveys conducted by the National Weather Service (NWS) and result in an estimated wind speed and Enhanced Fujita (EF) ranking for tornadic events through a visual evaluation of the degree of damage to structures and/or trees. To determine the strength of a tornado after an extreme wind event occurs, the NWS evaluators survey the damage to estimate the tornado's wind speed. The survey team's task is to gather data to recreate a tornado's lifecycle, including where it struck, when and where it initially touched down and lifted (path length), width, and magnitude. The investigative teams are sometimes tasked with determining whether damage may have been caused by straight-line winds or tornadoes and assessing the magnitude of straight-line winds and tornadoes.

The Enhanced Fujita Scale became operational on February 1, 2007, and based on estimated wind speeds and related damage, it is used to assign a tornado a rating. When conducting surveys, damage caused by tornadoes is assessed against a set of Damage Indicators (DIs) and Degrees of Damage (DOD), aiding in the estimation of the probable wind speeds generated by the tornado. This information is then used to assign a rating ranging from EF0 to EF5. The windspeeds related to the EF scale are estimated wind speeds from damage; they are not measured. Continued research is needed to validate the wind speed values associated with each DI and DOD (Wurman et al., 2013; Wurman et al., 2010; Wurman et al., 2007; Haan et al., 2010; Prevatt et al., 2011; NOAA, 2017). If there is no DI path of a tornado, it is not possible to estimate the maximum speed of the tornado at that location. Direct measurements using probes placed in the path of tornadoes and/or remote sensing using Doppler radar technology can provide definitive wind speed values. With this thought in mind, the upper boundary for the wind speed range for EF5 is not specified. Table 2.1 below highlights different EF classifications and their 3-second wind gusts.

Table 2.1: Enhanced Fujita Scale for rating tornado magnitude (Adapted from Texas Tech University, 2006).

Category	3 – Second Gust (mph)
EF0	65 - 85
EF1	86 - 110
EF2	111 - 135
EF3	136 - 165
EF4	166 - 200

The National Weather Service (NWS) is the sole federal entity tasked with issuing official EF scale classifications. The goal is to determine the EF scale category by assessing the maximum wind speed recorded within the area of damage. Skilled personnel will select the

relevant damage indicator (DI) from a list of over 28 indicators utilized in the rating process (Table 2.2).

Table 2.2: NWS damage indicators (highlighted indicators represent commercial structures).
(Adapted from Texas Tech University 2006).

NUMBER	DAMAGE INDICATOR	ABBREVIATION
1	Small barns, farm outbuildings	SBO
2	One- or two-family residences	FR12
3	Single-wide mobile home (MHSW)	MHSW
4	Double-wide mobile home	MHDW
5	Apt, condo, townhouse (3 stories or less)	ACT
6	Motel	M
7	Masonry apt. or motel	MAM
8	Small retail bldg. (fast food)	SRB
9	Small professional (doctor's office, branch bank)	SPB
10	Strip mall	SM
11	Large shopping mall	LSM
12	Large, isolated ("big box") retail bldg.	LIRB
13	Automobile showroom	ASR
14	Automotive service building	ASB
15	School - 1-story elementary (interior or exterior halls)	ES
16	School - jr. or sr. high school	JHSH
17	Low-rise (1-4 story) bldg.	LRB
18	Mid-rise (5-20 story) bldg.	MRB
19	High-rise (over 20 stories)	HRB
20	Institutional bldg. (hospital, govt., or university)	IB
21	Metal building system	MBS
22	Service station canopy	SSC
23	Warehouse (tilt-up walls or heavy timber)	WHB
24	Transmission line tower	TLT
25	Free-standing tower	FST
26	Free-standing pole (light, flag, luminary)	FSP
27	Tree - hardwood	TH
28	Tree - softwood	TS

*Shaded DIs represent commercial buildings

The description or construction of a building ought to match with the DI under review, and identified damage should correspond with the degrees of damage (DODs) linked to the chosen DI. The NWS surveyors will evaluate and assess within the confines of the specified upper and lower wind speed limits, along with the anticipated or expected value for the specific

DOD. This process is repeated for multiple structures and trees before arriving at a definite EF rating. Table 2.3 shows the DODs and wind bounds for Strip Malls.

Table 2.3: Strip Mall Degree of Damage and Wind Bounds
(Adapted from: Texas Tech University 2006).

DOD*	Damage description	EXPECTED	LOWER BOUND	UPPER BOUND
1	Threshold of visible damage	65	51	80
2	Uplift of roof covering at eaves and roof corners	80	66	100
3	Broken windows or glass doors	88	72	105
4	Uplift of the roof decking	101	84	122
5	Collapsed façade or parapet walls	103	185	125
6	Covered walkways uplifted or collapsed	103	86	125
7	Uplift or collapse of entire roof structure	122	103	143
8	Collapse of exterior walls; closely spaced interior walls remain standing	140	117	165
9	Complete destruction of all or a large section of building	171	147	198

The DODs for a particular DI range from damage initiation (lower bound) to total destruction (upper bound) of the building or structure. Each DI has several DODs [6 – 10, according to Mehta, 2013], and there are more than 200 levels of damage (DODs), which describe damage in the range between commencement of damage and total destruction. The DODs are in sequence, so each subsequent one has a higher expected wind speed than the previous one (Table 2.3).

The strategy of DIs consists of an expected, upper, and lower bound wind speed. The wind speed range includes both the upper and lower bounds, which accommodate circumstances that influence the actual wind speed's effect on a given DOD within normal conditions. This approach, therefore, assumes that there is no apparent discontinuity in the load path, construction quality is traditional, appropriate building materials are utilized, compliance with local building

codes is maintained, and maintenance is uninterrupted (Masoomi et al. 2018a). Traditional construction quality means construction procedures are considered appropriate in most similar DIs in an area. Proper building materials fit their specific use and the area's environment. Regular maintenance implies that the facility has not run down or deteriorated over time (Amini and van de Lindt, 2014).

Each damage indicator depicts the typical construction for that category indicator. For example, typical construction for one- or two-family residences may include tile, asphalt shingles, metal roofing, or slate. They may have brick veneer, wood panels, stucco, vinyl, metal siding, and an attached single-car garage (Texas Tech, 2006). Once the structure has been assigned a damage indicator, the team will thoroughly analyze the building structure and construction. The survey team will allocate a degree of damage to the structure or tree in question.

While Damage Indicators (DIs) and Degrees of Damage (DOD) provide valuable insights into the assessment of tornado-related damage, it is essential to look into the details of damage characterization and limit States. Damage States and limit states are often utilized to summarize the structural response under extreme wind loading conditions.

2.3 Damage Characterization and Limit States

In the context of tornado vulnerability assessments, Damage States (DS) serve as critical benchmarks for evaluating the extent of structural damage incurred by buildings during tornado events. These Damage States are integral components of widely used frameworks such as Hazus-MH and FEMA guidelines. Hazus-MH categorizes Damage States into Slight, Moderate, Extensive, and Complete, providing a standardized methodology for quantifying the severity of

tornado-induced damage. Building damage states are given as a probability of the wind load exceeding the resistant capacity of a structure's MWFRS and C&C (walls, connections, roofing, and so on). Similarly, FEMA employs a classification system encompassing categories such as Destroyed, Major, Minor, Affected, and, for those buildings that cannot be reached for assessment, Inaccessible (FEMA, 2011), offering a comprehensive spectrum of damage severity levels (Table 2.4).

Table 2.4: FEMA Damage States (Adapted from FEMA, 2010)






		Damage description
Destroyed	1	Complete failure of two or more major structural components, e.g., collapse of basement walls, foundation, load-bearing walls, or roof
	2	Only foundation remains
	3	A residence that is in imminent threat of collapse because of disaster-related damage or confirmed imminent danger – e.g., impending landslides, mudslides, or sinkholes
Major		
	1	Failure or partial failure to structural elements of the roof to include rafters, ceiling joists, ridge boards, etc.
	2	Failure or partial failure to structural elements of the walls to include framing, sheathing, etc.
	3	Failure or partial failure to foundation to include crumbling, bulging, collapsing, of more than six inches
	4	Residences with a water line 18 inches above the floor in an essential living space, a water line above the electrical outlets, or a water line on the first floor when basement is completely full
Minor		
	1	Nonstructural damage to roof components over essential living space to include large areas of shingles, e.g., roof covering, fascia boards, soffit, flashing, and skylight
	3	Non-structural damage to the interior wall components to include drywall, insulation; exterior components to include house wrap, missing doors, broken window framings; or substantial loss of exterior covering, such as missing siding, vinyl, stucco, etc.
	4	Multiple small vertical cracks in the foundation
	5	Damage to chimney to include, tilting, fallen, cracks, or separated from the residence
	6	Damage to or submersion of mechanical components, e.g., furnace, boiler, water heater, HVAC, electrical panel, pressure tanks or well pressure switch, etc.
	7	Water line less than 18 inches in an essential living space
		Damage or disaster related contamination to a private well or septic system
Affected		
	1	Partial missing shingles or siding (non-continuous/sporadic), home kept roof structure intact.
	2	Cosmetic damage, such as paint discoloration or loose siding
	3	Broken screens
	4	Gutter damage and debris
	5	Damage to an attached structure such as a porch, carport, garage, or outbuilding not for commercial use
	6	Damage to landscaping, retaining walls, or downed trees that do not affect access to the residence or has not collapse into residence
	7	Any water line in the crawl space or basement when essential living space or mechanical components are not damaged or submerged

These Damage States enable consistent and objective assessment of structural integrity and facilitate efficient allocation of resources for post-disaster response and recovery efforts.

Understanding the implications of different Damage States is paramount for developing effective mitigation strategies and enhancing community resilience in tornado-prone regions. For example, in their study, Memari et al. (2018) used four damage states, Slight, Moderate, Extensive, and Complete, to assess the building's performance relative to tornado loading. These damage states explained the performance of physical damage sustained by the building envelope, roof structure, and exterior walls.

A significant number of studies have been conducted over the last several decades, mainly focusing on evaluating and understanding the damage to infrastructure due to tornado loads (Haan et al., 2010; Prevatt et al., 2012). Beyond the familiar classifications of the EF scale's Degrees of Damage (DODs) and DIs for buildings, the StEER Damage rating in Table 2.5 provides a comprehensive overview of wind damage ratings. Aligning with the Hazus-MH (FEMA 2010) nomenclature, four distinct damage states (DS) – Minor, Moderate, Severe, and Destroyed – ensure consistency. Referencing Table 2.5, if any shaded damage indicators in a given row manifest, the corresponding building or structure is categorized into the associated damage state. For example, a building earns the designation of damage state 4 (Destroyed) only when it experiences roof structural failure or load-bearing wall failure. In damage state 4, the first three damage indicators will also typically occur, likely leading to DS4.

Table 2.5: Wind damage rating criteria for components. Quantitative guidelines for assigning overall wind damage rating. (Adapted from VAST Handbook: DE/QC, 2019)

Damage State [1]	Short Description	Illustrative Example	Presence or Extent of Failure in:				
			Roof or Wall cover	Window or door	Roof or Wall sub-structure	Roof struct.	Wall struct. [2]
0 No damage or very minor damage	No visible exterior damage		0%	No	No	No	No
1 Minor damage	Damage confined to envelope		> 2% and ≤ 15%	1	No	No	No
2 Moderate damage	Load path preserved, but significant repairs required		> 15% and < 50%	> 1 and ≤ the larger of 3 and 20%	1 to 3 panels	No	No
3 Severe Damage	Major impacts to structural load path		> 50%	> the larger of 3 and 20% and ≤ 50%	> 3 and ≤ 25%	≤ 15%	No
4 Destroyed	Total loss. Structural load path compromised beyond repair.		> 50%	> 50%	> 25%	> 15%	Yes
Notes: [1] A building is considered to be in the damage state if any of the shaded damage indicators in the corresponding row are observed. [2] Wall structure refers to walls in living area only. The ground floor of elevated structures often have breakaway walls that can be easily damaged by storm surge. This damage should be ignored in assigning the overall damage rating.							

Having established a comprehensive understanding of extreme weather, tornado formation, and the impact of tornadoes, this dissertation focuses on the existing body of knowledge surrounding the assessment of building tornado fragility. The subsequent section reviews pertinent literature, exploring the methodologies, findings, and gaps in our current understanding of how structures respond to tornadoes.

2.4 Review of the Current State of Building Tornado Modeling Failure of Structural Components Using Fragilities

The fragility curve development methodology, expressed mathematically, defines fragility as the conditional probability that a specific random variable related to the response or performance of a structure or structural component will surpass a predefined capacity under

given conditions, typically represented by various loads such as extreme wind events. Within this framework, tornadic fragility quantifies the likelihood that a building or its component will exceed a specific limit state under the influence of extreme wind events. The chosen limit states align with the building's operational or functional aspects and are synonymous with building resistive capacity (Amini et al., 2014).

Previous studies of post-event storm surveys have documented common failure modes of residential and commercial buildings. Common observations include substandard brick veneer attachments (LaFave et al., 2016), poor roof performance associated with loss of roof sheathing, and failure of the roof-to-wall connection due to uplift, which in some cases results in multiple wall collapses (Gardner et al., 2000; Marshall, 2002; Pan et al., 2002; Jordan, 2007; Peng, Rouche and Prevatt, 2013), and load path deficiencies (Prevatt et al., 2011; van de Lindt et al., 2012). Numerical studies have modeled tornado damage fragility functions for buildings (Amini and van de Lindt, 2014) and have begun incorporating tornado fragility functions into regional simulations for risk assessments (Masoomi et al., 2018b; Memari et al., 2018).

Tornado fragility curves, defined as conditional probability curves that give the likelihood of damage given a wind speed (Memari et al., 2018; Masoomi and van de Lindt, 2016; Koliou et al., 2017; Masoomi et al., 2018b; Attary et al., 2017), have been found to be valuable tools for modeling potential damages to structures. Fragility curves are the relationship between the probability of a failure and an intensity measure of a hazard. In tornadic fragility functions, the primary failure mode is generally defined as excessive stress or displacement greater than given thresholds resulting from extreme wind-induced loadings (Koliou et al., 2017). The intensity measure of loading is selected as the peak wind loading, and the failure probabilities are

described as dependent variables of the intensity measure on the fragility curve (Lee J et al., 2016).

Fragility curves of buildings using probabilistic techniques help quantify potential damage to structural components or the entire building system during tornadoes. The integration of these fragility models into tornadic risk assessments provides an opportunity to screen buildings susceptible to tornadic wind loading to project anticipated damage and tornadic wind loading losses or support post-event inspection. Ultimately, fragility curves enable us to evaluate the resilience of buildings and communities to tornado events and develop targeted strategies to enhance preparedness and reduce vulnerability. Fragility curves relating the probability of failure to the intensity of some hazards are reliable for the failure assessment of structural systems (Shafieezadeh et al., 2014; Padgett and DesRoches, 2009; Shafieezadeh et al., 2011). For example, Li and Elingwood (2009) and Ham et al. (2009) generated fragility relationships for residential home components and industrial buildings, respectively, by using reliability analysis with respect to wind speeds. Reliability analysis involves quantifying the likelihood that a structure or its components will exceed a certain threshold of response (e.g., damage or failure) when subjected to different levels of loading. This analysis typically incorporates factors such as material properties, geometric configurations, environmental conditions, and uncertainties associated with input parameters.

Fragility curves require reliability analysis to calculate the probability of an event in which a structure undergoes a certain level of damage. Lombardo et al. (2023) developed an approach using tornadic fragility curves to quantify the likelihood and magnitude of misclassifying tornado characteristics (e.g., peak wind speed, damage length, and width) using

damage to residential structures in typical rural configurations. This study found that, from an intensity perspective, EF4 tornadoes are most likely to be correctly identified through damage, with EF4 ratings being favored for strong to violent tornadoes. However, accurately estimating the intensity of violent tornadoes based solely on residential damage proves challenging, suggesting limitations in identifying "true" EF5 tornadoes from residential damage alone.

An example is given by Lee, Ham, and Kim (2013) for investigating a structure based on roof covering, roof structure, and exterior windows. In determining the response of building components to extreme wind loadings, the variability of many factors leads to a great deal of uncertainty. The turbulent nature of wind loadings on different topographic terrains produces fluctuating aerodynamic forces on the various parts of a building. Aside from this, the building components' resistance varies due to their innate material properties and construction. To account for these, fragility curves are used to quantify the probability of a particular damage state that a structure will experience as a function of demand, given a set of parameters, such as roof covering type and condition, roof structure design and integrity, exterior windows' properties and quality, topographic terrain features influencing wind flow patterns, aerodynamic forces acting on different parts of the building, material properties of building components, construction quality, and standards.

Studies have developed fragility functions for some building archetypes in a community to perform damage and resilience modeling at a community level. The study by Memari et al. (2018) develops tornado fragility functions for several building types, creating 19 building archetypes. Other authors (Amini and van Lindt, 2014; Standohar-Alfani and van de Lindt, 2016) form a reasonably comprehensive portfolio, termed a minimal building portfolio (MBP) tornado

building fragilities for community-level spatial damage analyses. These fragilities are used to assign damage states to different types of buildings using Monte Carlo Simulations (MCS).

The estimation of loss due to wind hazard has been previously well outlined through the Federal Emergency Management Agency's (FEMA) HAZUS. It has been established based on a building's damage state. As mentioned in the previous section, building damage states are given as a probability of the wind load exceeding the resistant capacity of a structure's MWFRS and C&C (walls, connections, roofing, and so on). Such fragilities have been developed previously on an individual building basis (Unanwa et al., 2000; Rosowsky et al., 2002; Rosowski et al., 2004; Ellingwood et al., 2004; Hwang et al., 2004; Koliou et al., 2014; Amini et al., 2014; Masoomi et al., 2016; Koliou et al., 2017; Masoomi et al., 2018a; 2018b; Gill et al., 2021. Refan et al., 2020). van de Lindt and Dao (2012) point out that "more than 80% of the total building stock in the United States and more than 90% of the residential buildings in North America are wood-frame construction, a type of construction that is quite vulnerable to wind damage". As a result, Masoomi et al. (2018b) investigated performance enhancement strategies for wood-frame residential buildings. They explored blends of roof coverings, roof sheathing nailing patterns, and roof-to-wall connections. They further considered a total of nine construction product combinations and later looked into the damage fragilities of five wood-frame building archetypes for the "four damage states defined based on the performance of the building envelope, including roof coverings, doors and windows, roof sheathing, and roof-to-wall connections."

The methodology to develop tornado fragility of components, as developed by Memari et al. (2018), is shown in the flowchart below:

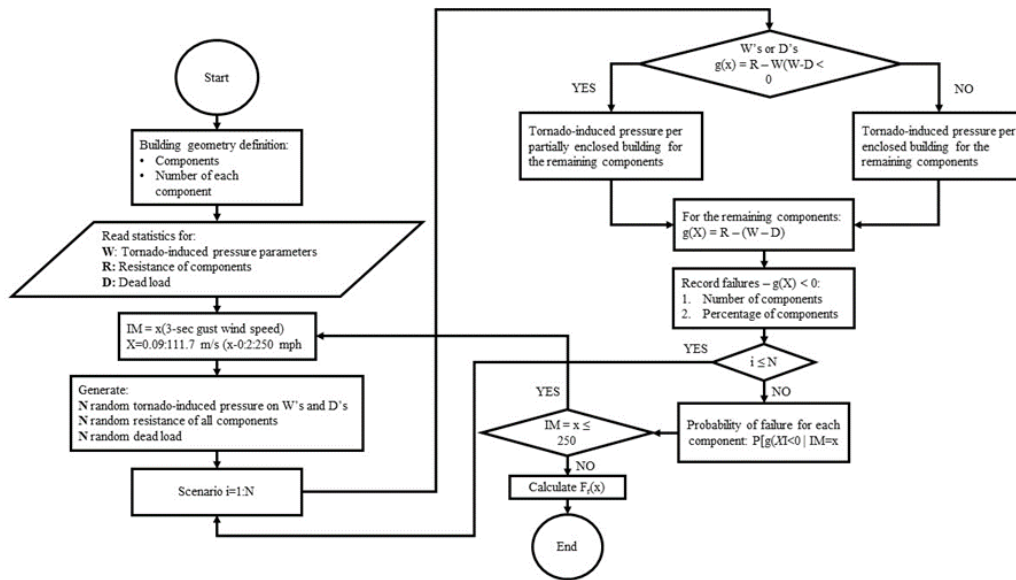


Figure 2.2: Flowchart showing methodology to develop tornado fragility of components.
(Adapted from Mehmari et al. 2018)

Figure 2.3 below shows an example of a set of fragility curves. The vertical axis represents the probability that the wind load on the structure will meet or exceed a certain limit state, while the horizontal axis in fragility curves generally varies within different predefined conditions, such as the intensity of the 3-sec gust wind speed.

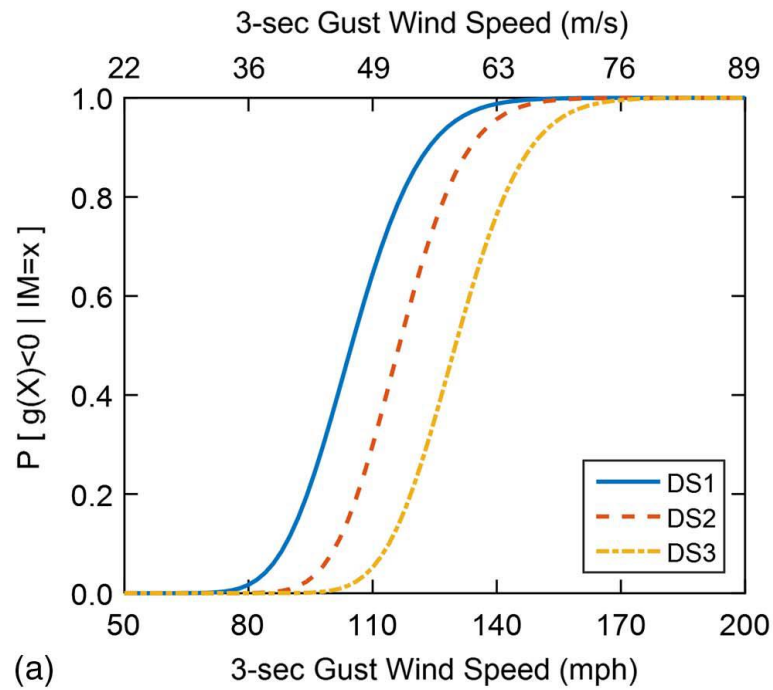


Figure 2.3: Example of fragility curves for doors and windows. (Adapted from Memari et al. 2018)

2.5 Limitation of Current Approaches

While current approaches in utilizing fragilities concentrate on evaluating the vulnerability of buildings in their pristine state, a notable gap exists in addressing the impact of deterioration and maintenance deficiencies on structural performance. These approaches traditionally overlook the potential effects of deterioration and maintenance deficiencies on a building's structural performance. Current practices involve wind damage ratings determined through visual assessments of the main wind force-resisting systems (MWFRS) and components & cladding (C&C) of damaged buildings. The condition of these structures is contingent upon factors such as hazard strength, building materials, construction quality, and the potential state of deterioration, which is closely linked to ongoing maintenance efforts. Continuous maintenance, which ensures the longevity and resilience of a facility (Lacasse, 2020), is pivotal in mitigating deterioration caused by various factors such as age, overcapacity, and lack of planning or

preventative maintenance. This is particularly significant when buildings are left unoccupied after reaching the end of their useful life.

Current literature on the use of fragility functions for modeling the probability of failure from extreme winds lacks consideration of the effects of aging, which is in contrast to the thorough exploration of *seismic* fragility in bridge studies, where Choe et al. (2008, 2009) have probed the impact of deterioration on the capacity and fragility of typical single-bent bridges in California. Choe et al.'s work highlights the necessity of capturing the effects of deterioration on seismic fragility, leading to the development of time-dependent fragility curves that incorporate uncertainties in bridge component capacity models. Building upon this foundation, subsequent researchers, such as Ghosh and Padgett (2010, 2012), Simon et al. (2010), and Alipour et al. (2010), have explored the broader understanding of the effect of aging on system response and fragility. Their studies consider the vulnerability of multiple components and incorporate simultaneous aging, thereby constructing time-dependent fragility curves with a specific emphasis on corrosion-induced deterioration. Recognizing the inevitability of material and structural deterioration, extending this line of inquiry to extreme wind event fragility studies for buildings is imperative, bridging the current research gap and enhancing the comprehensiveness of modeling failure of structural components using fragilities.

Building upon the foundation laid by seismic fragility studies, particularly the work of Ghosh and Padgett (2012), there is an opportunity to adapt and extend these methodologies to address the deterioration effects in extreme wind event fragility studies for buildings. Recognizing the inevitability of material and construction practices' deterioration, extending this line of inquiry to extreme wind event fragility studies is imperative. Doing so would enhance the

comprehensiveness of modeling the failure of structural components using fragilities, thereby contributing to developing more resilient structures in the face of extreme wind events.

2.6 Deterioration

Deterioration plays an essential role in influencing the vulnerability of buildings during extreme wind events. For example, previous studies by Auld et al. (2010) identify that the quality of construction, maintenance of building stock, and state of deterioration also strongly influence their damage potential and extent of claims following extreme wind events. Studies done by Swiss Reinsurance (1997) and Munich Reinsurance (2005) state that lower-quality construction and poor maintenance or premature deterioration over time can rapidly worsen the marginal damages for each threshold of wind or other climate parameters, leading to higher loss and, therefore, claims following an extreme wind event.

This section explores the various dimensions of deterioration, ranging from the lifespan of building materials to predictive models and methodologies. To provide a comprehensive understanding, the research examines the concept of service life and its connection to building materials, followed by insights into the process of facility condition assessments (FCA) and the challenges posed as buildings approach the end of their useful life. This section also considers the process of modeling deterioration using Markovian models to predict deterioration, providing a statistical foundation for understanding the dynamic changes in building conditions. Finally, this section explores deterioration degrees and rates, highlighting their impact on structural response under dynamic loading.

Deterioration, in terms of facilities management, means a loss of the estimated value of real estate resulting from its technical (physical), functional (utility), and environmental

deterioration. Aging, design flaws, assembly defects, material structural changes over time, damage from external factors, and inadequate service/maintenance contribute to deterioration (Uzarski, 2008). Elements exhibit varying lifecycles, deteriorating unevenly, and therefore have disparate service lives (Dziadosz & Meszek, 2015).

2.6.1 Service Life of Materials

The service life of building materials can be defined as the period after installation during which the essential properties meet or exceed minimum acceptable values (Dziadosz & Meszek 2015, 2018). This time-based parameter serves as a critical benchmark for evaluating the longevity and durability of building elements. Each material or component in a building system has an expected service life; for instance, structural members are expected to perform their intended functions for at least the lifetime of a building, while materials such as roofing membranes usually have shorter service lives and require periodic repair or replacement during the lifetime of the building (Schoen, 2010). These distinctions are crucial in understanding how each material contributes to a structure's overall performance and functionality.

Collecting data on the service life of building materials involves a combination of experiential knowledge and systematic testing methodologies (Masters & Brandt, 1999). These approaches aim to provide insights into the expected performance and longevity of materials within the built environment. Experience-based data on service life are derived from the historical performance of materials in real-world conditions. Building professionals, researchers, and facility managers contribute to this wealth of knowledge by observing the behavior of materials over time (Konior, 2021). By documenting the lifespan of various components and structures, valuable information is gathered on the durability and reliability of different materials.

On the other hand, systematic testing serves as a scientific approach to assessing the service life of building materials. Laboratory exposure, field exposure, and assessments of in-service performance are common methods employed. These tests simulate environmental conditions, stressors, and usage patterns to evaluate how materials respond and degrade over time (Dziadosz & Meszek, 2015). The data from such controlled experiments contribute to a more comprehensive understanding of material performance.

Schoen (2010), through a peer-reviewed preventative maintenance guidebook, created a list of systems, materials, and their average useful life in years. The caveat in his study was that many factors can affect the average useful life, and like any average, individual systems and components will have lifetimes far from average. Lifetimes can often be extended significantly through robust maintenance programs that go beyond the norm, and many facilities currently have functioning equipment older than the lifetimes listed in the study. Climatic conditions and challenging environments introduce additional complexities to predicting service life. Wet locations, saltwater proximity, or heavy industrial activity exposure can accelerate deterioration. These external factors interact with material properties, influencing the rate of deterioration and the overall longevity of building components.

2.6.2 Facility Condition Rating

As building assets deteriorate, it is important for commercial and government building owners and facility managers to maintain them systematically, ensuring their optimal performance throughout their operational lifespan. Typically, building owners conduct annual Facility Condition Assessments (FCAs) to monitor their assets. These inspections typically involve visually inspecting each component within a building and assigning a condition rating on

a scale of one to five, with one indicating optimal condition and five requiring immediate attention (Lewis and Payant, 2000). The primary purpose is to monitor the condition and performance of these assets over time. FCAs are essential aspects of proactive facility management, providing a valuable understanding of the current state of building functionality and guiding decision-making for maintenance strategies. The methodology of FCAs involves a comprehensive inspection of each item within a building. Trained professionals, often facility managers or inspectors, visually assess various components and systems. The assessment considers factors such as structural integrity, functionality (how well facilities are performing for their assigned use), and environmental conditions (Mayo and Karanja, 2018). The goal is to create a holistic understanding of the building's condition by assigning a condition rating.

The condition ratings, as depicted in Table 2.6, serve as crucial tools for owners and facility managers, offering insights into the current performance of their assets and guiding maintenance scheduling with a focus on addressing deteriorated elements (IPWEA, 2009).

Table 2.6: Condition States following FCA

Condition State	Component Condition	Condition Description
1	Very good	The element is as new
2	Good	The element is sound; minor damage and minor maintenance required
3	Moderate	Moderate damage; moderate maintenance required
4	Poor	Major damage; major maintenance required
5	Very poor	Very poor. Serious damage; element should be replaced

By categorizing elements into different condition states, FCAs facilitate prioritization. Elements high in poorer condition (higher condition states) are flagged for immediate attention

and major maintenance, guiding owners in allocating resources where they are most needed.

Examples of these elements are shown in Table 2.7.

Table 2.7: Example of Building Systems and their Elements: Uniformat II Format

ID	Components	Sub-Components
A.	Substructure	Foundation: Walls, columns, pilings
		Basement: Materials, insulation, slab, floor underpinnings
B.	Shell	Superstructure / structural frame: columns, pillars, walls
		Roof: Roof surface, gutters, eaves, skylights, chimney surrounds
		Exterior: Windows, doors, and wall finishes (paint and masonry)
		Shell appurtenances: Balconies, fire escapes, gutters, downspouts
C.	Interiors	Partitions: walls, interior doors, fittings such as signage Stairs: Interior stairs and landings Finishes: Materials used on walls, floors, and ceilings
D.	Conveyance	Lifts: any other such fixed apparatuses for the movement of goods or people
E.	Plumbing	Fixtures, Water distribution, Sanitary waste, Rain water drainage
F.	HVAC (heating, ventilation, and air conditioning)	Energy supply
		Heat generation and distribution systems
		Cooling generation and distribution systems
		Testing, balancing, controls, and instrumentation
G.	Fire Protection	Chimneys and vents
		Sprinklers, Standpipes, Hydrants, Hydrants, and other fire protection specialties
H.	Electrical	Electrical service & distribution
		Lighting & branch wiring (interior and exterior)
		Communications & security
		Other electrical system-related pieces, such as lightning protection, generators, and emergency lighting

Condition ratings help owners understand which components are functioning optimally (lower condition states) and which may require attention, repair, or replacement. FCAs provide a basis for creating maintenance schedules. The frequency and intensity of maintenance activities can be tailored based on the condition ratings (Uzarski, 2008). Regular maintenance for elements in good condition can prevent deterioration, while more intensive efforts may be directed toward elements in poorer condition.

As buildings approach the end of their useful life, several challenges emerge in the area of continuous maintenance (Bailey & Galecka, 2008). The meticulous care and maintenance practices observed throughout their operational lifespan may encounter hurdles or diminish, introducing complexities that impact the continued functionality and safety of the building. According to Laraia (2018), at the end of the service phase of a facility, there is a relatively high number of facilities left in a semi-abandoned state for many years. Structural deterioration can occur when a building is neglected or left for a prolonged period without proper maintenance, making it vulnerable to damage during an extreme hazard event. The strength of the components of any structural system, in general, is a time-dependent property that may decrease resistance along the structure's service life. Structural components may be weakened, making the building more susceptible to damage.

In the context of tornado modeling failure of structural components using fragilities, the challenges associated with the maintenance of a building approaching the end of its useful life are critical. The state of deterioration can significantly influence the structural response to wind loading during a tornado event, necessitating accurate modeling for finite element analysis. As buildings age and maintenance declines, safety risks may increase. Deterioration of critical

structural elements can compromise the safety of occupants and surrounding areas. The safety implications are particularly relevant in extreme events like tornadoes, where the structural integrity of a building is crucial. Neglected maintenance may contribute to higher levels of damage, posing risks to both property and lives (Auld, 2010). Deterioration may affect the structure's response under dynamic loading, such as wind loading. This research emphasizes deterioration consideration.

Addressing maintenance challenges as buildings approach the end of their useful life is vital for ensuring the continued functionality, safety, and resilience of structures. This becomes especially significant when modeling the failure of structural components using fragilities for extreme events, where accurately representing the building's condition is essential for predicting its response to dynamic forces such as tornadoes.

2.6.3 Deterioration Modeling

Modeling deterioration can be used to alter fragility functions, and its significance lies in capturing the dynamic interplay between structural integrity, material properties, and the aging process. As buildings deteriorate over time, their response to external forces, such as those generated by tornadoes, undergoes changes that significantly influence the fragility of the structure. This section explores the reasoning behind the importance of modeling deterioration when determining fragility functions that may change over time.

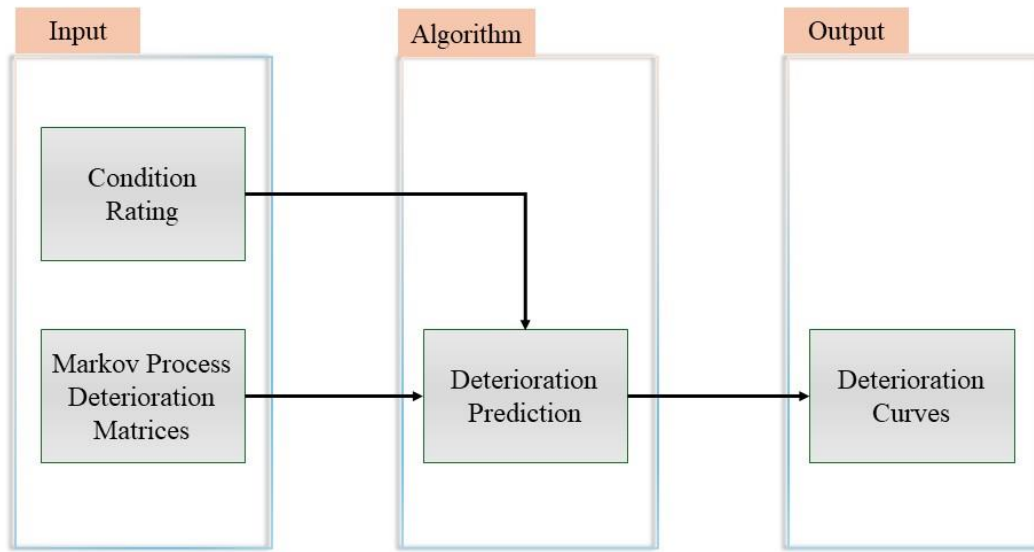
Tornado fragility curves depict the probability of structural damage or failure at varying intensity levels of tornadoes. The accuracy of these curves depends on how well the model captures the effects of deterioration on building vulnerability. Robust deterioration models may contribute to the derivation of accurate tornado fragility curves by allowing for the assessment of

how different levels of deterioration influence the likelihood and severity of damage under tornado conditions.

2.6.4 Markovian Models

Deterioration prediction is a significant stage in the whole life cycle of building management (Kleiner and Rajani, 2001). Deterioration prediction focuses on individual elements of the building and/or the building as a whole infrastructure system based on the condition data from the condition rating. Probabilistic models “predict the condition as the probability of occurrence of a range of possible outcomes” (Ortiz-Garcia et al., 2006). Statistical models have been used in engineering studies (Henley and H., 1992; Kuzin and Adams, 2005), and statistical or probabilistic modeling, such as Markov chain, ordinal regression, and linear discriminant analysis, is based on statistical theory for modeling phenomena with random noise in components.

Markovian models are the most studied stochastic techniques that have been used considerably in modeling the deterioration of infrastructure (Jiang et al., 1988; Butt et al., 1987). In their study, Jiang et al. (1988) mention the Markov decision process, which defines states of assets and statistically attains the probabilities of the assets' condition transitioning from one state to another during an inspection period. The methodology for deterioration prediction is summarized in Figure 2.4 below.



2.4: Deterioration Prediction

2.6.4.1 Markov Chain

Markovian models, particularly Markov chains, excel in capturing these probabilistic transitions between condition states. They provide a statistical framework for predicting the likelihood of moving from one state to another. Building assets are subject to changing conditions due to factors such as aging, environmental exposure, and usage. Markovian models quantify the probabilities of transitions between condition states, offering a predictive tool to anticipate how the building's health may evolve. By customizing transition probabilities based on observed data and asset-specific features, Markovian models provide a more accurate representation of how individual building elements or systems will likely degrade (Morcous 2002).

"A Markov chain has a stationary stochastic matrix which, once applied to an initial probability distribution, results in the next step's probability distribution" (Mohseni et al. 2012). A Markov chain is a sequence of events where the probabilities of the future only depend on the present. It is stochastic as the predictions are probabilistic and uncertain in nature. Markov chain

is more appropriate for developing and verifying a deterioration prediction model where continuous inspection data sets are unavailable. Also, the assumption of unit change of facility condition is unsuitable for building condition data because the deterioration of building components might undergo a multistate transition (i.e., jumping from condition three to condition six within a one-time step). Hence, the Markov chain is selected to derive the deterioration prediction model, as shown in Figure 2.5. Markov chain has been used for the analysis of different infrastructure such as stormwater pipes (Micevski et al., 2002; Tran, 2007), bridges (Madanat and Wan Ibrahim, 1995), and sewers (Baik et al., 2006). These statistical models simulate the randomness and uncertainty of the element's deterioration process using one or more variables.

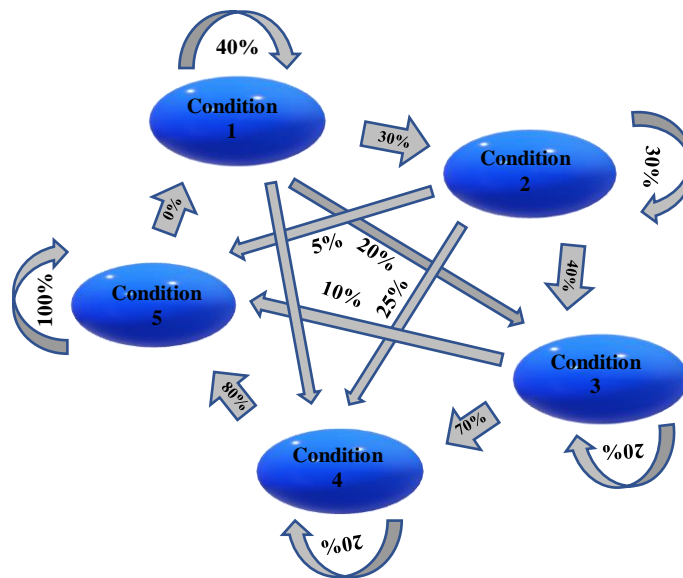


Figure 2.5: Example of a Markov chain deterioration model - Transition relations

Markovian models offer a powerful and versatile framework for predicting building asset deterioration. Their significance lies in their ability to systematically represent condition states, model probabilistic transitions, and adapt to variable time intervals. Applied to building assets,

these models enhance the accuracy of deterioration predictions, supporting informed decision-making for maintenance, risk mitigation, and the overall management of structural health over time. While Markovian models provide valuable insights into the probabilistic deterioration of individual building elements, this study's exploration extends beyond theoretical frameworks. Transitioning from the complex analysis of element-level deterioration, the following section looks at the broader perspective of material degradation, examining the tangible impact of deterioration rates or degrees on the overall structural response, particularly in the context of tornadic modeling failure of structural components using fragilities.

2.6.5 Deterioration Rates

Deterioration rates in engineering structures and infrastructure are best captured by a physics-based failure model. The connection between deterioration rates and the impact on structural response during dynamic loading, such as wind loading, is pivotal for understanding how the gradual loss of building integrity influences its behavior under external forces. The time-dependent nature of deterioration implies that a building's response to dynamic loading, such as wind, can be influenced by the evolving condition of its components. Pandey et al. (2007) recommend modeling deterioration as a time-dependent stochastic process, wherein coefficients (e.g., rate of deterioration per unit time) are treated as random quantities.

Various methods exist to assess deterioration, with some defining building deterioration based on the overall wear of specific construction elements, while others evaluate the deterioration of individual building elements and materials. Konarsewska & Konarsewska (2006) state that the visual method is one such approach. However, an alternative and more dynamic method is the time flow methodology, requiring knowledge of usage duration and the envisioned

building lifespan. Determining the rate of deterioration or degree of deterioration involves understanding the service life durability of a building and its materials (Dziadosz & Meszek 2015), which the research discusses at length in section 2.6.1. Building facilities comprise numerous elements with varying degrees of technical deterioration influenced by diverse factors and their interactions. Predicting durability and service life proves challenging, and common methods yield estimated values with varying accuracy and labor requirements. Konior (2021) contends that time methodologies are prevalent, assuming that technical deterioration increases over time, contingent on maintenance accuracy and materials used in the building facility.

In both literature and practice, different formulae, such as Ross, Eytelwein, Unger, and Romstorfen, are employed to measure technical deterioration encompassing time methodologies and functional deterioration (Konior, 2021; Dziadosz & Meszek 2015, 2018). This division into different care levels regarding a building has historical roots dating back to the early 20th century in Poland. The formulae provided in Table 2.8 below characterize the degrees of technical wear in a building, reflecting different levels of care.

Table 2.8: formulae to determine deterioration (Adapted from Konior et al., 2018)

Formula to determine deterioration	
Traditional (Poor Maintenance of building)	$Z = \frac{t}{T}$
Unger (Average Maintenance)	$Z = \frac{t \cdot (t + T)}{2T^2}$
Romstorfen (Satisfactory Maintenance)	$Z = \frac{t \cdot (2t + T)}{3T^2}$
Eytelwein (Excellent Maintenance)	$Z = \frac{t^2}{T^2}$

Where:

Z = Deterioration rate or degree

t = Current stage of service life (years)

T = Service life (years)

An explanation of how these formulae are utilized is as follows:

Linear Formula of Proportionality:

When little care is given to the maintenance of the building, the linear proportionality formula is employed. This formula relates the deterioration rate (Z) to the current stage of service life (t) and the overall service life (T).

Ross and Unger (Average Maintenance)

When average care is taken with regard to the maintenance of the building, the Ross and Unger formula is used. This means that current and major repairs are done on time.

Romstorfen Formula (Satisfactory Maintenance):

Above-average care in maintenance leads to the application of the Romstorfen formula. This formula provides a more optimistic assessment of the deterioration rate under satisfactory maintenance conditions.

Ross and Eytelwein Formula (Excellent Maintenance):

Extreme maintenance care triggers the use of the Ross and Eytelwein formula. This formula reflects a scenario where the building receives meticulous care, resulting in slower deterioration rates.

These formulae can indirectly contribute to understanding structural response during dynamic loading. By quantifying the rate of technical deterioration, they offer insights into the potential vulnerabilities of building materials. The results from these formulae can guide decisions on maintenance, repair, or replacement of components that may influence the structural response to dynamic loading events like wind. The choice of the formula depends on the perceived level of maintenance care, and the outcomes directly impact the expected deterioration rates. Buildings with higher deterioration rates may exhibit different responses to dynamic loading, emphasizing the importance of accurate deterioration modeling for reliable structural assessments.

Deterioration in engineering structures involves gradually losing estimated real estate value due to physical, functional, and environmental factors. Elements experience wear and tear influenced by age, design flaws, assembly defects, material property deficiencies, and varying components' service life. Facility Condition Assessments monitor deterioration, and if robust maintenance practices follow this, it can extend the building's lifespan. Deterioration prediction, a crucial stage in whole-life building management, utilizes probabilistic models like Markov chains and ordinal regression, accounting for randomness and uncertainty. Assessing deterioration degree/rates involves modeling it as a time-dependent stochastic process, considering various methods, and emphasizing the impact of maintenance accuracy and materials. Formulae like Ross, Eytelwein, Unger, and Romstorfen measure technical deterioration. The historical division into different care levels underscores the importance of proactive maintenance in building management.

3.1. Summary

The insights gained from this chapter provide the necessary groundwork for the subsequent development of tornadic modeling failure of structural components using fragilities methodologies. Accurate prediction of deterioration and proactive maintenance strategies are integral to enhancing the resilience of buildings. The research discussed herein aims to bridge gaps considering the deterioration effect by exploring the relationship between building material deterioration and tornado fragility, offering a more comprehensive approach to building fragility under extreme wind events. The methodologies developed will advance tornadic modeling failure of structural components using fragility practices and contribute to broader discussions on resilient infrastructure in the face of natural hazards.

CHAPTER 3: RESEARCH METHODOLOGY

This chapter provides an overview of the research methodology employed, elucidating the research questions and strategies utilized to investigate them. In the following sections, the research details the methodologies employed to address the research objectives, emphasizing the systematic approach taken to ensure the reliability and applicability of its findings.

To recap, the research questions developed for the research are as follows:

1. During facility condition assessments (FCAs), are facility managers prioritizing the same components as those conducting post-event storm surveys?
2. Does deterioration have an effect on the tornadic wind-loading response of building materials? How significant are the shifts in material tornadic fragilities of deteriorating buildings when compared to non-deteriorating (pristine) buildings?
3. Would a structure's age and material deterioration ultimately impact how tornadoes are ranked on the EF-scale?

3.1 Facility Condition Assessments

3.1.1 Introduction

As mentioned in the literature review section, the estimation of loss due to wind hazards has been previously well outlined through the Federal Emergency Management Agency's (FEMA) HAZUS-MH and has been established based on a building's damage state. Building damage states explain the performance of physical damage sustained by the building envelope, roof structure, and exterior walls and are given as a probability of the wind load exceeding the resistant capacity of a structure's MWFRS and C&C (walls, connections, roofing, door, and so on).

In the context of increasing environmental hazards and aging infrastructure, FCAs are particularly significant in evaluating building vulnerabilities. They provide a proactive approach to assess the resilience of buildings to various stressors, including natural disasters, extreme weather events, and the gradual effects of time and wear. By identifying vulnerabilities and potential points of failure, FCAs empower stakeholders to implement preventive measures and enhance the overall resilience of buildings against external threats. It is, therefore, essential to compare the focus of facility managers' FCAs with NWS post-event storm surveys to address the alignment between pre- and post-tornado surveys, shedding light on potential discrepancies.

An FCA is defined by Rugless (1993) as “a process of systematically evaluating an organization’s capital assets to project repair, renewal, or replacement needs that will preserve their ability to support the mission or activities they are assigned to serve.” The FCA holds paramount significance within the asset management process, serving as the cornerstone for other functions, such as decisions regarding repair or replacement. In the context of condition assessment, it is imperative to decompose a building into its principal components hierarchically. This hierarchical breakdown aims to classify and group these components into distinct categories. For instance, a building can be segmented into various disciplines or systems (such as structural, electrical, mechanical, building façade, etc.), which can then be further subdivided into more detailed component levels (e.g., interior doors/exterior doors, ceilings, windows, etc.). Adopting a standardized and consistent format for defining a building hierarchy can facilitate data sharing within an organization's Facility Management department. Elhakeem's study (2005) amalgamated the advantages of existing hierarchies. It proposed a five-level building hierarchy (system, subsystem, component, type/element, and instance) aligned with the Organizational Breakdown Structure (OBS) of educational institutions (e.g., school boards). The primary

advantages of this proposed hierarchy include streamlining the process of revising assessed components, assessing each facility's performance in maintaining its components in a safe and satisfactory condition and enabling the organization to allocate funds effectively. Various endeavors have been made to establish a hierarchy of building components, which have been discussed within building information modeling and in proprietary initiatives by government agencies to develop asset management systems.

This consistency in data organization facilitates data sharing within a Facility Management (FM) department, ensuring the assessment process's accuracy and reliability. This structured approach to building hierarchy is the foundation for collecting and cleaning data pertinent to our research question: ‘During FCAs, are facility managers prioritizing the same components as NWS during post-event storm surveys?’ Understanding and aligning the priorities of facility managers with those of NWS post-event storm surveys are crucial for ensuring the effective allocation of resources, timely repairs, and, ultimately, the structural integrity and safety of buildings in the face of extreme weather events. To address Research Question 1, data on current FCAs, specifically those related to decommissioned buildings, must be collected, as these are the most vulnerable to unmitigated deterioration.

3.1.2 Data collection and cleaning

Data for FCAs is obtained from a wider survey conducted in 2022 regarding decommissioning practices in commercial buildings. The survey encompasses a diverse range of building owners, facility managers, and stakeholders involved in designing, managing, and maintaining commercial properties. The research discusses a survey whose data are collected through a Qualtrics platform survey targeting professionals within the built environment,

including architects, engineers, building owners, facility managers, project managers, and construction managers. These participants are selected from the American Institute of Architects (AIA) and International Facilities Management Association (IFMA) databases due to both organizations' international reach. The respondents are subsequently divided into three professional groups:

- Group I - architects;
- Group II - facility managers and building owners; and
- Group III - construction managers, project managers, and engineers.

The survey grouping of respondents is based on their functional roles and responsibilities within the building lifecycle to ensure targeted analysis of relevant perspectives. Architects (Group I) are categorized together due to their shared involvement in the design and planning phases of construction projects, while facility managers and building owners (Group II) are grouped based on their mutual focus on building operations, maintenance, and asset management. Construction managers, project managers, and engineers (Group III) are clustered together owing to their collective roles in overseeing construction activities and providing technical expertise.

Data cleaning, quality management, and statistical analysis are carried out using the IBM Statistical Package for Social Sciences (SPSS version 27.0) software tool. This involves checking for potential data errors, such as formatting errors, duplication, and missing data where participants failed to respond. Survey responses that contain missing data are marked, and respondents are contacted via email. Respondents who did not reply with the information necessary to fill in this data are excluded from the subsequent analysis.

3.1.3 Questionnaire

The survey instrument is designed to gather comprehensive information on the condition of building components, maintenance priorities, and decision-making processes related to decommissioning. Key areas of focus include:

- 1) planning for decommissioning;
- 2) ***condition assessments***;
- 3) guidelines; and
- 4) general information.

In the interest of evaluating discrepancies between damage surveys and FCAs, the discussion herein focuses on the second key area: ***condition assessments***. By investigating the relationships between professionals' roles and condition assessments, this research aims to compare the focus of facility managers' FCAs with NWS post-event storm surveys to address the alignment between pre- and post-tornado assessments, shedding light on potential discrepancies. Table 3.1 shows the questions under the section "condition Assessments."

Table 3.1: Research Variables under the Condition Assessment Section of the Research

<i>Section</i>	<i>Variables</i>
Condition Assessments	<ul style="list-style-type: none"> ✓ Frequency of condition assessments on unoccupied commercial buildings. ✓ Asset prioritization for condition assessments on unoccupied commercial buildings. ✓ Additional assets that should be included in condition assessments of unoccupied commercial buildings.

The condition assessment questions concern specific building assets as garnered from the American Society for Testing and Materials (ASTM's) UNIFORMAT II (Charette & Marshall,

1999) and MasterFormat (CSI, 2020; Waugaman et al., 2022), the standards for organizing specifications for most commercial building design and construction projects in North America. Particular reference is given to UNIFORMAT II's Chart 4.5 (Charette & Marshall, 1999), where the relationship between UNIFORMAT and MasterFormat is described. Data collection is based on a taxonomy of building assembly systems in UNIFORMAT II for Building Elements. Classifications of these building assembly systems provide a commonly used outline for data collection and permit comparison between institutions, including Level 1 - Major Group Element, Level 2 - Group Elements, and Level 3 - Individual Elements.

3.1.4 Comparative Analysis

The data and results from the 2022 survey are analyzed to compare the building components that are the focus of facility managers during FCAs with that of NWS during post-event storm surveys, as shown in Table 3.2, as listed in Jain et al. (2020).

Table 3.2: Critical building components during NWS post-event storm survey (Adapted from Jain et al. 2020)

No.	Building Component
1	Roof Structure
2	Roof Covering
3	External Walls
4	Windows
5	Doors
6	Wall Cover (Cladding and Siding)
7	Roof-to-wall Connections
8	Roof and Wall Sheathing

This comparative analysis aims to assess the alignment between pre- and post-tornado assessments and identify any discrepancies or areas for improvement in vulnerability assessments. The collected survey data are subjected to both quantitative and qualitative analysis to derive meaningful insights and conclusions. Quantitative analysis uses statistical methods to

summarize and interpret numerical survey responses, such as frequency distributions, descriptive statistics, and inferential analyses.

Qualitative analysis, on the other hand, focuses on interpreting open-ended survey responses to identify recurring themes, patterns, and trends. Textual data are coded and categorized to facilitate systematic analysis and interpretation, allowing for qualitative insights and participant feedback extraction.

Within the scope of this research, descriptive analyses are used to determine the overall percentages of the responses relative to each variable. This is accomplished by using cross-tabulation, which involves grouping each of the variables shown in Table 3.1, tabulating these, and examining the relationship in tabulated data to show any potential association between these variables and the respondents' role in the industry.

Inferential statistics are also explored using the Chi-Square Test for Independence to examine the relationship between the respondents' current role in the industry and the categorical variables listed under the sections planning, condition assessments, and procedures & guidelines. The Chi-Square Test for Independence test determines relevant associations between the variables and whether these associations are statistically significant. The null hypothesis (H_0) assumes that the variables related to condition assessments are independent of the professionals' role in the industry. The alternative hypothesis (H_a) assumes a significant association between the variables. The significance level (α) is set at 0.05 (5%) in the research. A Chi-Square Test for Independence is conducted for each variable shown in Table 3.1 against the single variable of "current role in the industry." The formula for Chi-Square is as follows:

$$\chi^2_{df} = \sum \frac{(O_i - E_i)^2}{E_i} \quad (\text{Eq 3.1})$$

Where:

df = degrees of freedom = $(r - 1)(c - 1)$, where r is the number of rows, c is the number of columns, O is the observed cell frequencies, and E is the expected cell frequencies.

Cramer's V tests are also conducted to identify the strength of these associations between the variables in Table 3.1 under the condition assessment section and the industry's current role. The formula for Cramer's V is:

$$V = \sqrt{\frac{\chi^2}{(N) \min(r-1, c-1)}} \quad (\text{Eq 3.2})$$

Where χ^2 is the chi-square statistic for the cross-tabulation, N represents sample size, and $\min(r - 1, c - 1)$ indicates the number of rows or the number of columns in the contingency table, whichever is smaller.

According to Cohen (1988), a V between 0.1 and 0.3 indicates a weak association, a V between 0.4 and 0.5 points at a medium association, and a V greater than 0.5 indicates a strong association. To regulate for multiple comparisons and to lower the risk of Type I errors¹, the alpha significance level is adjusted using the Bonferroni correction post-hoc procedure to $0.05/[(\text{number of tests conducted})]$.

Some of the survey questions are single-answer selections. However, the survey also includes questions with multiple responses (select all that apply). In analyzing these types of questions, cross-tabulation allows us to investigate each of the responses separately. Recoding

¹ Rejecting the null hypothesis when it is actually true.

the response data to read zero (0) = no and one (1) = yes results in only responses coded as one (1) to be counted as an affirmative response. Therefore, the analysis provides the percentage of participants who answer with an affirmative response within each answer based on "select all that apply," giving a richer source of data to understand the respondents' answers better. All personal identifiers are removed in the analysis to safeguard the participants' privacy and anonymity.

3.1.5 Integration with Post-Tornado Surveys

The findings from the comparative analysis are integrated with post-event storm surveys conducted by the NWS to evaluate the effectiveness of FCAs in identifying vulnerable building components and informing resilience strategies. This analysis aims to determine if the building components being evaluated in FCAs align with those noted within damage surveys. By leveraging insights from both pre- and post-event storm surveys, this research seeks to enhance the understanding of building vulnerabilities and strengthen risk management practices in the face of extreme weather events.

3.2 Deterioration Prediction and Deterioration Rates

3.2.1 Introduction

In order to establish an effective strategic asset management plan that facilitates proactive maintenance and rehabilitation strategies, it is imperative to employ a reliable method for predicting the condition states of assets. Predicting deterioration allows asset owners to accurately forecast costs based on condition data gathered during inspections, ensuring predictability regarding the future condition of assets and the necessary intervention criteria and timing aligned with service level expectations. As discussed in Chapter 2 (Literature Review),

traditional deterministic approaches to deterioration prediction may not adequately capture the stochastic nature of degradation, especially when dealing with numerous buildings, elements, and factors influencing degradation trends. Deterioration prediction stands at the forefront of proactive building management and maintenance, offering valuable insights into built infrastructure's long-term performance and resilience. This section provides the methods used for deterioration prediction within this research. Deterioration prediction refers to the process of forecasting the degradation and aging of building materials and components over time.

In an era characterized by aging infrastructure, climate change, and evolving environmental stressors, and how that affects a building's ability to withstand extreme loading conditions, deterioration prediction plays a critical role in enhancing building resilience and sustainability. By understanding how materials degrade under different conditions and stressors and how that affects a building's ability to withstand extreme loading conditions, stakeholders can implement targeted interventions to prolong the lifespan of buildings, optimize resource allocation, and further promote the safety and well-being of inhabitants.

3.2.2 Deterioration Prediction Model

As described in the literature review section, this research adopts the stochastic approach of the Markov Chain process, utilizing discrete data sets to depict the degradation patterns of components in commercial and government buildings. Morcous et al. (2002) note that the Markov chain theory remains a widely employed method in numerous statistical models. The International Infrastructure Management Manual (IIMM, 2006) states that organizations need asset data that will indicate those assets are reaching the end of their useful life and will require further attention in the immediate future. It also suggests that assets are interconnected, thereby

affecting their aging process. In pursuing a comprehensive understanding of deterioration within building materials, this research leverages valuable insights obtained from a prior investigation.

Modeling the deterioration process involves probabilistic factors arising from the uncertainty of environmental influences on assets over their lifespan and the variability among individual assets. Therefore, simulating and forecasting this process within the context of stochastic models is preferable. However, validating and identifying parameters of a stochastic model rely on the accessibility and structure of data, whether from controlled experiments or field assessments (Zhang and Augenbroe, 2005). Madanat and Ibrahim (1995) state that “Markovian transition probabilities have been used extensively in the field of infrastructure management to provide forecasts of facility conditions.” This section provides a comprehensive explanation of this research's methodology employed in utilizing the Markov Chain Model, including the state transition process, model assumptions, and parameter estimation techniques.

3.2.3 Data Collection

The data utilized in predicting deterioration patterns is sourced from Hessam Mohseni’s (2017) research on the Markov process for deterioration modeling and asset management of buildings, a seminal work that documents the degradation of building components over time. The data utilized in this research stems from Mohseni’s (2017) rigorous research that employs the Markov Process to predict the deterioration of key building elements, including roofs, walls, windows, doors, services, and the entire superstructure. The research tracks the condition of buildings over a specified period and creates an abundant dataset.

While the data from Hessam Mohseni’s (2017) research provides a robust foundation for our predictive models, it is essential to acknowledge its strengths and limitations. The extensive

duration of the original study and the comprehensive nature of data collection contribute to the reliability of the deterioration patterns observed. However, it does not recognize potential constraints, such as the environment, and assumes that asset conditions stay the same or worsen (never better). Additionally, Mohseni's (2017) research considers an assumption or notion that the forthcoming condition of a facility is solely reliant on its present state and disregards its historical condition, which is regarded as unrealistic.

Building upon the insights gathered from the previous study, this research utilizes the discrete-time Markov Chain to extrapolate and refine deterioration predictions within the context of roofs, walls, doors, windows, wall cladding, and wall-to-roof connections. Integrating the data from Mohseni's (2017) study with the current research's methodologies allows us to draw upon established patterns with methods used to enrich our understanding of material responses over time. The research aims to enhance the precision and applicability of deterioration predictions, contributing to a complex understanding of material responses to environmental stressors.

3.2.4 Markov Process Application

At the core of the Markov Chain Model are state transitions, wherein the condition of a building component evolves over discrete time intervals based on probabilistic state changes. The model defines a finite set of condition states, each representing a distinct level of deterioration or degradation. Through the state transition process, the model captures the probability of transitioning between different condition states over successive periods, reflecting material degradation's dynamic nature.

The development of the Markov Chain Model entails several key assumptions that underpin its applicability and validity. These assumptions include:

- Stationarity: The probability of transitioning between condition-states remains constant over time.
- Markov Property: The future state of the building component depends solely on its current condition and is independent of previous states.
- Homogeneity: Transition probabilities are consistent across all building components and are unaffected by external factors or interventions.

By adhering to these assumptions, the Markov Chain Model provides a simplified yet effective framework for characterizing the deterioration process and projecting future condition states with a certain degree of reliability.

In deterioration modeling, the characteristics of a model undergo random fluctuations over time. A Markov chain is a probabilistic model featuring a finite state, depicting a specific stochastic process that progresses through discrete time points according to fixed probabilities (Sharabah et al., 2006). It employs a stationary stochastic matrix and utilizes an initial probability distribution matrix to define the deterioration process. The Markov matrix employed in this research is “right stochastic,” with vectors in a row summing up to 1, reflecting its stochastic nature as it evolves probabilistically and uncertainly over time. The probability of one random variable in a Markov process depends solely on the preceding variable in the sequence.

Consequently, future states are contingent solely on the present state, independent of any preceding state in a Markov chain. Each Markov chain comprises an initial distribution matrix derived from inspected condition data and a transition matrix containing finite sets of states represented in rows and columns $S (1,2,3...n)$ alongside probabilities P_{ij} for transitioning from state i to state j within a single time interval. This research uses a discrete-time Markov chain,

assuming discrete input data, including discrete time intervals and states (conditions). An example of such a matrix is shown below:

$$\begin{array}{ccc} P_q & C_1 & C_2 \\ C_1 & 0.4 & 0.3 \\ C_2 & 0 & 0.3 \end{array}$$

The characteristics of the Markov model utilized in the research are outlined below:

- A stationary (time-homogeneous) Markov chain has been employed based on the data accessibility within the research;

$$P(X_{n+1} = a \mid X_n = b) = P(X_n = a \mid X_{n-1} = b)$$

- A transition matrix that is right stochastic, depicted as an upper triangular matrix or a right triangular matrix, illustrating the deterioration trend;
- An irreversible Markov Chain is adopted to reflect the inherent deterioration characteristics and to distinguish the maintenance from degradation process;

$$P(X_{n+1} = a \mid X_n = b) \neq P(X_n = a \mid X_{n-1} = b)$$

The transition matrices have the absorbing condition state denoted as 5, characterized as the most severe state.

$$P_{55} = 1$$

$$P_{5j} = 0 \text{ for } j = 1, 2, 3 \& 4$$

In other words:

$$((X_n = i) \rightarrow S_i \text{ as } n \rightarrow \infty$$

The first step in using Markov Chain modeling involves assessing the condition of building elements (Sharabah et al., 2007). A standard rating scale is used, with 1 indicating the best condition and 5 indicating the worst, as illustrated in Table 3.3.

Table 3.3: Condition Rating Scale

Condition State	Component Condition	Condition Description
1	Very good	The element is as new
2	Good	The element is sound; minor damage and minor maintenance required
3	Moderate	Moderate damage; moderate maintenance required
4	Poor	Major damage; major maintenance required
5	Very poor	Very poor. Serious damage; element should be replaced

Although the deterioration process occurs continuously, for the sake of simplicity, these processes are represented over discrete time steps. The current condition inspection for buildings in Mohseni's (2017) research was conducted using a discrete data collection method. Hence, in the current research, a discrete-time Markov chain is considered a model for predicting the life cycle of building elements.

3.2.4.1 Discrete-Time Markov Chain

According to Sharabah et al. (2006), a discrete-time Markov Chain is a stochastic process with a finite number of states where random variables are observed at specific time intervals. When an element is in state "i," there exists a fixed probability, P_{ij} , of transitioning into state j after the next time step. P_{ij} is commonly referred to as the "transition probability." The matrix P , whose ij^{th} entry is P_{ij} , is known as the transition matrix. This matrix encompasses a finite set of

states represented by $S (1,2,3 \dots n)$ along with the probability P_{ij} of transitioning from state i to state j in one-time step t . In a Markov Chain, the transition probabilities P_{ij} must satisfy the following two conditions:

$$P_{ij} \geq 0,$$

$$\sum_j p_{ij} \leq 1$$

This implies that if a component is in state i , it is denoted as P_{ii} probability that the component will remain in state i and a probability of $(1 - P_{ii})$ probability that it will transition to the subsequent state j .

Current state at time t is i : $X_t = i$

Subsequent state at time $t + 1$ is:

$$j: X_{t+1} = j$$

The conditional probability statement of Markovian property:

$$\Pr\{X_{t+1} = j \mid X_0 = k_0, X_1 = k_1, \dots, X_t = i\} = \Pr\{X_{t+1} = j \mid X_t = i\}$$

Discrete-time means $t \in T = \{0, 1, 2, \dots\}$

Figure 2.5 in Chapter 2 displays a typical transition matrix using a condition rating system scale of 5 states, while Figure 3.1 below outlines the probability transition relationships depicted in the Markov transition matrix presented in Figure 2.5. The depiction of the probability of an element occupying a particular state at a specific time point can be illustrated using a series of curves, as will be shown in the subsequent chapter, Chapter 4.

p_{ij}	C.1	C.2	C.3	C.4	C.5
C.1	0.4	0.3	0.2	0.1	0
C.2	0	0.3	0.4	0.25	0.05
C.3	0	0	0.2	0.7	0.1
C.4	0	0	0	0.2	0.8
C.5	0	0	0	0	1

Figure 3.1: Transition Matrix

The Chapman-Kolmogorov theorem, relying on joint probability theory for its demonstration, describes the behavior of a Markov chain progressing over time. It is used to compute the probabilities of future states in a Markov chain, given the transition probabilities between states at each time step. It is a powerful tool for analyzing Markov chains' long-term behavior and properties, such as steady-state distributions and expected time to reach certain states. Employing a bivariate discrete distribution, as evident in the available data on building conditions, the Chapman-Kolmogorov equation implies the following for the transition matrix at the n^{th} -step transition matrix.

$$\mathbf{P}^{(n)} = \mathbf{P}^{(n)} \quad (\text{Eq 3.3a})$$

This results from:

$$\mathbf{P}_{ij}^{(a+b)} = \sum_{m \in S} \mathbf{P}_{im}^{(a)} \mathbf{P}_{mj}^{(b)} \quad (\text{Eq 3.3b})$$

$$\mathbf{P}_{ij}^{(n)} = \sum_{m \in S} \mathbf{P}_{ik}^{(m)} \mathbf{P}_{kj}^{(n-m)} \quad (\text{Eq 3.3c})$$

This equation essentially says that to transition from state i to state j in n steps, one can consider all possible intermediate states k and compute the probability of transitioning from i to k

in m steps and then from k to j in $n-m$ steps. In practical terms, the Chapman-Kolmogorov theorem is used to compute the probabilities of future states in a Markov chain, given the transition probabilities between states at each time step. It is a powerful tool for analyzing Markov chains' long-term behavior and properties, such as steady-state distributions and expected time to reach certain states (Sharabah et al., 2006).

For a Markov chain with a state space of S , formally, the Chapman-Kolmogorov theorem states that for a finite-state Markov chain with transition probabilities $P_{ij}(n)$, where i and j are states in the Markov chain, the n -step transition probability can be computed as the sum of all intermediate states m .

Sharabah (2007) introduced an initial distribution ' v ,' which is represented as a single-row matrix indicating the number of elements in each state. Following a single time step, the updated distribution is derived in a Markov chain by multiplying the initial distribution v by the transition matrix P .

The distribution after one step is expressed as vP . Subsequently, the distribution after another step, obtained by further multiplication by P , is calculated as $(vP)P = vP^2$.

Hence, the distribution after two steps is denoted as $= vP^2$

Similarly, the distribution after n steps can be obtained by vP^n , where P_n represents the n -step transition matrix. This implies that the ij^{th} entry in P^n signifies the probability of the system transitioning from state i to state j in n steps.

In certain industries, the transient probabilities of the Markov chain for deterioration prediction are adjusted using expert judgments. When there is insufficient data for calibration,

engineering judgment in defining Markov matrices serves as the best estimate for forecasting the future condition of an element. However, in scenarios where sets of inspection data are available, the calibration process involves determining the elements of the transition matrices through data sets and mathematical methods. In the research project conducted by Mohseni (2017), which involves six county councils as project partners, data collected by the councils were utilized to identify the elements of the transition matrices. Additionally, a regression-based optimization method is applied to the same data in this research project to calibrate the Markovian transition matrices. Since Mohseni's (2017) research project data had six county councils, the data collected by the councils is used to identify the transition matrices' elements. This research project utilizes a regression-based optimization method on the same data to calibrate the Markovian transition matrices.

3.2.4.2 Model Calibration Process

This research uses a regression-based optimization method on the same data to calibrate the Markovian transition matrices. As outlined in Chapter 2, Madanat et al. (1995) describe the regression-based optimization technique as employing a nonlinear optimization function. This function aims to minimize the total sum of absolute differences between the regression curve, which accurately fits the condition data, and the conditions projected by the Markov chain model adopted. The formulation of the objective function and constraints for this optimization problem is articulated as follows (Madanat et al., 1995):

Minimize

$$\sum_{n=1}^N |Y_n(t) - E(t_n, P)|$$

If $0 \leq P_{ij} \leq 1$ for $i, j = 1, 2, \dots, k$

$$\sum_{i=1}^k P_{ij} = 1 \quad (\text{Eq 3.4})$$

where

‘ N ’ is the total number of facilities;

‘ $Y_n(t)$ ’ is the expected condition of the structure ‘ n ’ at age ‘ t ’ using the regression model;

‘ P ’ is the transition probability matrix;

‘ P_{ij} ’ is the probability of transition from state ‘ i ’ to state ‘ j ’;

‘ $E(t_n, P)$ ’ is the expected condition of facility ‘ n ’ at age ‘ t ’

This is using the transition probability matrix ‘ P ’;

‘ k ’ is the maximum value for the condition rating.

3.2.4.3 Model Validation & Performance Evaluation of the Calibrated Model

Validation or evaluation of the performance of the deterioration models adjusted in this research concerns the alignment between the projected values and the actual observations. The projected values are obtained from the adjusted transition matrices using the Markov chain process. At the same time, the actual observations are independent values employed to examine disparities in the Markov model's predictions compared to an exact, known dataset.

As discussed earlier in this chapter, Mohseni's (2017) research used data retrieved between 2007, 2009, and 2011 inspections. These datasets are used to calibrate the Markovian deterioration models within this research. The datasets employed to derive the deterioration transition matrices, known as the training datasets, should not be utilized to calibrate (or train) the model in order to

assess it effectively. According to Tran (2007), a test dataset (observed data) is necessary for this purpose. There are two prevalent approaches to calibrate and validate models while ensuring the separation of training and testing datasets. One method involves randomly dividing the dataset into the calibration (training) and testing datasets. Alternatively, another approach, which may lead to a more realistic validation process, entails using an additional independent dataset. This research employs a 2018 inspection data set as the observed (or test) data set to validate the method.

3.2.4.3.1 Pearson's Chi-Squared Goodness-of-Fit test

According to Montgomery et al. (2004), two possible hypotheses are possible when testing for goodness-of-fit. The first type occurs when the population or probability distribution is understood, and the hypothesis concerns the parameters of that distribution. The second type of hypothesis, which is commonly encountered, arises when the underlying distribution of the population is unclear, and the aim is to assess whether a specific distribution is adequate as a population model. In this scenario, the probability distribution of building component conditions is unknown, and notably, the observed sample used to test the hypothesis may conform to an unknown probability distribution. To evaluate this latter hypothesis, Pearson's chi-squared test is utilized to validate the transition matrices developed for predicting building deterioration.

As the number of elements inspected in each building age group is inconsistent in the test inspection dataset, the number of elements inspected is adjusted to represent the proportion of elements in each condition. In other words, the *distribution* in each year group is considered for the validation process. The same data preparation process is conducted to eliminate outlier data from the test data set.

Pearson's chi-squared test evaluates the adequacy of a model to align with a set of observed data. This assessment, known as a goodness-of-fit test, is predicated on the null hypothesis that the observed frequency matches the predicted frequency (Micevski et al., 2002). Typically, this test requires a confidence level ranging from 90% to 95% for hypothesis acceptance (Montgomery et al. 2004). The chi-square distribution is utilized to determine whether a given dataset conforms to a specified theoretical probability model (Dowdy et al., 2011). Moeller (2012) advocates employing the chi-squared goodness-of-fit test in models where the failure distribution comprises a single parameter.

Montgomery et al. (2004) explain that the procedure necessitates a random sample of a certain sample from a population whose probability distribution is unknown. These observations are organized into a histogram with bins (Montgomery et al., 2004). The chi-square goodness-of-fit test procedure can be expressed as follows (Dowdy et al., 2011):

H_0 : Sample from distribution A

H_a : Sample not from distribution A

Significance level: α

Test Statistics:

$$X^2 = \sum_{i=1}^k \frac{(O_i - E_i)^2}{E_i} \quad (\text{Eq). 3.5}$$

Where;

O_i = Observed number of outcomes in category A_i (from the test data set 2011)

E_i = Expected number of outcomes

$W_i - nP(A_i)$ [from the Markov chain probabilities, calibrated from the training data set 2007 and 2009 (expected)].

$$n = \sum_{i=1}^k O_i \quad (\text{Eq). 3.6}$$

Region of rejection:

$$X^2 \geq X_{\alpha, v}^2$$

$$v = k - 1 - r \quad (\text{Eq). 3.7}$$

Where

v is the degrees of freedom,

k is the number of categories or groups being compared,

r is the number of estimated parameters in distribution 'A' estimated from the sample.

(r equals zero in this case)

The critical values depending on v and α are given in Figure 3.2.

Upper-tail critical values of chi-square distribution with ν degrees of freedom					
ν	Probability less than the critical value				
	0.90	0.95	0.975	0.99	0.999
1	2.706	3.841	5.024	6.635	10.828
2	4.605	5.991	7.378	9.210	13.816
3	6.251	7.815	9.348	11.345	16.266
4	7.779	9.488	11.143	13.277	18.467
5	9.236	11.070	12.833	15.086	20.515
6	10.645	12.592	14.449	16.812	22.458
7	12.017	14.067	16.013	18.475	24.322
8	13.362	15.507	17.535	20.090	26.125
9	14.684	16.919	19.023	21.666	27.877
10	15.987	18.307	20.483	23.209	29.588
11	17.275	19.675	21.920	24.725	31.264
12	18.549	21.026	23.337	26.217	32.910
13	19.812	22.362	24.736	27.688	34.528
14	21.064	23.685	26.119	29.141	36.123
15	22.307	24.996	27.488	30.578	37.697
16	23.542	26.296	28.845	32.000	39.252
17	24.769	27.587	30.191	33.409	40.790
18	25.989	28.869	31.526	34.805	42.312
19	27.204	30.144	32.852	36.191	43.820
20	28.412	31.410	34.170	37.566	45.315
21	29.615	32.671	35.479	38.932	46.797
22	30.813	33.924	36.781	40.289	48.268
23	32.007	35.172	38.076	41.638	49.728
24	33.196	36.415	39.364	42.980	51.179
25	34.382	37.652	40.646	44.314	52.620
26	35.563	38.885	41.923	45.642	54.052
27	36.741	40.113	43.195	46.963	55.476
28	37.916	41.337	44.461	48.278	56.892
29	39.087	42.557	45.722	49.588	58.301

Figure 3.2: Critical values of Chi-Square distribution for ν degrees (NIST 2012)

3.3 Summary

This section examines the methodology for predicting the deterioration patterns of key building components, including roofing, walls, windows, and doors, under various maintenance scenarios. The following section quantifies deterioration rates for the materials comprising these components. By analyzing deterioration rates, this research aims to develop comprehensive fragility curves that capture the vulnerability of building materials to tornado events. This

transition allows this research to aid in bridging the gap between theoretical predictions and practical considerations. By comparing these trends to real-world data and stakeholder priorities, we can enhance our understanding of building vulnerabilities and inform targeted mitigation strategies to bolster resilience against extreme weather events.

3.4 Deterioration Rates

3.4.1 Introduction

This research now explores the methodology for determining deterioration rates. This step delves deeper into the quantitative assessment of material degradation over time, laying the groundwork for developing robust fragility curves.

To model the time-dependent deterioration rates for poorly, averagely, satisfactorily, and excellently maintained buildings, the research utilizes a methodology based on the concept of building materials' service life and degradation processes. The deterioration rates are determined using established formulae derived from the literature and adapted to suit the specific maintenance conditions of the materials under study. Although time-dependent deterioration rates for all condition states are modeled, it is essential to note that this research focuses on buildings that are at the end of their useful lives and are, therefore, poorly maintained. This also allows for further discussion regarding the importance of standardizing the decommissioning of buildings.

3.4.2 Materials Selection for Commercial and Government Buildings

The selection of building materials and components plays a crucial role in developing fragility curves since different materials have different strengths and resistive capacities. This section provides an overview of the materials selected for inclusion in fragility curves for this

research, highlighting their properties, vulnerabilities, and implications for structural resilience and risk assessment.

The materials included in fragility curves represent various building components commonly found in commercial and government structures. These may include:

- Roofing materials: Asphalt shingles, clay tiles, metal roofing
- Structural elements: Wood frame, reinforced concrete, steel frame
- Exterior cladding: Brick, stone, stucco, aluminum siding
- Doors and windows: Wood, steel, aluminum, fiberglass

The selection of building materials plays a pivotal role in determining commercial and government buildings' performance, durability, and resilience. This section provides an overview of the materials selected for key building components, highlighting their suitability, advantages, and considerations within the context of building management and resilience.

Roofing Materials:

Asphalt and clay tiles are commonly used for roofing in commercial and government buildings due to their durability, weather resistance, and aesthetic appeal. Asphalt shingles offer cost-effectiveness and ease of installation, making them a popular choice for a wide range of building types. Clay tiles provide superior thermal insulation, longevity, and architectural charm, particularly suitable for buildings with historical or aesthetic considerations (Barbhuiya & Das, 2023; Zhang & Braun, 2023)

Structural Wall Materials:

Wood frames and concrete masonry units (CMUs) are prevalent choices for structural walls in commercial and government buildings, each offering unique advantages and considerations. Wood frame construction provides flexibility, affordability, and energy efficiency, making it suitable for various building applications. CMUs provide durability, fire resistance, and sound insulation properties, making them ideal for high-traffic areas or buildings requiring enhanced structural integrity (Mattinzioli & Jiménez del Barco, 2022; Zhang & Braun, 2023).

Exterior Siding Materials:

Brick-facing and aluminum siding are commonly used for exterior cladding in commercial and government buildings, providing protection against the elements and enhancing the building's aesthetic appeal. Brick-facing offers durability, weather resistance, and timeless aesthetics, suitable for facilities seeking a traditional or historic appearance. Aluminum siding provides lightweight, low-maintenance, and customizable options, allowing for modern design, flexibility, and sustainability (Mattinzioli & Jiménez del Barco, 2022; Zhang & Braun, 2023).

Doors and Window Materials:

Wood is often selected for doors in commercial and government buildings due to its natural beauty, versatility, and insulation properties. Metal casement windows and steel doors offer durability, security, and energy efficiency, providing ample natural light and ventilation while enhancing the building's aesthetics and functionality (Mattinzioli & Jiménez del Barco, 2022).

3.4.3 Data Collection

Service life data for various building materials, components, and fasteners are obtained from reputable sources, including the preventative maintenance guidebook by Schoen (2010) and data provided by the Building Owners and Managers Association. This data includes information on the average useful life of materials used in constructing and manufacturing roofs, walls, doors, windows, 16d toenails, and H2.5 hurricane clips.

A building component model is defined to determine the necessary major repairs and component replacements in a building and to justify the timing of that work to optimize the savings per repair dollar invested. This model is constructed by creating an inventory of components that comprise the building as influenced by the building component model. The inventory of building components categorizes the facility into primary building systems, subsequently delineating the individual components constituting those systems. This classification is based on the ASTM Unifomat II hierarchy (ASTM E 1557-02). Each component within the building model is equipped with designated characteristics determined by its material, type, age, and position. For instance, a window (component) could be constructed from metal, vinyl, or wood. These various material types exhibit diverse reactions to environmental factors over time, possess distinct anticipated service lifespans, and necessitate varied maintenance actions at different stages of their lifecycle. Consequently, the building component and its corresponding attribute data serve as the fundamental unit for building lifecycle asset management and condition monitoring. Table 3.4 shows a subset of the building components.

Table 3.4: Building Component Inventory

System	Component	Material	Service Life (yr.)
Structural	Walls	Wood Frame	100
Structural	Walls	Concrete	100
Structural	Roof Cover	Clay tiles/Metal	75
Roofing	Roof Cover	Asphalt	50
Exterior	Walls	Concrete Block	50
Exterior	Walls	Aluminium Siding	50
Exterior	Walls	Brick Facing	100
Exterior	Doors	Wood	40
Exterior	Windows and Glazed Walls	Metal Casement	40

Hurricane straps and clips (shown in Figure 3.3) exhibit remarkable longevity, often enduring for the entire lifespan of a building due to their construction from steel. Steel's inherent durability and reasonable corrosion resistance due to anti-corrosion coating render hurricane straps and clips ideal for regions susceptible to high winds and frequent storms. These structural elements significantly bolster a building's structural resilience by withstanding winds and seismic forces, thereby becoming indispensable requirements in areas prone to hurricanes, extreme storms, and earthquakes. In contrast, toenails, consisting of diagonal nails driven through the side of the roof truss into the top of the wall plate, are common in older homes but offer comparatively limited wind resistance for the roof.

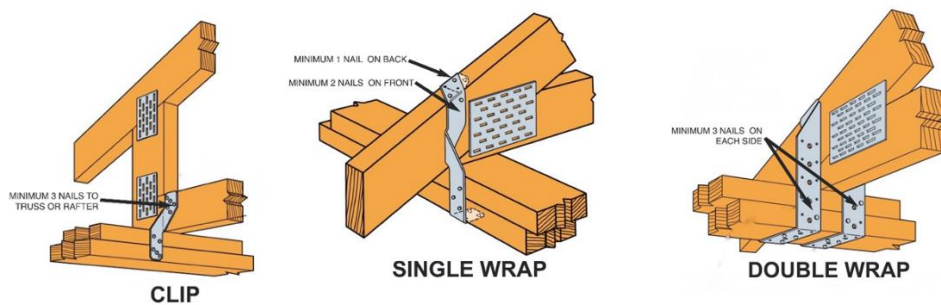


Figure 3.3: Hurricane clips

It is essential to define what we mean by service life. The Home Quality Mark one, Technical Manual SD239, England, Scotland & Wales, published in 2018, defines “service life” as: “The period after installation during which a building, or its part, meets or exceeds the performance requirements” (BRE, 2018)

3.4.4 Formulation of Deterioration Models

Four deterioration models are developed using the acquired service lives to represent different maintenance conditions, ranging from poor to excellent maintenance practices. The formulas used to calculate deterioration rates are as follows:

Table 3.5: Deterioration Models

Formula to determine deterioration	
Traditional (poor maintenance of building)	$Z = \frac{t}{T}$
Unger (average maintenance)	$Z = \frac{t \cdot (t + T)}{2T^2}$
Romstrofen (satisfactory maintenance)	$Z = \frac{t \cdot (2t + T)}{3T^2}$
Eytelwein (excellent maintenance)	$Z = \frac{t^2}{T^2}$

Where:

Z = Deterioration rate or degree

t = Current stage of service life (years)

T = Service life (years)

While the models are developed to represent a range of maintenance conditions, this research focuses on commercial and government buildings that have reached the end of their service life and may have been left unattended for a long time. Therefore, the deterioration rates corresponding to poorly maintained facilities are selected for further analysis and integration into the fragility function framework. The model formulation is based on the concept that the degree of deterioration in a building component is proportional to the ratio of its current stage of service life to its total service life. As the building component ages and approaches the end of its service life, the deterioration rate increases, reflecting the cumulative effects of environmental factors, wear and tear, and maintenance neglect. Interpretation of the model equation suggests that the deterioration rate Z is directly influenced by the ratio of t to T , with higher values indicating a more advanced stage of deterioration relative to the total service life of the building component. The research uses the average maintenance model, which utilizes a quadratic equation to estimate the rate of deterioration over time, with the rate increasing as the material approaches the end of its service life, to validate the results of the poor maintenance model.

The selected deterioration rates are incorporated into the modeling failure of structural components using fragilities models to quantify the vulnerability of building components under tornado loading conditions. By considering the effects of material degradation over time, the determined fragility functions provide insights into the structural resilience of abandoned commercial buildings. It informs risk management strategies for mitigating the impacts of extreme weather events.

The methodology for modeling deterioration rates is based on several key assumptions:

1. The model assumes a linear relationship between the current stage of service life and the degree of deterioration, with deterioration occurring constantly over time.
2. The model assumes uniform deterioration across the building component, neglecting variations in deterioration rates due to localized factors or environmental conditions.
3. The model focuses solely on the underlying deterioration of poorly maintained buildings, neglecting the potential effects of maintenance interventions or repairs on the rate of deterioration.

It is, therefore, for this reason that validation using deterioration rates for buildings with average maintenance is incorporated into the analysis.

3.5 Summary

This section outlines the methodology for quantifying deterioration rates of building materials, a critical step in developing robust time-dependent fragility curves. Leveraging a simple linear model, $Z = t/T$, the research systematically examines the factors influencing material degradation over time. This approach encompassed thorough materials selection and comprehensive data collection to ensure the accuracy and reliability of the deterioration models.

3.6 Building Materials Fragilities

3.6.1 Introduction

The strength of buildings or any structural system's components is generally a time-dependent property that may decrease resistance along the structure's, components, and materials' service life. Fragility parameters are required at different times throughout the service life to assess and forecast the susceptibility of deteriorating buildings consistently. Tractable functions for time-dependent fragility models provide an efficient way to achieve this by

adopting curve-fitting methods regarding parameters as a variable of time. For example, Shafieezadeh et al. (2014), in introducing seismic fragilities, illustrate the effect of corrosion in bridges at five different points in time; the median Peak Ground Acceleration (PGA) and dispersion of the lognormal fragility curves for each damage state are assessed for a case study bridge at a total of 10 different temporal designations along its service life. Analytical functions are evaluated to represent the change in median and dispersion values in time due to corrosion. Such time-dependent models have a notable advantage in that they allow for the estimation of fragility parameters at any given point for the bridge and corrosion parameters without the necessity of conducting full fragility analyses each time.

In other words, instead of repeatedly performing comprehensive analyses to determine the fragility parameters of the bridge and corrosion over time, time-dependent models provide a mechanism to predict these parameters at any specific time. This capability streamlines the process and saves computational resources, as researchers can input the relevant data into the time-dependent model to obtain the desired fragility parameters without requiring extensive reanalysis.

To provide a mechanism to generalize results, 1-story commercial buildings are used as baseline structures. This research looks into time-dependent fragility curves of materials used in the construction of roofs, walls, windows, wall cladding, doors, steel roof joists, and roof-to-wall connections at a total of 5 different points in time along the materials' service life. These materials are asphalt shingles, clay tiles, steel roof joists, concrete blocks, metal casement windows (excluding glass), timber windows, steel doors, aluminum doors, steel in 16d toenails, one H2.5 clip, and two H2.5 clips. Each of these materials offers a unique structural resistance.

Analytical functions are evaluated to depict alterations in median and dispersion values of their resistive capacity over time as a result of deterioration.

Masoomi and Van de Lindt (2016) outlined a possible topology of community components in their study for non-deteriorating (pristine) buildings. The dependencies among components and the component properties required for subsequent damage simulations under a specified hazard assigned to each component in their model. A subsequent analysis, using the calculated fragility functions, examined the performance of community components under simulated tornado conditions. A set of tornado fragility curves corresponding to four prescribed damage states was developed: damage states 1, 2, 3, and 4. For roof covering, fragility curves are developed for three limit states. Memari et al. (2018) highlighted that damage to roof covering does not affect Damage State 4 because it is assumed that more than 50% of the roof covering would fail under the force of tornadic wind loads capable of inflicting this degree of damage, as highlighted in Table 3.6.

Table 3.6: Damage states for commercial building Memari et al. (2018)

DS	Roof covering	Window/door	Exterior wall	Garage door	Roof Structure
1	>2% and ≤15% ^a	1 or 2 ^a	>2% and ≤25% ^a	No	No
2	>15% and ≤50% ^a	>1 or 2 and ≤25% ^a	>25% and ≤50% ^a	Yes ^a	No
3	>50% ^a	>25% ^a	>50% and ≤75% ^a	Typically Yes ^a	No
4	Typically >50% ^a	Typically >25% ^a	>75% ^a	Typically Yes ^a	Yes ^a

^aDamage states are defined according to the occurrence of any damage indicators in a given row.

3.6.2 Tornado fragility curves methodology and intensity measures

In the perspective of performance-based engineering, a probabilistic analysis of structural components and systems subjected to hazard – e.g., tornado or hurricane – provides a means by

which uncertainty in performance and reliability of structures can be evaluated. In order to conduct such an analysis, a set of limit states that denote a specified level of performance for the structural components and systems must be identified. For tornadic modeling failure of structural components using fragilities, the limit state function, $g(X)$, for a component is written as:

$$g(X) = R - (W - D) \quad (\text{Eq 3.8})$$

where X = vector of uncertain variables that explain the limit state condition; W = tornado-induced wind load; R = resistance of structural components; and D = resistive dead load.

Therefore, a component failure can be defined as $g(X) < 0$.

To create tornado fragility curves, the probability of exceeding a specified limit state for a given intensity measure (IM) of the hazard can be calculated as follows:

$$F_r(x) = P[g(X) < 0 | IM = x] \quad (\text{Eq 3.9})$$

Fragility curves are a common element in natural hazard damage modeling. These functions account for uncertainties in load calculation and resistance estimation. Various limit states are considered for different building components to develop fragility curves, each contributing to the formation of a damage state (DS) for the building. At the component level, a fragility curve is defined as the conditional probability of surpassing a limit state (LS) based on a specific demand parameter under a given hazard intensity. Mathematically, this can be expressed as follows (Ellingwood et al., 2004):

$$Fr(V) = P[LS \geq ls_i | X = x]$$

For ease of use and typically achieving a strong statistical fit, a fragility curve can be represented by fitting a cumulative distribution function (CDF) of the lognormal distribution.

The fragility curves are developed utilizing Monte Carlo Simulation as follows:

$$Fr(V) = \Phi\left[\frac{\ln(x) - \lambda_R}{\xi_R}\right] \quad (\text{Eq. 3.10})$$

where x = given intensity measure defined as 3-s gust wind speed (m/s or mph) for tornado fragility function;

$\Phi [^*]$ = standard normal cumulative distribution function;

λ_R = logarithmic median of capacity; and

ξ_R = logarithmic standard deviation of capacity.

Fragility curves for pristine buildings are plotted using Eq. (3.10), where the horizontal axis shows the intensity measure and the vertical one shows the conditional probability.

As mentioned earlier, the research performed herein borrows heavily from a study by (Ghosh and Padgett, 2017) on time-dependent seismic fragilities. Subsequently, based on work by the authors, time-dependent material level fragilities for this research are analyzed as follows:

$$F_{r,m(t)} = \Phi\left[\frac{\ln(x) - \ln[\lambda_m(t)]}{\xi_m(t)}\right] \quad (\text{Eq. 3.11})$$

where,

$\lambda_m(t)$ and $\xi_m(t)$ are the time-dependent median and dispersion parameters of the lognormal distribution representing the fragility $Pf, m(t)$ of the m^{th} material.

The research generates a set of $N = 1,000$ random resistances and wind loads (demand) for the materials of components that contribute to lateral and uplift resistance of the building under tornado-induced pressure, MWFRS, and C&C components. The research begins by selecting the material under examination, which defines the limit state function. Next, both demand and capacity are estimated. Here, 'n' represents the different wind speeds associated with the demand, while 'm' denotes the number of Monte Carlo simulations conducted.

Subsequently, a size $n \times m$ matrix is created to represent demand and capacity. The demand is determined by converting 143 different wind speeds (from 57 mph to 200 mph) from the EF-scale into pressures (loads), which are then used to calculate the demand placed on the selected materials. Meanwhile, resistive capacity is determined by considering the materials' dead load and uplift resistive capacity. The MCS considers 1000 trials to generate the $n \times m$ matrix, where 'n' is equal to 1000 and 'm' is equal to 143. This matrix serves to calculate the capacity of the materials.

The limit state function is then evaluated using Eq (3-1). The demand comprises wind pressure and forces acting as uplift forces on the MWFRS and C&C (Yang et al., 2013), which may occur in multiple directions. Random variables, such as dead load and uplift capacity, are defined based on probability distributions and assigned to each trial (i.e., 1000 random variables per trial). Once the random variables are generated, they are incorporated into the limit state equation alongside the wind pressures used for these models. This procedure is repeated for the duration of MCS, and a probability paper plot is applied to the fragility parameters (i.e., ζ and λ values). The residual R^2 is also calculated to examine how many data points surround the line of best fit, accounting for the accuracy of the data to validate the fragility parameters.

$$\ln(x_i) = \xi S_i + \lambda \quad (\text{Eq. 3.12})$$

where;

ξ represents the slope and

λ represents the intercept

High R^2 values indicate that the lognormal distribution best fits the MCS. Thus, the presented fragility models can be described using a lognormal distribution with ζ and λ .

The fragility curves developed using this model are for materials in pristine buildings and are the first step in creating fragility curves. In the second stage of the process, this research incorporates time-dependent deterioration rates for 0 – 50 years of age in 10-year intervals to structural resistive capacity parameters and then recreates the fragility curves. The format of time-dependent functions presented herein emulates those that Ghosh and Padgett (2010) presented. This approach offers an efficient method to capture the effect of aging and deterioration on bridge systems and is transferable to buildings and other structures.

The procedure for creating each fragility curve using Monte Carlo simulation (MCS) in this research is presented in flow chart form in Figure 3.5 below:

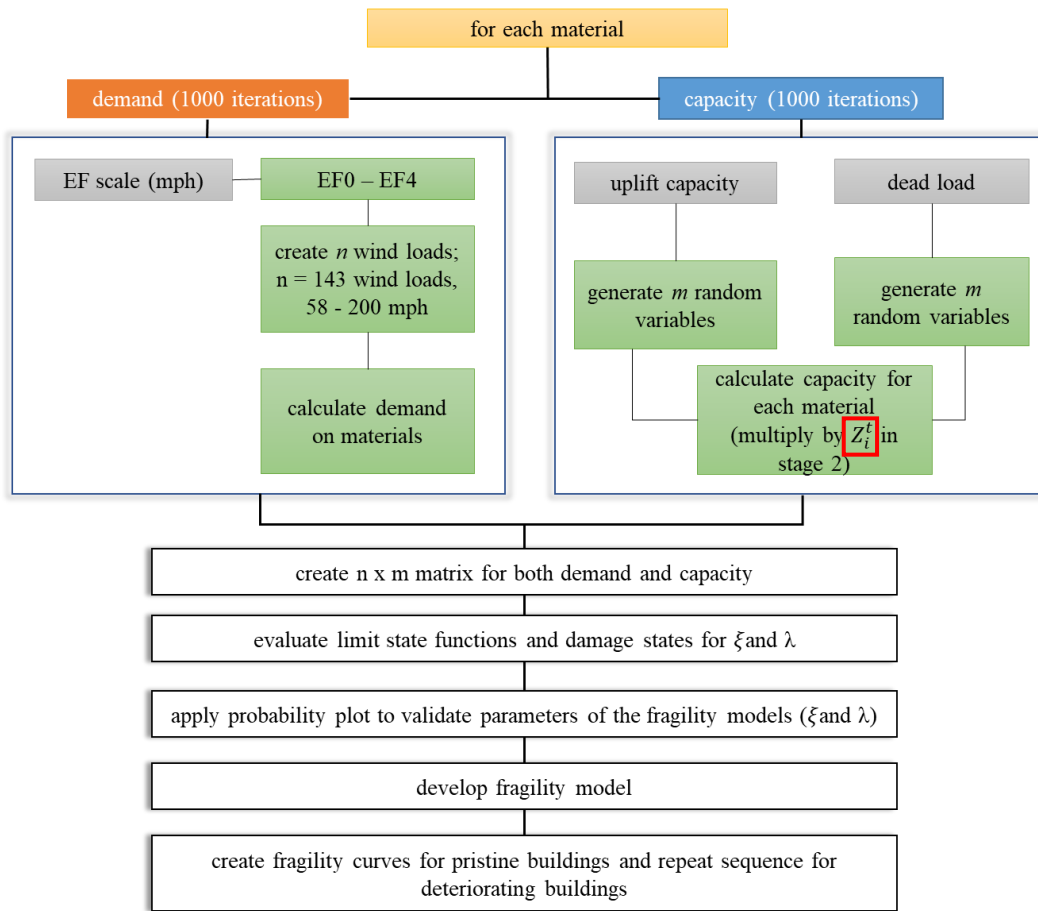


Figure 3.4: Flowchart for Developing Time-dependent Fragility Curves

*It is acknowledged that loads may differ from one side of the building at a point in time for larger buildings. However, the spatial effect across the building is neglected since the peak load from a 3-sec gust wind speed, i.e., a static analysis, is used.

3.6.2.1 Tornado Load Characterization

The methodology (Masoomi and van de Lindt 2016) adopted in this research to model tornado-induced wind loading is built on the ASCE 7 (2010, 2016) building code and the more current ASCE 7-22 (2022) methodology for both straight-line and tornado wind loading conditions. The use of tornado-specific wind loads, which are characteristically different from straight-line winds, is introduced into the ASCE 7 code as of 2022. This method adjusts the aerodynamic pressure coefficients by incorporating a tornado pressure adjustment factor. This

factor accommodates the atmospheric pressure deficit resulting from the vortex structure of the tornado, albeit without directly modeling the pressure deficit. Considering that the maximum wind speed can occur in any direction during a tornado and may result in the maximum pressure coefficient on buildings (Prevatt et al., 2013; FEMA, 2015), a conservative directional factor equal to 1.0 is selected. Although the ground surface roughness and the fetch length of the surrounding terrain may affect the tornado-induced loads (Sabareesh et al., 2013; Liu and Ishihara, 2016), Exposure C of the exposure categories in ASCE 7 (ASCE 2022) is considered in all analyses of this research, which is defined as “open terrain with scattered obstructions having heights generally less than 30 feet”.

Velocity pressure at height z , q_z , for straight-line wind is calculated as follows:

$$q_z = 0.613K_zK_{zt}K_dV^2(N/m^2) \text{ for } V \text{ in mph} \quad (\text{Eq. 3.13a})$$

$$q_z = 0.00256K_zK_{zt}K_dV^2(lb/ft^2) \text{ for } V \text{ in mph} \quad (\text{Eq. 3.13b})$$

where K_z = velocity pressure exposure coefficient; K_{zt} = topographic factor; K_d = wind directionality factor; and V = 3-sec gust wind speed. The velocity pressure at mean roof height h , q_z , is also calculated by Eq. (7). The wind pressure for the main wind force resisting system (MWFRS) is then determined using

$$p = qGC_p - q_i(GC_{pi}) \quad (\text{Eq. 3.14})$$

where q and q_i = velocity pressure calculated at height z or h ; G = gust effect factor, C_p = external pressure coefficient; and GC_{pi} = internal pressure coefficient. The wind pressure for components and claddings (C&C) is calculated as follows:

$$p = q_z[GC_p - (GC_{pi})] \quad (\text{Eq. 3.15})$$

where all variables are as defined previously.

This research implements the approach consistent with Memari et al. (2018) and Gill et al. (2021) to determine the tornado-induced pressure. The research then uses coefficients defined by ASCE/SEI 7-22 for tornado external pressure adjustment coefficients of 1.8 – 3.2 and 1.4 – 2.4. For internal pressure, adjustments for MWFRS and C&C are considered zero (i.e., no adjustment is needed). In this case, the tornado internal pressure adjustment for MWFRS is recommended as 1.0, whereas it is zero for C&C.

The tornado-induced pressure is then calculated as follows:

$$p = q_z [T_e(GC_p) - T_i(GC_{pi})] \quad (\text{Eq. 3.16})$$

Table 3.6 summarizes both T_e and T_i coefficients for MWFRS and C&C according to this approach. Tables 3.7 and 3.8 summarize statistics for wind pressure parameters per Eq. (3.16). The GC_p coefficient for roof covering varies depending on the roof angle and varies across different buildings. A normal distribution is applied to all variables.

Table 3.7: Tornado Pressure Adjustments (Adapted from ASCE 7-22, 2022)

Parameters Description				Parameter
Tornado Pressure Adjustment	Uplift Pressure	MWFRS	T_e	1.8 – 3.2
			T_i	0.0
	Lateral Pressure	C&C	T_e	1.4 – 2.4
			T_i	0.0
		MWFRS	T_e	1.0 – 1.5
			T_i	1.0
		C&C	T_e	1.2 – 2.0
			T_i	0.0

Table 3.8: Wind Load Statistics (Adapted from ASCE 7-22, 2022)

Wind Load Parameters	Parameter Description	Statistical Parameters		
		Mean	COV	Distribution
K_h	0 – 49.2 m	0.82	0.14	Normal
	65.6 m	0.84		
	82.0 m	0.88		
	98.4 m	0.94		
	131.2 m	1.00		
Gust-effect factor (G)	-	0.82	0.10	Normal
Internal pressure coefficient (GC_{pi})	Enclosed Buildings	± 0.15	0.33	Normal
	Partially Enclosed Buildings	± 0.46		
External pressure coefficient (C_p)	Wall	0.69	0.15	Normal
	Roof	-0.81		
External pressure coefficients (GC_p) – Approach A	Door and window	-0.68	0.12	
	Roof Cover – Zone 1	-0.95		
	Roof Cover – Zone 2	-1.71		
	Roof Cover – Zone 3	-2.66		
	Roof Deck – Zone 1	-0.90		
	Roof Deck – Zone 2	-1.24		
	Roof Deck – Zone 3	-1.52		
	Roof Joist – Zone 1	-0.86		
	Roof Joist – Zone 2	-1.05		
	Roof Joist – Zone 3	-1.05		

3.6.2.2 Resistance Characterization

Resistance data for all materials are gathered from currently available experimental results in the literature pertaining to wind loading. Table 3.9 shows all resistance data collected for components and materials contributing to the performance of buildings subjected to tornado hazards pertinent to this research.

Table 3.9: Component and Materials Structural Resistance Data

Component	Mean (kPa)	Mean (kN)	Coefficient of variance	Associated buildings	Reference
Asphalt shingles	0.10		0.10	Residential	Unnikrishnan and Barbato (2016)
Clay tiles dead load	0.96		0.10	Residential	Unnikrishnan and Barbato (2016)
Roof panel dead load	0.17		0.10	Residential	
Concrete block, side		19.00	0.20	Applicable for: fire station, strip mall	
Concrete block, gable		8.50	0.20	Applicable for: fire station, strip mall	
Bolted (steel joist to steel connection)		2,180	0.20	Light industrial	Average from Swanson and Leon (2000) (coefficient of variance assumed)
Anchors (steel joist to masonry wall)		112	0.25	Heavy industrial, shopping center	Average from Cook and Klinger (1992) (coefficient of variance assumed)
Metal deck clips	0.094		0.40	Fire station, light industrial, heavy industrial, shopping center, strip malls	Farquhar et al. (2005)
Roof-to-wall connection - two 16d toe nails		1.83	0.16	Residential	van de Lindt et al. (2013)
Roof-to-wall connection dead load	0.717		0.10	Residential	Ellingwood et al. (2004)
Roof-to-wall connection - two H2.5 clips		11.68	0.12	Residential	Reed et al. (1997)
Roof-to-wall connection - One H2.5 clip		5.84	0.12	Residential	Reed et al. (1997)
Steel roof joists	2.40		0.01	Light industrial (~16K2 steel joist)	
	8.40		0.05	Heavy industrial, shopping center (~26K5 steel joist)	
Walls					
Brick (solid MC)	501		0.31	Fire station	Kim and Bennet (2002)
Masonry (solid PCL)	1,564		0.30	Office strip malls, office	
Aluminum siding		0.91	0.38	Light industrial	Calculated average of all results for flat sheathing (Jacob 1952)
Note: MC = masonry cement; PCL = Portland cement/lime.					

3.6.2.3 Building Damage States

Four damage states (DS), namely light, moderate, extensive, and complete, are defined for each archetype building. Table 3.10 depicts the physical description of each damage state. These damage states describe the performance of physical damage sustained by the building envelope, roof structure, and exterior walls.

Table 3.10: Quantitative guidelines for assigning overall wind damage rating. Source: VAST Handbook: DE/QC - US Windstorm Building Resilience through Reconnaissance

DS identifier	DS Description	Physical damage description	LS description
1	Slight structural damage	Moderate roof cover loss that can be covered with a tarp to prevent additional water from entering the building.	Roof or wall cover failure: >2 and $\leq 15\%$; door failure: 1; roof deck or wall substrate failure: none; roof joist or wall substrate failure: none; wall failure: none.
2	Moderate structural damage	Major roof cover damage with a maximum of two roof deck and one door failure.	Roof cover failure: $\geq 15\%$ and $< 50\%$; window or door failure: >1 and \leq the larger of 3 and 20%; roof deck or wall substrate failure: 1 to 3 panels; roof joist failure: none; wall failure: none.
3	Extensive structural damage	Not able to be occupied, but repairable. Major loss of roof deck panels or joists as well more than one door broken door. Roof cover failure is certain and does not contribute in DS 3.	Roof cover failure: $< 50\%$; window or door failure: $>$ the larger of 3 and 20% and $\leq 50\%$; roof deck or wall substrate failure: > 3 and $\leq 25\%$; roof joist failure: $\leq 15\%$; wall failure: none.
4	Complete structural damage	Not able to be occupied and not repairable. Extensive roof system failure and some tilt-up wall failure. Roof cover and door failures are certain and do not contribute in DS 4.	Roof cover failure: $< 50\%$; window or door failure: $> 50\%$; roof deck or wall substrate failure: $>$; roof joist failure: $> 15\%$; wall failure: Yes.

If any damage state descriptions in a given row of Table 3.10 occur, the building or structure is considered to be in that damage state. For example, for a building to be deemed to have sustained Damage State 4 (Destroyed), the building must have sustained either roof structural or load-bearing wall failure. It's important to note that in damage state 4, the first three damage indicators usually manifest, indicating that damage state 4 is solely contingent upon roof cover failure and load-bearing wall failure.

Notably, fragility curves incorporating deterioration rates are subject to assumptions and uncertainties related to material properties, degradation mechanisms, and hazard interactions, which may influence model predictions and decision-making processes.

3.6.2.4 Probability of Exceedance – Average Percent Change

The research utilizes the concept of "average percent change" in the probability of exceedance to assess the relative shift in vulnerability between pristine (non-deteriorated) and deteriorated building materials. This metric serves as a vital indicator of how a building material's vulnerability is affected by varying maintenance levels.

The average percent change represents the relative difference in the probability of exceedance between two conditions. Specifically, it quantifies the magnitude of change in vulnerability or risk when transitioning from pristine maintenance conditions to poor maintenance conditions. The percent change in probability of exceedance would be calculated as follows:

$$\text{Average \% change} = \frac{\text{Probability of Exceedance (deteriorated)} - \text{Probability of Exceedance (pristine)}}{\text{Average Probability of Exceedance (pristine)}} \times 100$$

A positive percent change indicates an increase in vulnerability for deteriorated building materials compared to pristine building materials. Conversely, a negative percent change would indicate a decrease in vulnerability for deteriorated building materials, suggesting that the building materials exhibit greater resilience despite deterioration. Understanding the percent change in probability of exceedance is crucial for assessing the impact of deterioration on building vulnerability. Understanding the percent change in probability of exceedance is vital for assessing the impact of maintenance practices on building vulnerability.

3.7 Summary

In summary, data for FCAs is obtained from a broader survey conducted in 2022 regarding decommissioning practices in commercial buildings. The survey instrument is designed to gather comprehensive information on the condition of building components, maintenance priorities, and decision-making processes related to decommissioning. Comparative analysis assesses the alignment between pre- and post-event storm surveys, utilizing results from the 2022 survey and NWS post-event storm survey guidance.

From here, time-dependent deterioration rates are determined for poorly maintained buildings using established formulas derived from the literature, which are utilized to create fragility functions. Service life data for building materials and components are obtained from reputable sources, including the preventative maintenance guidebook by Schoen (2010) and data provided by the Building Owners and Managers Association. Four deterioration models are developed to represent different maintenance conditions, ranging from poor to excellent maintenance practices. Deterioration rates corresponding to poorly maintained buildings of

particular interest are selected for further analysis and integration into the modeling failure of structural components using a fragilities framework.

The selected deterioration rates are then incorporated into the fragility function models to quantify the vulnerability of building components under tornado loading conditions. Fragility curves are developed to quantify the probability of structural failure under tornado loading for pristine buildings and incorporate deterioration rates for various building materials. The comparative analysis assesses shifts in material tornadic fragilities between deteriorating and non-deteriorating (pristine) buildings (Research Question 2). Since NWS provides guidance on degrees of damage for building components for field survey teams, post-event, the fragility curves developed herein may highlight how building (facility) condition contributes to the ultimate determination of a tornado's EF ranking (Research Question 3).

CHAPTER 4: RESULTS AND DISCUSSION

This chapter presents the results of this research into the impact of material deterioration on building fragilities under tornadic events and discusses how these results may influence (1) FCAs, and (2) the determination of a tornado's EF ranking. This research addresses the research questions by comprehensively analyzing facility condition assessments (FCAs), deterioration prediction models, deterioration rates, and building fragilities. This research begins by examining the alignment between the priorities identified during FCAs conducted by facility managers and the post-event storm surveys. The predicted deterioration patterns of building components are addressed, followed by the development of deterioration rates for various construction materials. These findings set the stage for evaluating time-dependent fragility curves, comparing pristine and deteriorated building conditions, and discussing how building usage may ultimately impact EF ranking of a tornadic event.

4.1 Facility Condition Assessment

This section discusses results regarding the priorities identified during FCAs and their alignment with post-event storm surveys. The methodology involves surveying built environment professionals to gain insights into the components prioritized during FCAs.

Through analysis of survey responses, the research sought to answer Research Question 1: "During facility condition assessments (FCAs), are building managers prioritizing the same components as those conducting post-event storm surveys?" These findings show that while FCAs and post-event storm surveys equally value roofs and windows, there is a discrepancy regarding the importance of walls and doors. The following sections present and discuss the results that lead to this conclusion.

4.1.1 Respondents and Characteristics

A total of 881 respondents completed the questionnaire, with 720 respondents meeting the required criteria of currently working with commercial and government buildings for this research. The respondents represent 48 U.S. states, the District of Columbia, and Puerto Rico ($n = 438$, 85%), four Canadian provinces ($N = 13$, 3%), and 33 other countries ($N = 26$, 3%). These survey demographics are shown in Figure 4.1. Of note, 205 respondents did not indicate the country they worked in, but those respondents still completed the survey. Survey participants are members of IFMA and AIA with positions in facility management, architecture, engineering, construction management, or project management.

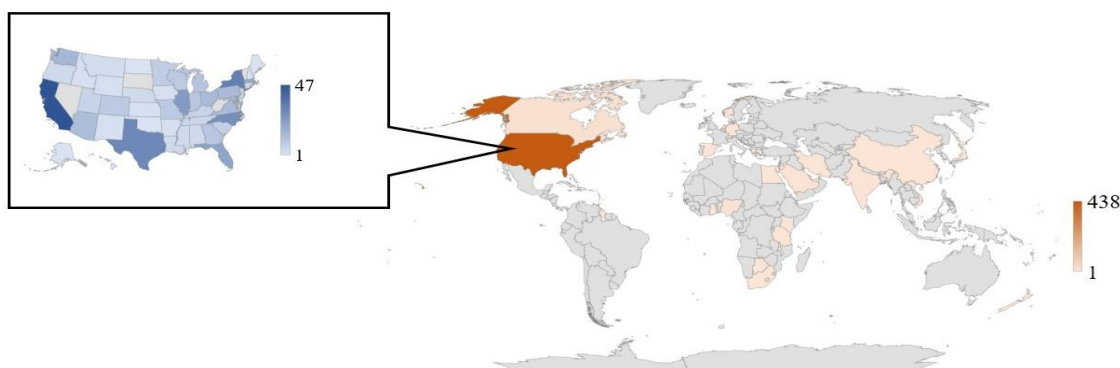


Figure 4.1: Distribution of Responses

The questionnaire is geared towards professionals who work with commercial ($n = 503$, 70%), government ($n = 191$, 27%), and private (non-residential) facilities ($n = 26$, 3%), resulting in 720 usable responses ($n = 720$) those mentioned above. The data are grouped to ensure they are not skewed towards one profession, as demonstrated in Figure 4.2. Group I consists of architects, Group II consists of facility managers and building owners, and Group III consists of construction managers, project managers, engineers, and others. These groupings are constructed such that the professions may have similar roles within the project lifecycle. For example,

facility managers and owners are more likely to deal with operations and maintenance than other professions. Of the respondents, 51% list their current role as architects, 29% identify as facility managers or building owners, and 20% identify as working as engineers, construction managers, or project managers. Results from respondents who declined to state their current role are eliminated from the analysis.

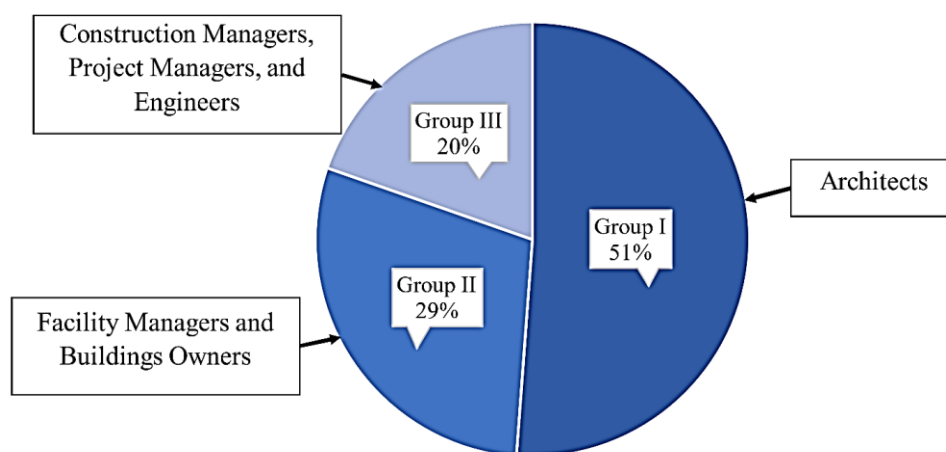


Figure 4.2: Characteristics of Respondents

Assets that should be considered for facility condition assessments when vacating a building.

In requesting that participants indicate which assets should be considered when vacating a building, respondents are able to select more than one asset. Shared responses across all groups are sprinklers and fire alarms, HVAC systems, roofing, and electrical systems. Respondents from Group II (facility managers and building owners) and Group III (construction managers, project managers, and engineers) also select security and access control systems as assets they deem essential to consider when vacating a facility (Table 4.1). These responses are compared to critical components highlighted in Jain et al. (2020) in no particular order.

Table 4.1: Assets for Which Condition Assessments Should be Carried Out When Vacating a Building

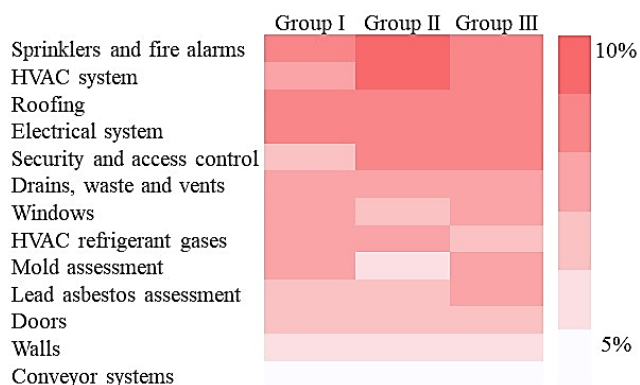
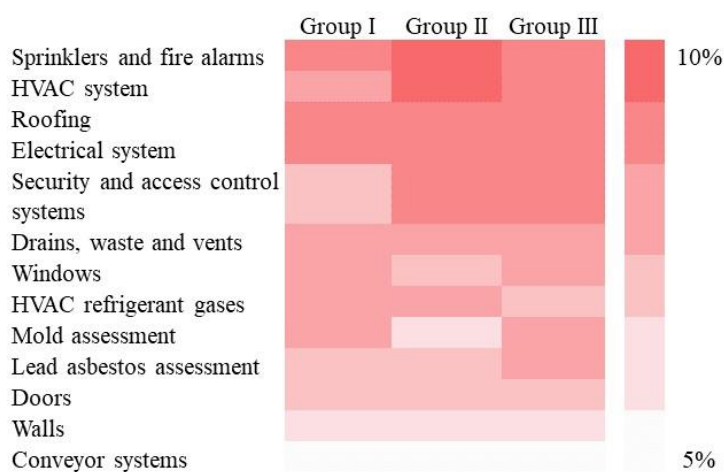


Table 4.2: Building Components During Post-storm Surveys

No.	Building Component
1.	Roof Structure
2.	Roof Covering
3.	External walls
4.	Windows
5.	Doors
6.	Wall Cover (Cladding and Siding)
7.	Roof-to Wall Connections
8.	Roof and Wall Sheathing

Table 4.3: Assets for Which Condition Assessments Should be Carried Out When Vacating a Building – United States Respondents Only



4.1.2 Inferential Statistics Summary

The results of the inferential statistics are summarized in Table 4.3. The calculated Chi-Square Test for Independence statistics results are 58.4 with 26 degrees of freedom. The p-value is less than 0.001, with the Cramer's V value, which measures the strength of association between the variables, at 0.25. Upon applying a Bonferroni correction and considering the Cramer's V results, this research reveals significant associations between the respondents' current role in the industry and the research variables shown in Table 4.3. These comprehensive

findings emphasize the interrelationships by industry that influence practices in commercial building decommissioning, as evidenced by the descriptive analysis.

Table 4.4: Association Between Respondent's Current Role and Research Variables and Their Strength

	Parameter	Valid cases	Degrees of freedom ^a	Chi-square statistic ^b	p-value	Cramer's V ^c	Effect size
Condition Assessments	Frequency of condition assessments	507	21	21.561	0.043	0.146	Moderate association
	Assets	530	26	58.363	<0.001	0.250	High association

^{a, b, c} Defined previously in the methodology chapter

4.1.3 Discussion regarding Research Question 1

The research's results indicate that roofing, sprinklers & fire alarm systems are critical assets to assess before vacating a building, coupled with windows, HVAC systems, HVAC refrigerant gases, and electrical systems, as shown in Table 4.1 for respondents globally and Table 4.3 for respondents in the United States only. Interestingly, the respondents from all professional disciplines did not rate walls and doors globally and nationally in the United States. When carrying out post-storm surveys, NWS evaluators concentrate on roofing, walls, windows, doors, and roof-to-wall connections, as shown in Table 4.2.

The apparent discrepancy in asset prioritization between facility managers during FCAs and NWS evaluators during post-storm damage surveys may raise concerns about the alignment between the two factions. While facility managers prioritize roofing, fire protection systems, windows, and certain mechanical and electrical components, NWS evaluators conducting post-event storm surveys focus on a broader range of structural elements, including walls, doors, and roof-to-wall connections. Despite these differences, several aspects contribute to the alignment

between the priorities of facility managers and NWS evaluators. First, facility managers, the wider built environment professionals, and NWS evaluators performing post-event storm surveys recognize the importance of critical building components such as roofs while carrying out FCAs or mitigating tornado-related damage. While their priorities may differ slightly, there is a common albeit inadvertent understanding of the key assets vulnerable to tornadic events, such as roofing systems and windows.

Secondly, looking at their complementary perspectives, facility managers and NWS evaluators carrying out post-event storm surveys bring different expertise and perspectives to the assessment process. While facility managers may prioritize assets based on operational considerations, occupant safety, regulatory compliance, and day-to-day functionality, NWS evaluators may prioritize components based on structural integrity, building codes, and risk analysis. While there is an overlap between these areas, such as occupant safety inherently encompassing structural integrity, each group may prioritize these aspects differently based on their specific roles and expertise. By integrating these complementary perspectives, stakeholders can develop comprehensive vulnerability mitigation strategies that address both operational and structural concerns.

Thirdly, effective collaboration across disciplines is essential for bridging the gap between asset prioritization during FCAs and asset vulnerability under extreme loading conditions. By fostering communication and coordination between disciplines, stakeholders can ensure that critical vulnerabilities are identified, assessed, and addressed in a timely manner. Collaborative efforts can also facilitate the implementation of proactive measures and targeted mitigation strategies to enhance building resilience against tornadoes.

The discrepancy in asset prioritization highlights opportunities for continuous improvement in assessment practices and communication channels between facility managers and NWS post-event storm evaluators. By soliciting feedback, sharing best practices, and aligning assessment methodologies, stakeholders can enhance the effectiveness of FCAs and post-event storm surveys, ultimately improving overall building resilience and tornado vulnerability mitigation efforts.

In summary, while there may be differences in asset prioritization between facility managers and NWS post-event storm surveyors during FCAs and post-event storm surveys, there is underlying alignment in their recognition of critical building components and shared commitment to enhancing building resilience against tornadic events. Effective collaboration, complementary perspectives, and a commitment to continuous improvement are key factors that contribute to bridging the gap and ensuring alignment between the two factions.

4.2 Building Material Deterioration Impacts to Fragility Curves

4.2.1 Deterioration Prediction Results

The deterioration of roofs, walls, doors, and windows is determined in 5-year intervals following the methods shown in section 3.2. Figures 4.3-4.6 depict the projected conditions of the four components. As mentioned earlier, while the absence of condition five data hinders full convergence to condition state 5, comparing the projected condition graphs validates the expected deterioration trend for building components. As evidenced in Figures 4.3 – 4.6, walls and roofs tend to deteriorate more rapidly than windows and doors.

In condition state 2 (as defined in figure 4.3), a notable spike is observed in all components at the 10-15-year mark, diminishing after 35 years. Windows exhibit the fastest

deterioration in this condition state with a probability of 0.45, followed by walls at 0.23, roofs at 0.15, and doors at 0.1. In condition state 3, a similar spike is observed at 15-35 years, with walls deteriorating fastest (probability of 0.6), followed by roofs at 0.5, doors at 0.55, and windows at 0.5. In condition state 4, a spike is observed much later in the service life of all components, at 40 years, with walls deteriorating fastest (probability of 0.65), followed by roofs at 0.6, doors at 0.55, and windows with a probability of 0.5. The probability of deterioration for all components continues in an upward trajectory to the end of service life.

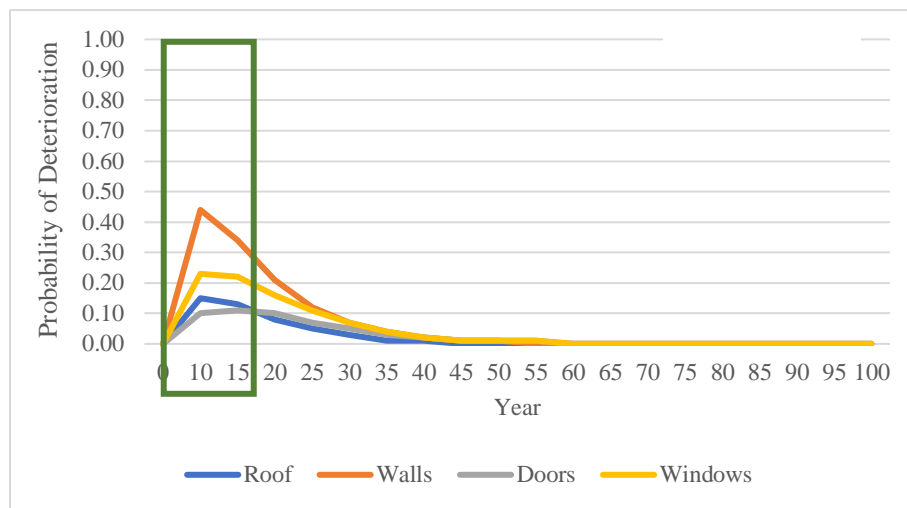


Figure 4.3: Condition State 2 Deterioration Trends for all Components

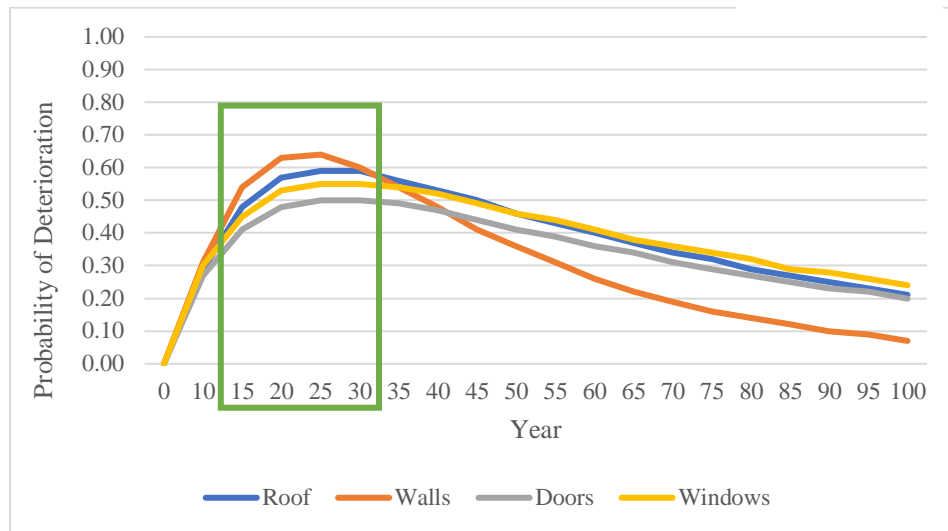


Figure 4.4: Condition State 3 Deterioration Trends for all Components

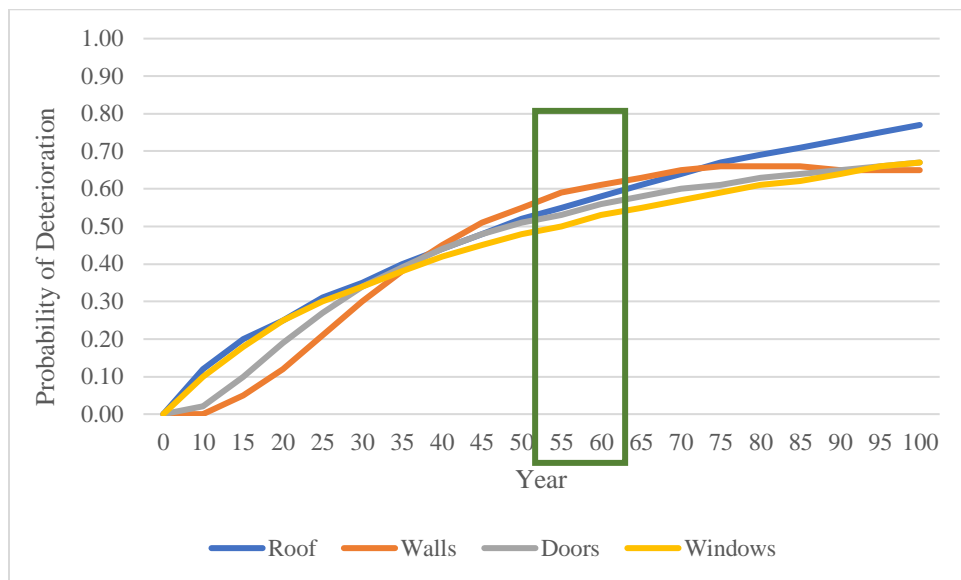


Figure 4.5: Condition State 4 Deterioration Trends for all Components

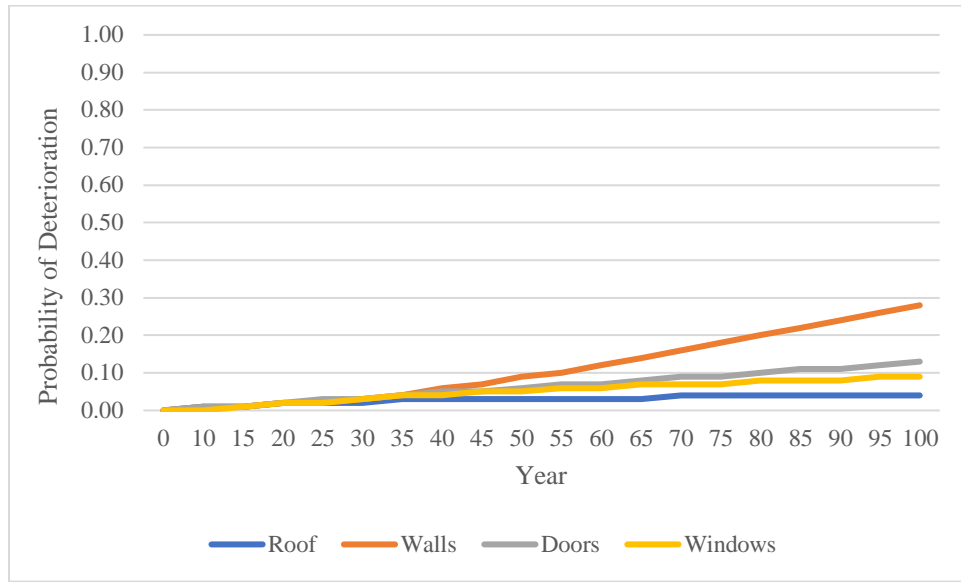


Figure 4.6: Condition State 5 Deterioration Trends for all Components

4.2.1.1 Model Calibration Process

As mentioned previously in Chapter 3, Madanat et al. (1995) explain the regression-based optimization method as a process that uses a non-linear optimization function to minimize the sum of absolute variances between the regression curve that best fits the condition data and the conditions predicted using the implemented Markov chain model. This regression curve is illustrated in Figure 4.7, while the transition matrices and transient probabilities are described in Appendix A. Optimization process samples and the optimization summary of services components are given in Appendix A. An explanation of the validation process for the calibrated transition matrices is provided in the following section.

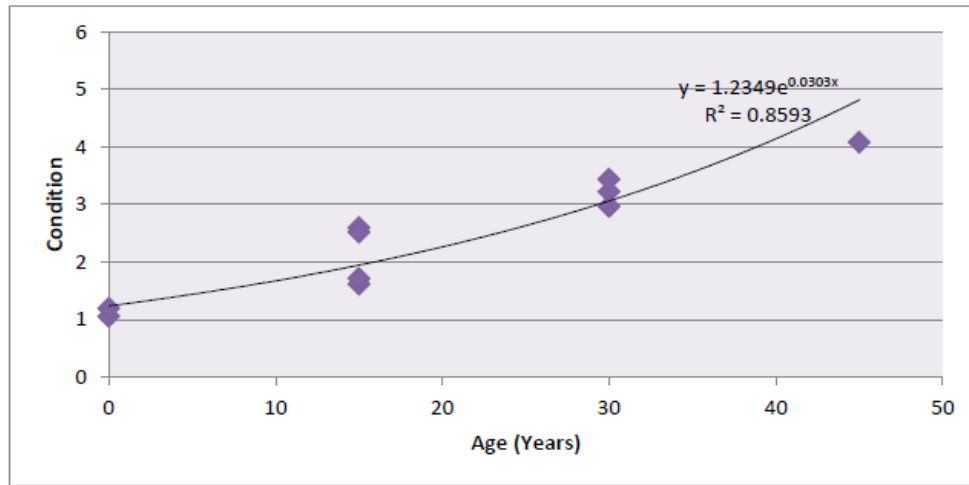


Figure 4.7: Exponential Regression Line Y_n

4.2.1.2 Validation & Evaluating Performance of the Calibrated Model

The validation or assessment of the performance of the deterioration models calibrated in this research concerns the consistency between predicted and observed values. Predicted values are derived from calibrated transition matrices using the Markov chain process, while observed values are independent data points used to examine differences in the predictions of the Markov model against real data.

As previously discussed in this chapter, the 2007 and 2009 inspection datasets are utilized to calibrate the Markovian deterioration models. These datasets, utilized to derive the 137 deterioration transition matrices, are referred to as the training datasets. To test the model effectively, the test dataset (observed data) should not be involved in calibrating or training the model (Tran, 2007). Two common methods for calibrating and validating models while maintaining separate training and testing datasets are employed. One method involves randomly dividing the dataset into the calibration (training) dataset and the testing dataset. Alternatively, another approach, potentially resulting in a more realistic validation process, entails using an

additional independent dataset. This research uses a 2011 inspection dataset as the observed (or test) dataset to validate the methodology.

The chi-square statistics (X^2), as calculated and contrasted with the chi-square critical value for a significance level of 0.05 and 2 degrees of freedom, shows that the Markov chain results as having been accepted by the chi-square hypothesis by having an acceptable chi-square value of 5.6 against the critical value of 5.99, confidence interval 95%. The critical values depending on ν and α are given in Figure 4.8.

Upper-tail critical values of chi-square distribution with ν degrees of freedom					
ν	Probability less than the critical value				
	0.90	0.95	0.975	0.99	0.999
1	2.706	3.841	5.024	6.635	10.828
2	4.605	5.991	7.378	9.210	13.816
3	6.251	7.815	9.348	11.345	16.266
4	7.779	9.488	11.143	13.277	18.467
5	9.236	11.070	12.833	15.086	20.515

Figure 4.8: Critical values of Chi-Square distribution for ν degrees (NIST/SEMATECH, 2012)

4.2.2 Resulting Deterioration Rates

The deterioration prediction leads to the analysis of the time-based deterioration rates for the components' materials. The deterioration rates are presented for each building material, highlighting any trends or patterns observed across different materials and environmental conditions.

The time-dependent analysis of deterioration rates reveals distinct time-based trends in material degradation over the service life of commercial and government buildings. For instance, roofing materials, asphalt shingles, and metal casement windows exhibit rapid deterioration, as shown in Table 4.4. Conversely, clay tiles, steel roof joists, poured concrete and timber walls,

mahogany and steel doors, hurricane clips, and 16d toenails show a more consistent deterioration rate across the lifespan, indicating stable material performance over extended periods.

Table 4.5: Individual Deterioration Rates of Materials

Building Component	Time (years)	Deterioration Rate
Roofs		
Asphalt Shingles	0	0
	10	0.2
	20	0.4
	30	0.6
	40	0.8
	50	1.00
Clay, Metal, Slate, and Steel Roof		
Joists	0	0
	10	0.13
	20	0.27
	30	0.4
	40	0.53
	50	0.67
Walls		
CMU, Poured Concrete, and Timber Frames	0	0
	10	0.13
	20	0.25
	30	0.38
	40	0.5
	50	0.63
Windows		
Metal Casement	0	0
	10	0.1
	20	0.2
Metal Casement and Timber	30	0.3
	40	0.4
	50	0.5
Doors		
Mahogany, Fiberglass, Steel (Fire Rated)	0	0
	10	0.17
	20	0.33
	30	0.5
	40	0.67
	50	0.83

Table 4.6: Individual Deterioration Rates of Materials (*cont.*).

Building Component	Time (years)	Deterioration Rate
Siding		
Aluminium and Brick Veneer	0	0
	10	0.2
	20	0.4
	30	0.6
	40	0.8
	50	0.9
Connections		
16d toenails and H2.5 clips - Steel	0	0
	10	0.1
	20	0.2
	30	0.3
	40	0.4
	50	0.5

These sequential trends in deterioration rates underscore the importance of considering time-dependent factors in modeling failure of structural components using fragilities.

Incorporating time-dependent deterioration rates into the fragility curve allows for a more accurate analysis of structural vulnerabilities over time. By capturing the time-based evolution of material degradation, the fragility curve can provide insights into the long-term resilience of commercial and government buildings under tornado events. Proactive maintenance strategies can be informed by time-based trends in deterioration rates, enabling building owners and managers to address vulnerabilities and mitigate the risk of structural failure over the lifespan of the building.

Time-based trends in deterioration rates provide valuable insights into how building components degrade and deteriorate over time. By understanding these trends, building owners and facility managers can implement proactive maintenance strategies to address vulnerabilities and mitigate the risk of structural failure through:

1. **Early Detection of Deterioration:** Monitoring deterioration rates allows building owners and facility managers to detect signs of degradation early on. By identifying areas where deterioration occurs more rapidly, they can prioritize maintenance efforts and address issues before they escalate into larger problems.
2. **Optimized Maintenance Scheduling:** Armed with data on deterioration rates, owners and managers can develop optimized maintenance schedules. Instead of relying on reactive maintenance practices, they can schedule inspections and repairs at intervals that align with each component's expected deterioration rate.
3. **Cost-effective Repairs:** Proactive maintenance based on deterioration trends can be more cost-effective in the long run compared to reactive repairs. By addressing issues early, before they lead to extensive damage, owners can avoid costly repairs and potential downtime associated with structural failures.
4. **Extended Lifespan of Building Components:** Implementing proactive maintenance strategies informed by deterioration rates can help extend the lifespan of building components. By promptly addressing deterioration, owners and facility managers can prevent premature failure and ensure that building systems remain functional and reliable for extended periods.
5. **Enhanced Safety and Resilience:** Regular maintenance based on deterioration trends helps ensure the safety and resilience of the building. By proactively addressing vulnerabilities, owners and managers can minimize the risk of structural failure during extreme events such as storms, earthquakes, or high winds, thereby protecting occupants and minimizing property damage.

Overall, time-based trends in deterioration rates serve as a valuable tool for building owners and facility managers to effectively manage the maintenance and upkeep of their facilities, ultimately leading to improved safety, resilience, and cost-effectiveness over the building's lifespan.

4.2.3 Time-dependent Materials Fragilities

The findings on deterioration rates provide time-based patterns of material degradation, laying the groundwork for assessing the impact of deterioration on building material fragility under tornado events. In this section, the research presents and analyzes the comparison of pristine (non-deteriorated) and deteriorated fragility curves for various building materials under tornado events. The objective is to assess the impact of deterioration on material vulnerability, focusing on shifts in the probability of exceedance, EF scale, and Degree of Damage 3-sec wind gust thresholds.

Fragility curves are developed using a lognormal distribution to achieve this objective, incorporating deterioration effects based on the established deterioration rates. This methodology enables the examination of differences in material vulnerability between pristine and deteriorated states, shedding light on the dynamic nature of material degradation under tornado conditions. Furthermore, the analysis explores the effects of deterioration on material fragility under different EF scale wind gust scenarios, providing insights into how shifts in wind speed thresholds may impact building resilience. Additionally, the research explores variations in Degrees of Damage to understand the implications of building material fragilities on damage state classification.

The research places significant emphasis on the role of poor maintenance in exacerbating structural vulnerability to tornado events based on the aforementioned study on decommissioning practices of commercial buildings carried out in 2022. In the study, poor maintenance, characterized by neglect, deferred repairs, and abandonment, emerged as a critical factor influencing the degradation of building materials and overall structural integrity. Deterioration rates corresponding to averagely maintained facilities are selected for further analysis and integration into the fragility function framework to validate the results.

This analysis aims to provide insights into the dynamics of material vulnerability under tornado events to answer Research Question 2: "Does deterioration have an effect on the tornadic wind-loading response of building materials? How significant are the shifts in material tornadic fragilities of deteriorating buildings when compared to non-deteriorating (pristine) buildings?"

4.2.4 Fragility Curves

The methodology for developing fragilities for the materials used in roof coverings, steel roof joists, walls, doors, windows, 16d toenails, and H2.5 clips is explained in the previous chapter. As discussed previously, the fragility of a structural system can be modeled using;

$$F_r(x) = \Phi \left[\frac{\ln(x) - \lambda_R}{\xi_R} \right]$$

where x = specified intensity measure defined as 3-sec gust wind speed (m/s or mph) for tornado fragility function; $\Phi[*]$ = standard normal cumulative distribution function; λ_R = logarithmic median of capacity; and ξ_R = logarithmic standard deviation of capacity. This procedure is employed to fit the results of the fragility curves for both pristine (non-deteriorating buildings) and deteriorating buildings at intervals of 0, 10, 20, 30, 40, and 50 years.

A probability paper plot is applied to the fragility parameters (i.e., ζ and λ values). The residual R^2 is also calculated to examine how many data points surround the line of best fit, accounting for the accuracy of the data to validate the fragility parameters. For this research, the R^2 value is 0.967, shown in Figure 4.9, which is a high R^2 value. High R^2 values indicate that the lognormal distribution best fits the MCS. Thus, the presented fragility models can be described using a lognormal distribution with ζ and λ .

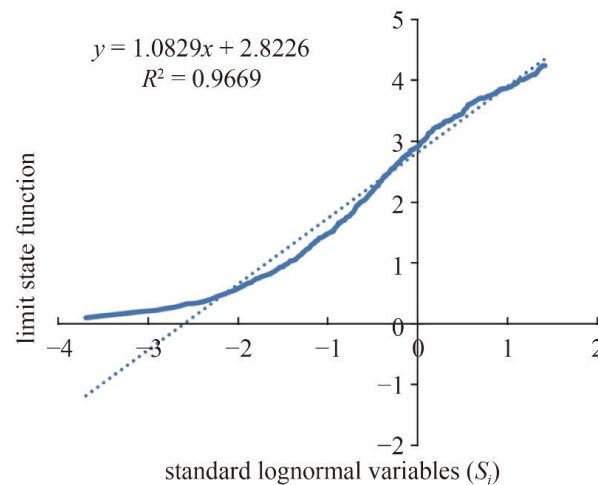


Figure 4.9: Best Fit Model for Monte Carlo Simulation

Figure 4.10 shows examples of the best fit for fragilities obtained for asphalt shingles at the 10, 30, and 50-year intervals of the material's service life.

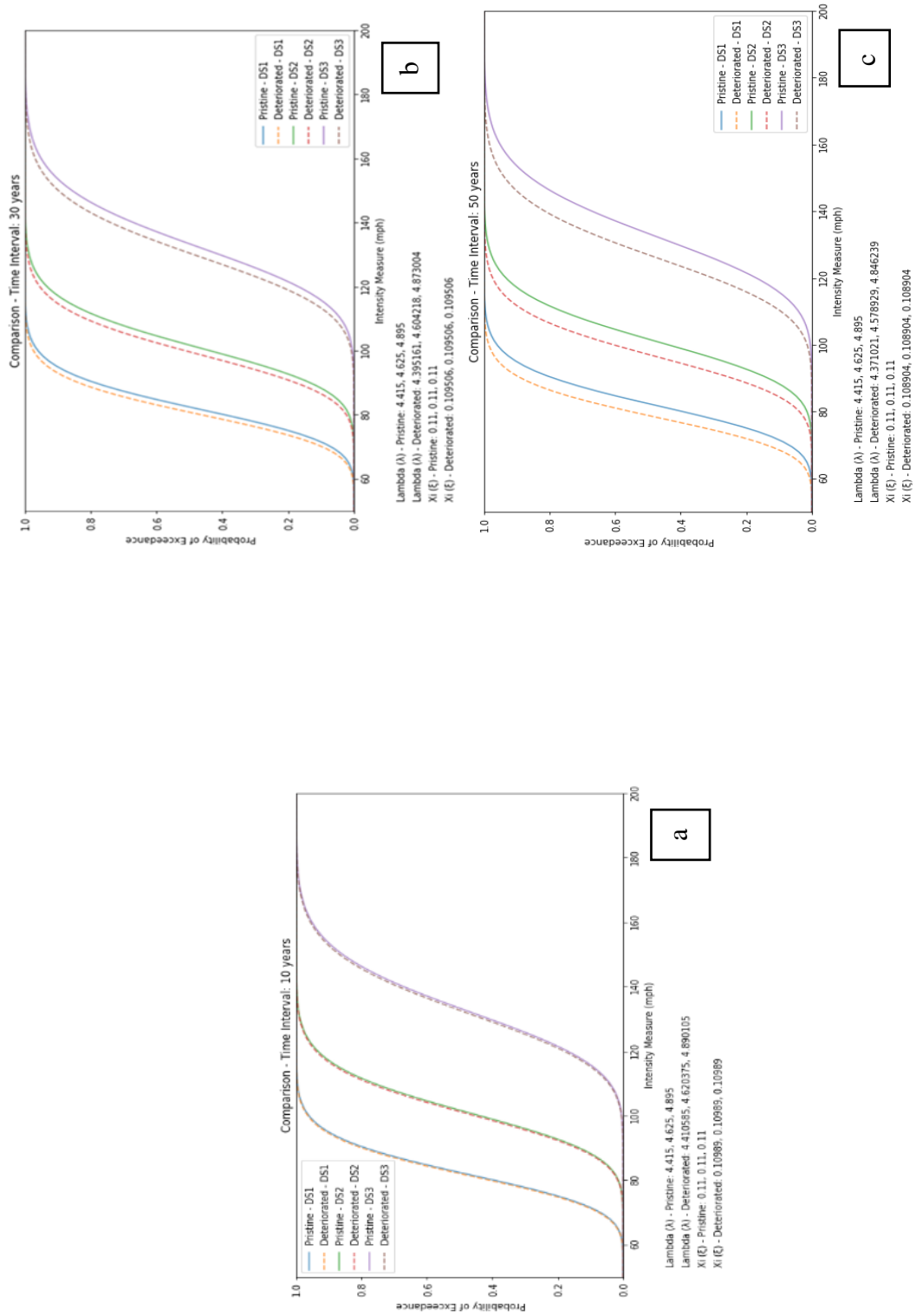


Figure 4.10: Lognormal best-fitted asphalt shingles fragilities at (a) 10-year interval, (b) 30-year interval, and (c) 50-year interval

This section evaluates the impact of deterioration on the response of building components by developing time-evolving building fragility curves for building materials used in roofs, walls, doors, windows, and wall-to-roof connections. Such time-dependent fragility curves quantify the impact of deterioration on building material vulnerability to tornadic wind damage along the service life of the building. The analysis focuses on fragility curves obtained for materials such as asphalt shingles, clay tiles, timber and metal casement windows, mahogany and steel doors, aluminum siding, steel roof joists, 16d toe-nails, and one or two H2.5 steel clips. These findings are validated through a comparative analysis with materials sourced from buildings with average maintenance. This comparison provided valuable insights into the differential vulnerability profiles of buildings based on maintenance practices.

Figures 4.11 – 4.16 illustrate a leftward shift in fragility curves for deteriorated materials compared to pristine ones. These figures showcase fragility curves for asphalt shingles, walls, and two H2.5 hurricane clips at different time intervals into their service life, highlighting the increasing vulnerability of deteriorated materials over time. These figures include the wind speed thresholds for each EF-Scale ranking, with the transition point between rankings called out. The overlay shows an increased probability of failure for asphalt shingles, walls, and H2.5 clips at the wind speed.

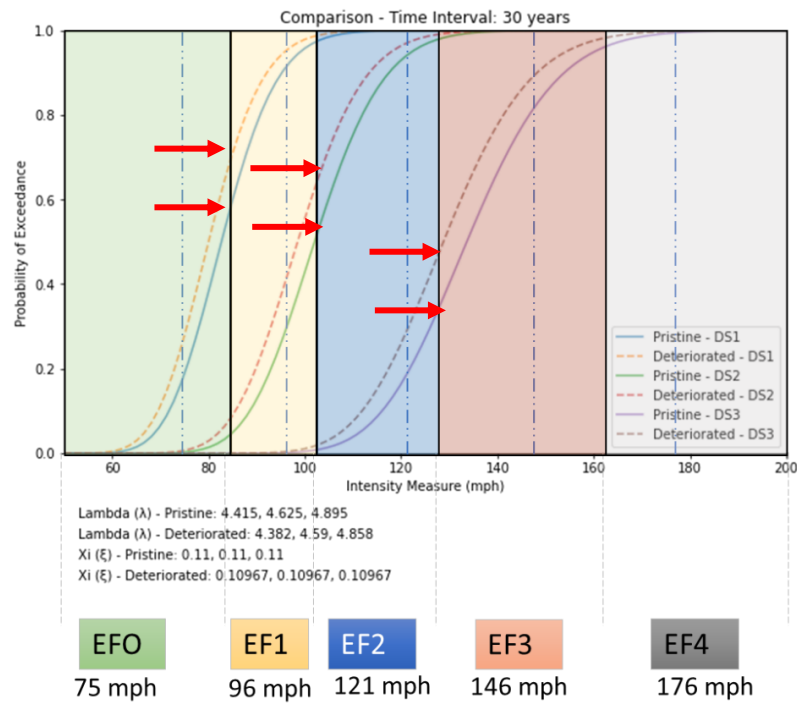


Figure 4.11: Fragilities for asphalt shingles at a 30-year time interval – Poor Maintenance

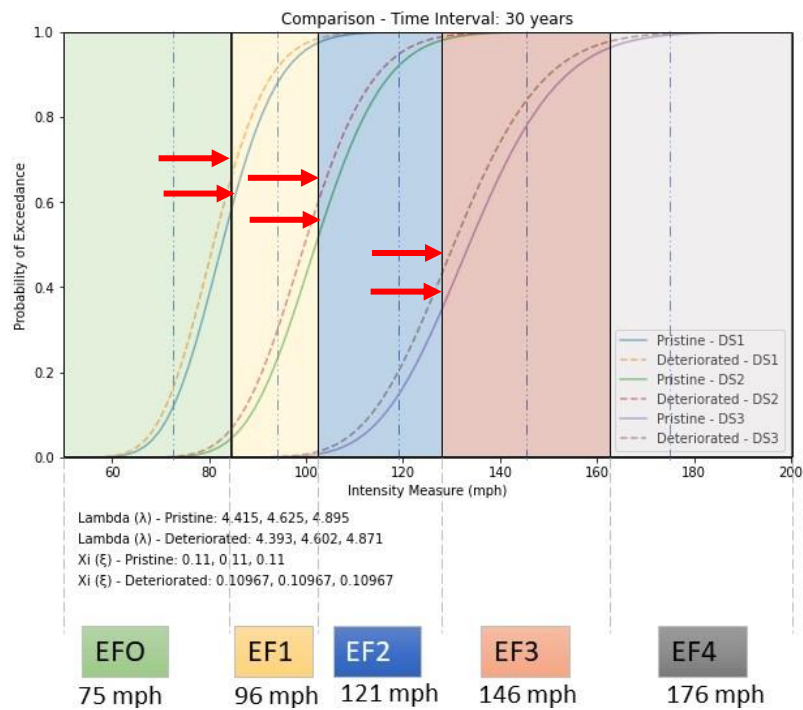


Figure 4.12: Fragilities for asphalt shingles at a 30-year time interval – Average Maintenance

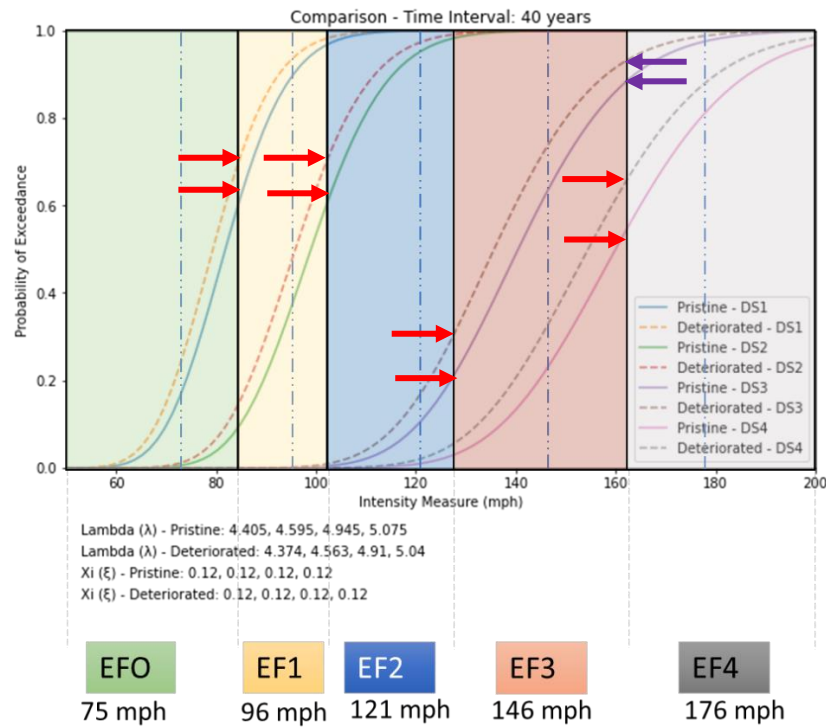


Figure 4.13: Fragilities for walls at a 40-year time interval – Poor Maintenance

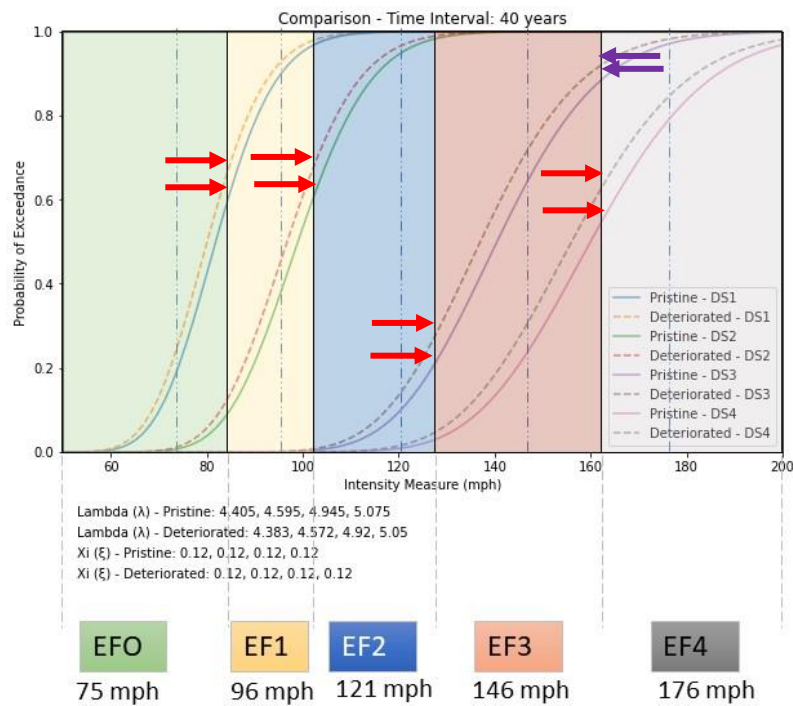


Figure 4.14: Fragilities for walls at a 40-year time interval – Average Maintenance

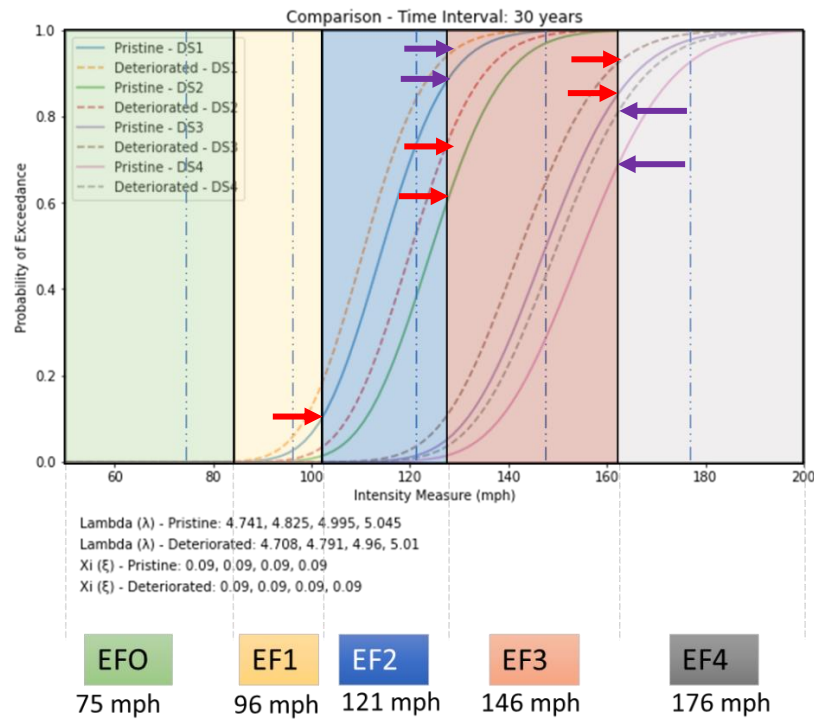


Figure 4.15: Fragilities for two H2.5 clips at a 30-year time interval – Poor Maintenance

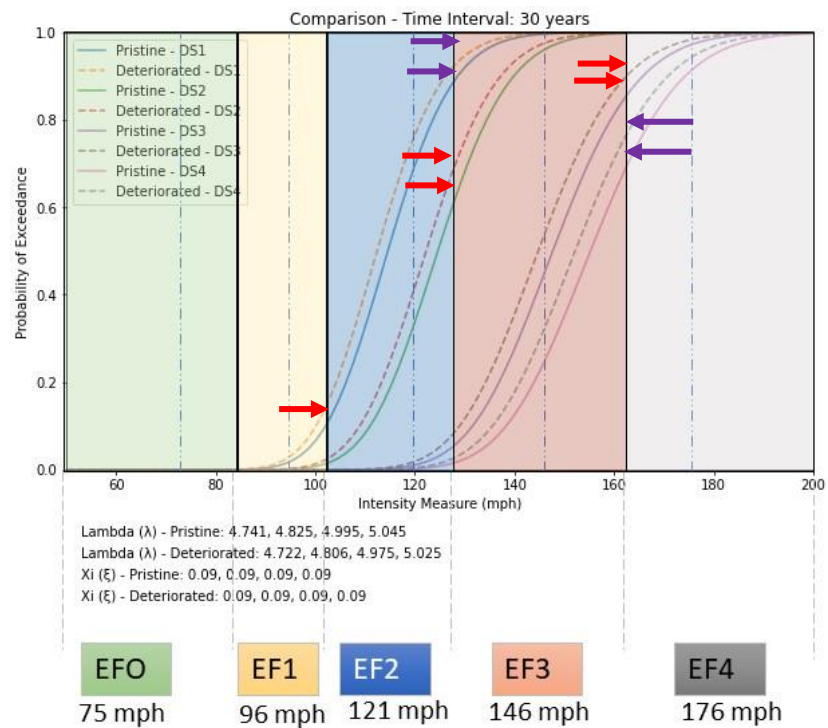


Figure 4.16: Fragilities for two H2.5 clips at a 30-year time interval – Average Maintenance

By quantifying the leftward shift in wind speed thresholds, the research observes an average percentage decrease of 4% in wind speed thresholds across all EF scale categories for asphalt shingles, walls, and H2.5 clips compared to pristine counterparts across all time intervals, for poorly maintained materials. The comparison with fragilities for materials in buildings that receive average maintenance reveals a similar leftward shift, resulting in an average decrease of 3% in wind speed thresholds across all EF scale categories for asphalt shingles, walls, and H2.5 clips in materials with average maintenance.

These findings shed light on the dynamic relationship between material deterioration and tornado vulnerability, particularly concerning the leftward shift in wind speed thresholds observed across the various building materials and time intervals. The observed decrease in wind speed requirements for damage initiation highlights the increased susceptibility of structures to wind-induced damage as materials degrade over time. While a 4% decrease (for poorly maintained building materials) on average in wind speed thresholds may seem modest, its cumulative effect over time can significantly compromise the structural integrity of buildings, leading to heightened risks of damage and failure, which is discussed further in the next section.

4.3 EF Scale Analysis

The previous analysis for all materials revealed a consistent leftward shift in fragility curves for deteriorated building materials compared to those of pristine buildings across all designated time intervals (10, 20, 30, 40, and 50 years) for each damage state (DS1, DS2, DS3, and DS4). This shift indicates that material deterioration leads to increased vulnerability to tornadic wind-loading events at lower wind speeds, resulting in a notable decrease in wind speed thresholds for damage initiation. In response to Research Question 3, “Would a structure’s age

and material deterioration ultimately impact how tornadoes are ranked on the EF-scale?”, as would be expected, the observed trend suggests that deteriorated materials are more susceptible to wind-induced damage at lower wind speeds than their pristine counterparts, regardless of the initial condition. Despite the relatively modest decrease in wind speed thresholds, Figure 4.14 illustrates the potential impact of such deterioration on asphalt shingles, highlighting the heightened risk of material deterioration.

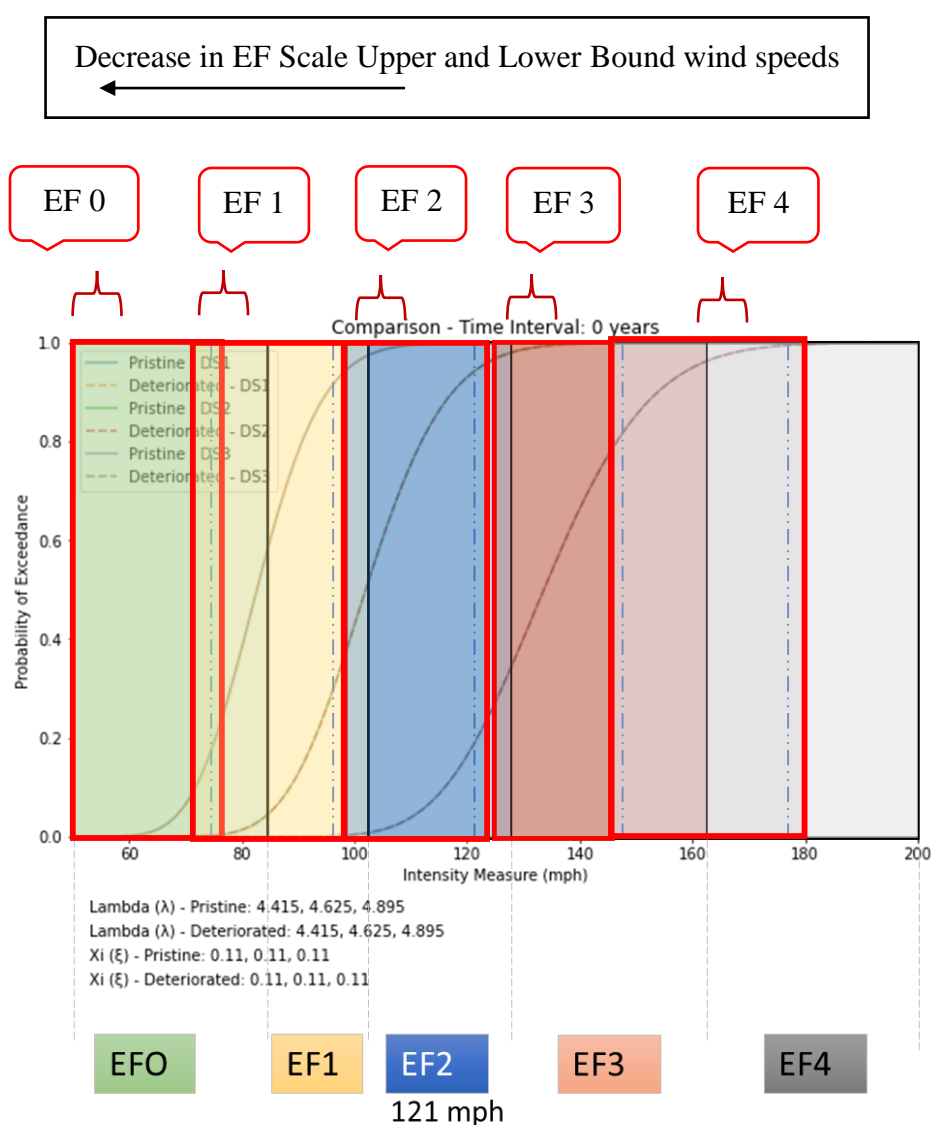


Figure 4.17: Leftward shift of EF scale wind speed thresholds for asphalt shingles

Table 4.5 provides the original lower and upper bound thresholds, per NWS, and assigns them as affiliated with assumed pristine conditions. The results from the fragility curves for deteriorated material are then used to define new lower and upper bounds within the EF-Scale.

Table 4.7: Upper and Lower Bound wind speed thresholds for pristine (non-deteriorated) and deteriorated asphalt shingles

EF Scale	Lower Bound (mph) Pristine	Lower Bound (mph) Deteriorated	Upper Bound (mph) Pristine	Upper Bound (mph) Deteriorated
EF 0	65	58	85	76
EF 1	86	77	110	99
EF 2	111	100	135	121
EF 3	136	125	165	148
EF 4	166	149	200	180

EF0 – The lower bound threshold wind speed for the deteriorated asphalt of 58 mph surpasses EF0’s Lower Bound threshold for pristine asphalt shingles, which is 65 mph.

EF 1 – The lower bound threshold wind speed for asphalt shingles of 77 mph overlaps with EF0’s threshold for pristine asphalt shingles between 65 and 85 mph.

EF 2 – The lower bound threshold wind speed for asphalt shingles of 100 mph overlaps with EF1’s threshold for pristine asphalt shingles between 86 and 110 mph.

EF 3 – The lower bound threshold wind speed of 125 mph overlaps with EF2’s threshold for pristine asphalt shingles between 111 and 135 mph.

EF 4 – The lower bound threshold wind speed for deteriorated asphalt shingles of 136 mph overlaps with EF3’s threshold between 166 and 200 mph.

Tables 4.7 – 4.9 provide the mean probability of exceedance for each EF scale category, further supporting the observed increase in the likelihood of damage occurrence for deteriorated materials. Statistical analyses, including paired t-tests and analysis of variance (ANOVA), highlight the significance of these shifts, with p-values < 0.05 indicating a statistically significant difference in the probability of exceedance between pristine and deteriorated materials. For statistically significant results ($p < 0.05$) and as an example, the research observes an average percentage increase in the probability of exceedance of 23%, 24%, and 34% across all EF scale categories for deteriorated asphalt shingles, walls, and single H2.5 hurricane clips respectively. All results for all materials are available in Appendix D.

Table 4.8: Probabilities of Exceedance for Asphalt Shingles (boxed area corresponds to Figure 4.10)

	DS1				DS2				DS3			
	EF0		EF1		EF1		EF2		EF2		EF3	
	Pristine	Deteriorated	Pristine	Deteriorated	Pristine	Deteriorated	Pristine	Deteriorated	Pristine	Deteriorated	Pristine	Deteriorated
Year												
0	0.59	0.59	0.9	0.9	0.56	0.56	0.9	0.9	0.37	0.37	0.8	0.8
10	0.59	0.59	0.9	0.92	0.56	0.58	0.9	0.9	0.37	0.39	0.8	0.8
20	0.59	0.68	0.9	0.95	0.56	0.58	0.9	0.95	0.37	0.41	0.8	0.95
30	0.59	0.64	0.9	0.95	0.56	0.61	0.9	0.95	0.37	0.43	0.8	0.95
40	0.59	0.78	0.9	0.95	0.56	0.71	0.9	1	0.37	0.59	0.8	0.95
50	0.59	0.82	0.9	1	0.56	0.81	0.9	1	0.37	0.7	0.8	1
Mean probability	0.590	0.683	0.900	0.945	0.560	0.642	0.900	0.950	0.370	0.482	0.800	0.908
T-Test (p-value)	0.066		0.023		0.097		0.041		0.094		0.027	
Variance	0.006		0.001		0.006		0.001		0.010		0.006	0.006
Standard Deviation	0.078		0.031		0.075		0.038		0.102		0.078	
Average Change	16%		5%		15%		6%		30%		14%	

Table 4.9: Probabilities of Exceedance for Walls (boxed area corresponds to Figure 4.11)

	DS1						DS2						DS4	
	EF0			EF1			EF2			EF0			EF1	
	Pristine	Deteriorated		Pristine	Deteriorated		Pristine	Deteriorated		Pristine	Deteriorated		Pristine	Deteriorated
Year														
0	0.59	0.59	0.95	0.95	0.99	0.99	0.99	0.99	0.1	0.1	0.61	0.61	0.56	0.56
10	0.59	0.59	0.95	0.95	0.99	0.99	0.99	0.99	0.1	0.1	0.61	0.61	0.56	0.57
20	0.59	0.62	0.95	0.98	0.99	1	0.99	1	0.1	0.12	0.61	0.64	0.56	0.6
30	0.59	0.64	0.95	0.99	0.99	1	0.99	1	0.1	0.13	0.61	0.67	0.56	0.62
40	0.59	0.7	0.95	0.99	0.99	1	0.99	1	0.1	0.16	0.61	0.74	0.56	0.68
50	0.59	0.79	0.95	1	0.99	1	0.99	1	0.1	0.2	0.61	0.78	0.56	0.76
Mean probability	0.590	0.655	0.950	0.977	0.990	0.997	0.990	0.997	0.100	0.135	0.610	0.675	0.560	0.632
T-Test (p-value)	0.096		0.029		0.025		0.000		0.078		0.074		0.069	
Variance	0.004		0.000		0.000		0.000		0.001		0.003		0.004	
Standard Deviation	0.060		0.019		0.005		0.005		0.031		0.056		0.061	
Average Change	11%		3%		1%		1%		35%		11%		13%	

Table 4.10: Probabilities of Exceedance for H2.5 clips (boxed area corresponds to Figure 4.12)

	DS1		DS2		DS3		DS4	
	EF2		EF2		EF3		EF3	
Year	Pristine	Deteriorated	Pristine	Deteriorated	Pristine	Deteriorated	Pristine	Deteriorated
0	0.9	0.9	0.61	0.61	0.86	0.86	0.68	0.68
10	0.9	0.95	0.61	0.66	0.86	0.9	0.68	0.78
20	0.9	0.96	0.61	0.7	0.86	0.91	0.68	0.79
30	0.9	0.97	0.61	0.78	0.86	0.95	0.68	0.81
40	0.9	0.98	0.61	0.8	0.86	0.97	0.68	0.88
50	0.9	0.99	0.61	0.87	0.86	0.98	0.68	0.91
Mean probability	0.900	0.958	0.610	0.737	0.860	0.928	0.680	0.808
T-Test (p-value)	0.007		0.024		0.015		0.012	
Variance	0.001		0.008		0.002		0.007	
Standard Deviation	0.036		0.089		0.045		0.083	
Average Change	6%		21%		8%		19%	

As discussed previously, this research places significant emphasis on the role of poor maintenance in exacerbating structural vulnerability to tornado events. Poor maintenance, characterized by neglect, deferred repairs, and abandonment, emerged as a critical factor influencing the degradation of building materials and overall structural resilience. This focus is informed by insights gained from the 2022 survey on decommissioning.

These findings underscore the detrimental impact of poor maintenance on material degradation and structural integrity. Neglected buildings exhibited a probable accelerated deterioration of roofing materials, walls, doors, windows, and structural connections, leading to decreased wind resistance and heightened vulnerability to tornado-induced damage. Building materials in deteriorated buildings exhibited higher probabilities of exceeding damage thresholds across all EF scale categories, indicating a greater susceptibility to tornado-induced damage.

These findings emphasize the importance of considering material deterioration in assessing building vulnerability to tornadic wind events. While the above results are provided in terms of Damage States, the determination of EF-Scale is based on the Degree of Damage (DOD) as defined by NWS Damage Indicators (Texas Tech, 2006). The EF-Scale encompasses a diverse range of Damage Indicators, including damage to small retail buildings (SRB), small professional buildings (SPB), strip malls (SM), large shopping malls (LSM), and large isolated retail buildings (LIRB), each category characterized by multiple DODs. This is in keeping with the research's focus on commercial and government buildings.

The leftward shift in fragility curves signifies a quantifiable decrease in wind speed thresholds required to initiate damage across all DOD categories for deteriorated materials compared to pristine counterparts. This reduction in wind speed thresholds highlights the

heightened risk posed by material deterioration and underscores the increased susceptibility of buildings to wind-induced damage over time.

For instance, Figures 4.15 – 4.18 show the effect of the leftward shift in deterioration curves for roof covering and walls, for example, to small retail buildings and large isolated buildings for damage states 1, 2, 3, and 4 at different time intervals into their service life, highlighting the increasing vulnerability of deteriorated materials over time. The DODs, used to identify the wind speed, are also shown to indicate how this leftward shift may cause a change in EF ranking.

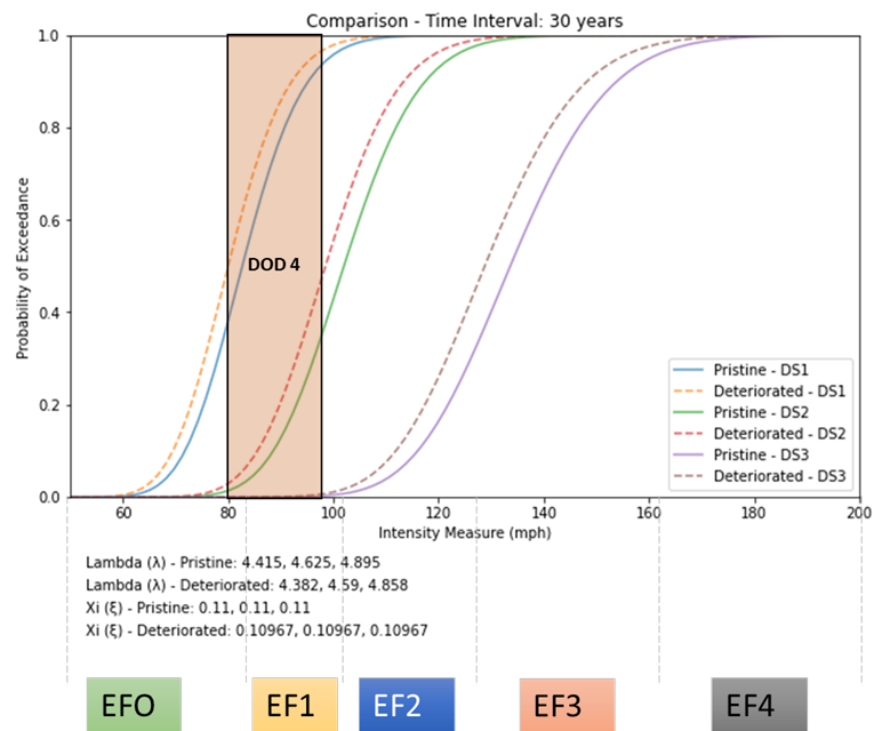


Figure 4.18: Fragilities for Asphalt Shingles with DOD 4 bounds for a Small Retail Building

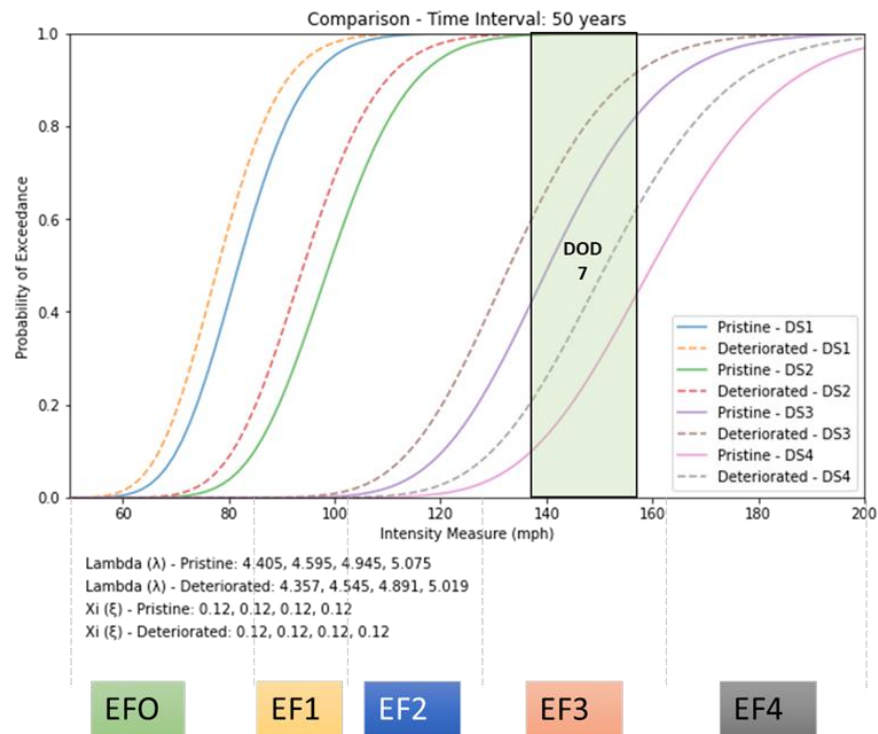


Figure 4.19: Fragilities for Walls with DOD 7 wind speed bounds for a Small Retail Building

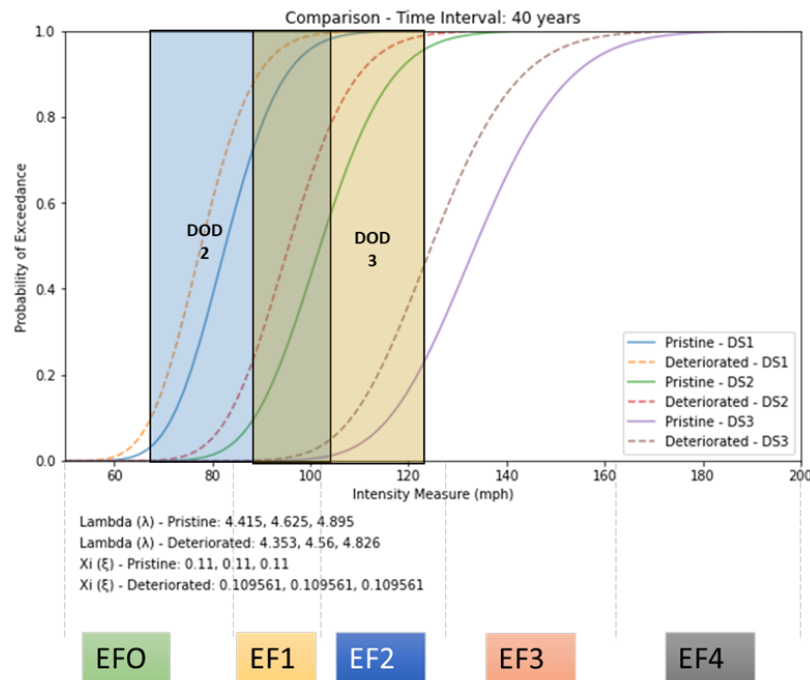


Figure 4.20: Fragilities for Asphalt Shingles with DOD 2 and 3 wind speed bounds for a Large Isolated Retail Building

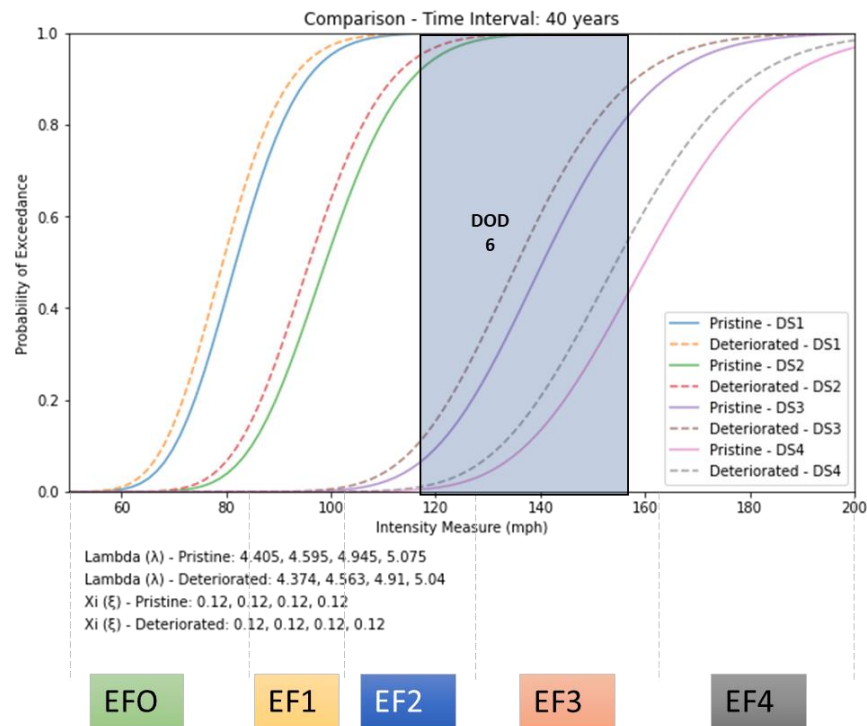


Figure 4.21: Fragilities for Walls with DOD 6 wind speed bounds for a Large Isolated Retail Building

Table 4.9 shows the results of quantifying the shift in wind speed thresholds, and the research observes an average percentage decrease of 3% – 7% across DOD categories for roofs and walls in small retail buildings (DOD 4 and DOD 7, respectively) and large isolated retail buildings (DOD 2, DOD 3 and DOD 6 respectively). The table also compares Upper- and Lower-bound wind speed thresholds for materials in pristine (non-deteriorated) and deteriorated small retail buildings (SRB) and large isolated retail buildings (LIRB) due to this decrease in percentage.

Table 4.11: Percentage Change in Fragility Parameter Lambda and the Upper and Lower bound wind speed thresholds for materials in pristine (non-deteriorated) and deteriorated Small Retail Buildings (SRB) and Large Isolated Retail Building (LIRB)

Damage Indicator	DOD ⁺	Damage Description ⁺⁺	Component	Material	Age of Material (Years)	% Change (Fragility Functions)	Lower bound (mph) ^{***}	Upper bound (mph) ^{***}
Small Retail Building	4	Uplift of roof decking; significant loss of roof covering (>20%)	Roof	Asphalt Shingles	30	4%	76 (81)	111 (119)
Small Retail Building	7	Collapse of exterior walls; closely spaced interior walls remain standing	Wall	Concrete	50	5%	105 (120)	139 (159)
Large Isolated Building	2	Loss of roof covering (<20%)	Roof	Asphalt Shingles	40	7%	60 (68)	90 (103)
Large Isolated Building	3	Uplift of roof decking; significant loss of roof covering (>20%)	Roof	Asphalt Shingles	40	7%	76 (87)	108 (123)
Large Isolated Building	6	Inward or outward collapse of exterior walls	Wall	Concrete	40	3%	109 (118)	146 (158)
				Masonry Units				

⁺DOD- Degree of Damage

⁺⁺Adapted from Texas Tech (2006)

^{***}Lower and Upper Bound wind speeds for pristine buildings (undeteriorated) are shown in brackets for comparison.

Despite the relatively modest decrease in wind speed thresholds, Figure 4.19 shows the potential impact of this reduction on the susceptibility of roofs to wind-induced damage in Large Isolated Retail Buildings at different time intervals, DOD 3, highlighting the leftward shift in wind speed and therefore the heightened risk posed by material deterioration.

At year 10's Lower Bound threshold, the wind speed for deteriorated roof covering of 86 mph surpasses the Lower Bound threshold for pristine roof covering between 87 and 83 mph. This trend continues with the Lower Bound threshold at year 20 decreasing to 86 mph, 85 mph at year 30, 76 mph at year 40, and 68 mph at year 50.

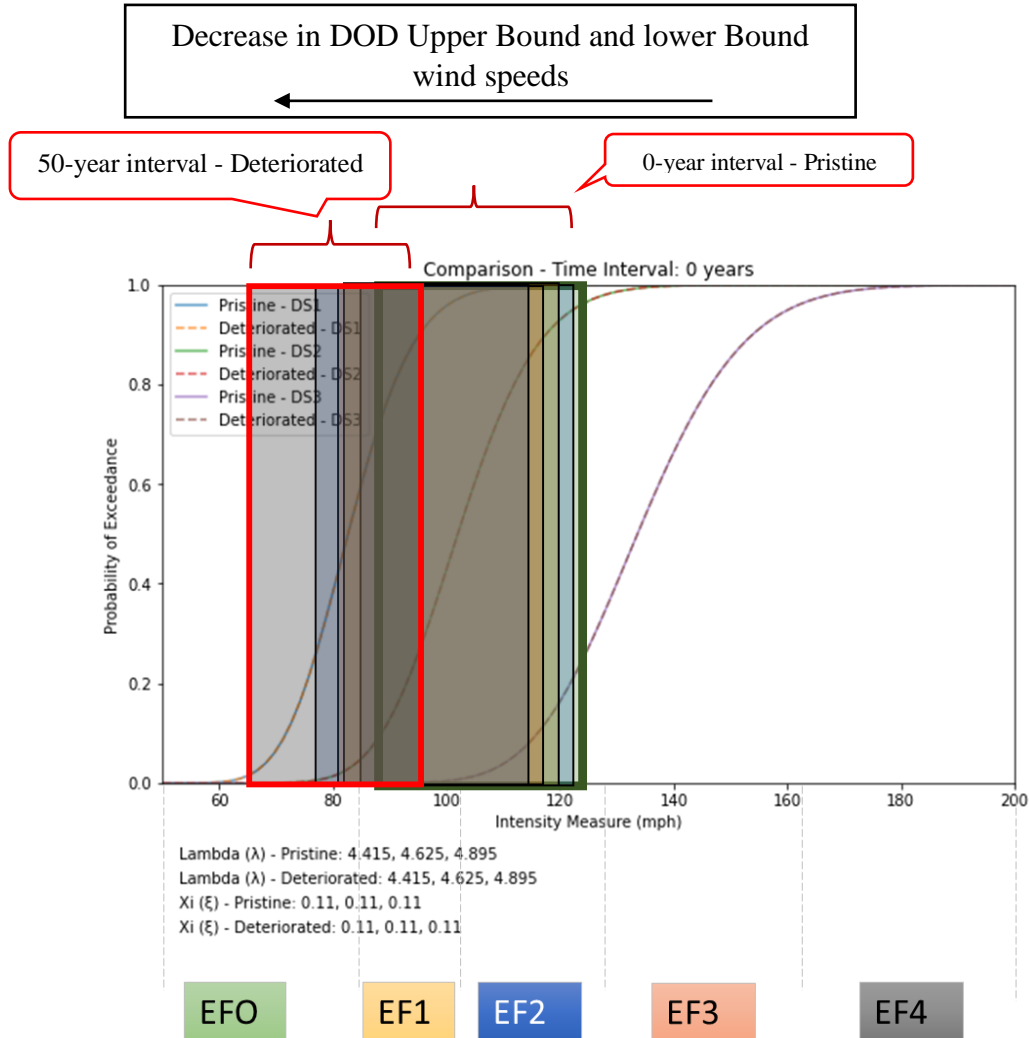


Figure 4.22: Leftward shift of DOD threshold wind speeds for roof covering to a Large Isolated Retail Building at 0-50-year intervals. Year 0 and year 50 thresholds are boxed.

4.3.1 Discussion on EF Scale Analysis

This research investigates building materials' time-dependent deterioration fragility curves, focusing on shifts in wind speed thresholds and changes in mean probability across EF Scale and Degree of Damage (DOD) analyses. Findings reveal significant leftward shifts in the fragility curves for various building materials, which would result in shifts in wind speed thresholds relative to the EF Scale. These findings indicate a decrease in wind speed

requirements for damage initiation in deteriorated materials compared to pristine counterparts, which is the assumption for the damage indicators for the EF-Scale. Additionally, observations highlight an average change in mean probability of exceedance across some of the analyzed scenarios, with statistically significant findings ($p < 0.05$) reinforcing the robustness of the results. The average increase in mean probability indicates a heightened likelihood of experiencing damage across different damage states, reflecting the progressive deterioration of building materials over time. This trend is more pronounced in cases where p-values are less than 0.05, signifying statistically significant changes that cannot be attributed to random variation alone. In the research, we utilize the concept of "average percent change" in the probability of exceedance to assess the relative shift in vulnerability between pristine (non-deteriorated) building materials and deteriorated building materials, as highlighted in Chapter 4, the methodology section. This metric serves as a vital indicator of how building resilience is affected by varying maintenance levels.

The leftward shift in fragility curves for deteriorated materials suggests reevaluating the EF scale ranking and DOD thresholds to account for the increased susceptibility of deteriorated materials to wind-induced damage. The decrease in wind speed thresholds required to initiate damage in deteriorated materials may lead to reassessing the EF scale categorization, potentially resulting in a higher EF scale ranking for tornado events. Previous damage surveys that followed the DOD guidance result in EF rankings based on an assumed pristine building condition prior to the tornado event. For example, a wind speed threshold previously associated with EF2 damage in pristine materials may now correspond to EF3 damage in deteriorated materials, reflecting the heightened vulnerability of the built environment to tornadic wind loading.

Deteriorated materials are more prone to damage at lower wind speeds, necessitating adjustments to the existing DOD thresholds to accurately reflect the extent of damage incurred by deteriorated buildings. This may entail revising DOD classifications or introducing new criteria to account for the differential vulnerability of deteriorated materials.

The variability in the magnitude of leftward shifts across different time intervals highlights the complex nature of material deterioration processes. While shorter time intervals may exhibit relatively minor shifts, the cumulative effects of environmental exposure and aging mechanisms become more pronounced over longer durations. Understanding the underlying drivers of this variability is crucial for developing proactive strategies to mitigate the impacts of material degradation on structural resilience. Further understanding of these drivers may ultimately highlight the need for structural integrity research, evaluation, and/or modeling to consider not only the physical aspects of a constructed building but also *how* that building is utilized and/or maintained over time.

4.4 Summary

Routine FCAs evaluate building components, which include roofing, HVAC systems, sprinklers, and fire alarms, electrical system, security and access control, drains, waste & vents, windows, HVAC refrigerant gases, lead and asbestos assessment, doors, walls, and conveyor systems within a building, which is found to overlap, in part, with surveys of a damaged facility post- extreme event. Often, storm surveys look at roof structure, roof covering, external walls, windows, doors, wall cover (cladding and siding), roof-to-wall connections, and roof & wall sheathing to determine an EF ranking for a tornadic event. If a tornado-damaged building was a decommissioned building and, therefore, no longer being maintained (poor maintenance), the

wind speed required to reach certain damage states may be significantly lower (depending on the age). When conducting a storm survey, damage indicators may have degrees of damage discussing the upper and lower wind bounds that cause between >2% (DS1) up to >50% (DS4) loss of roof covering, loss of 1 door or window (DS1) up to loss of >25% (DS4) of windows and doors, loss of >2% (DS1) and up to >75% (DS4) of exterior walls, and no loss (DS1) up to complete loss (DS4) of a roof structure.

With consideration of the results of this research, those upper and lower bounds, which help define the experienced wind speed and, therefore, the resulting EF ranking (as necessary), may be altered significantly based on the building maintenance practices. If storm surveys involve an evaluation of, for example, walls, but FCAs have that as a low priority, then there is a discrepancy in how buildings are being assessed pre- and post-extreme events. This potential mismatch will then transfer into the subsequent wind speed designations and EF rankings (for tornado events) from NWS post-event storm surveys. The analysis reveals a consistent leftward shift in fragility curves for deteriorated materials compared to pristine counterparts, indicating decreased wind speed thresholds for damage initiation. This shift underscores the increased vulnerability of structures to wind-induced failure due to material aging and degradation. Furthermore, quantifying the percentage shift in wind speed thresholds highlights the magnitude of this vulnerability, with deteriorated materials exhibiting significant reductions in wind speed thresholds across different EF scales and Degree of Damage categories.

Tornadoes, though prevalent in the United States, also occur in other countries around the globe. Adaptation of fragility analysis methodologies is necessary to suit local contexts, including adjusting input parameters like wind speeds and building characteristics. Despite

regional differences, universal fragility analysis principles can guide curve development, allowing for effective assessment of building vulnerability to tornadoes. Local factors are crucial for applying this methodology across diverse geographical contexts.

4.5 Assumptions and Limitations

Notably, fragility curves incorporating deterioration rates are subject to assumptions and uncertainties related to material properties, degradation mechanisms, and hazard interactions, which may influence model predictions and decision-making processes. This section discusses the assumptions and limitations of the research.

1. The analytical models in this study are built on assumptions about building material behavior and deterioration progression. These include a linear relationship between service life, deterioration rate, and uniform deterioration across components. While these assumptions are supported by literature and empirical evidence, they introduce uncertainties and limit generalizability. Validation using data from buildings with average maintenance is conducted to assess these assumptions' impact and quantify associated uncertainties. Linear models assume constant rates of change, but real-world phenomena may exhibit nonlinear interactions or threshold effects, oversimplifying linear models.
2. The research operates under the assumption of homogeneity, suggesting uniformity or consistency in building materials or environmental conditions within the study sample. However, it's essential to acknowledge that variations or heterogeneity may exist across different buildings or regions, potentially influencing the study findings.

3. The results of this study may be sensitive to variations in input parameters, such as material properties, environmental conditions, socio-economic conditions, and maintenance practices. For instance, differences in material properties between buildings, variations in local environmental conditions, disparities in socio-economic status, and diverse maintenance practices across regions or building types could introduce significant variability in the outcomes. Therefore, while this study provides valuable insights, it's essential to recognize that the findings may be influenced by the context and conditions under which the analysis was conducted.
4. While the research utilizes statistically significant findings to analyze the probability of exceedance, it acknowledges the existence of null results. Although this acknowledgment is important to prevent potential distortions in the body of evidence, which could lead to overestimating the effect sizes or generalizability, the study focuses on utilizing reliable data. This decision aims to enhance the robustness of the research findings.

Based on the limitations and assumptions identified in this study, several opportunities for future research are identified, including refining analytical models, expanding the scope of analysis, and addressing data quality issues. Future research may include conducting similar studies in diverse settings to enhance the findings' generalizability and validate the analytical models' robustness.

CHAPTER 5: KEY FINDINGS, CONTRIBUTIONS, AND FUTURE RESEARCH RECOMMENDATIONS

Tornadoes are among the most devastating natural disasters, especially for smaller communities. Despite the widespread use of fragility curve methods, the impact of material deterioration on tornado vulnerability has been largely overlooked. Through a comprehensive examination of the impact of material deterioration on tornado fragility, the research aims to fill this critical gap by investigating the impact of material deterioration on tornado fragility, focusing on commercial and government buildings at the end of their useful life. The objective is to quantify the impact of individual building material deterioration on the EF-scale tornado ranking and wind speed values associated with each DI and DOD. Additionally, the research aims to identify whether building or facility managers prioritize the same components as NWS officials during post-event storm surveys.

5.1 Key Findings

Facility Condition Assessments (FCAs): Through survey analysis, the research uncovers differences between the priorities of facility managers during FCAs and NWS during post-event storm surveys. While facility managers often focus on operational and maintenance concerns, NWS post-event storm surveys prioritize structural integrity and safety. Though there is an overlap between these areas, such as occupant safety inherently encompassing structural integrity, each group may prioritize these aspects differently based on their specific roles and expertise. This misalignment underscores the importance of harmonizing pre- and post-event storm surveys to ensure comprehensive risk mitigation strategies. The research reveals that roofing, sprinklers & fire alarm systems are prioritized assets during FCAs, with windows,

HVAC systems, HVAC refrigerant gases, and electrical systems also receiving significant attention. However, there is a notable misalignment between the components that facility managers and NWS post-event storm surveys prioritize, such as walls and doors, which are a focus during post-event storm surveys, highlighting potential gaps in risk perception and mitigation strategies. While there may be differences in asset prioritization, there is underlying alignment in their recognition of critical building components and shared commitment to enhancing building resilience against tornadic events. Effective collaboration, complementary perspectives, and a commitment to continuous improvement are key factors that contribute to bridging the gap and ensuring alignment between the two factions.

Building Material Deterioration Impacts to Fragility Curves: Using a Markov chain modeling approach, the research predicts time-based deterioration trends for various building components, including roofs, walls, doors, and windows. The models reveal distinct degradation patterns over time, with some walls and roofs exhibiting accelerated deterioration under certain conditions, while doors project a lower overall deterioration probability in condition states 2, 3, and 4. These insights provide valuable guidance for proactive maintenance strategies and asset management practices. Additionally, deterioration rate models for different maintenance scenarios, ranging from poor to excellent maintenance practices, are developed. Analysis of deterioration rates for various building materials reveals significant variability in degradation patterns, with implications for the development of fragility curves.

The findings following the development of fragility curves shed light on the dynamic relationship between material deterioration and tornado vulnerability, particularly concerning the leftward shift in wind speed thresholds observed across the various building materials and time

intervals, bringing attention to an observed decrease in wind speed thresholds. The observed decrease in wind speed requirements for damage initiation highlights the increased susceptibility of structures to wind-induced damage as materials degrade over time. While a 4% decrease on average in wind speed thresholds may seem modest, its cumulative effect over time can significantly compromise the structural integrity of buildings, leading to heightened risks of damage and failure. By quantifying the impact of deterioration on building components over time, the research highlights the importance of accurately incorporating time-dependent fragilities into vulnerability studies to assess tornado risk.

Fragility Functions and EF Scale Analysis: Through a comparative analysis of pristine and deteriorated fragility curves, the research reveals consistent leftward shifts in fragility curves for deteriorated materials compared to pristine counterparts across designated time intervals, indicative of a progressive increase in vulnerability over time. These shifts underscore the impact of material deterioration, leading to decreased wind speed thresholds for damage initiation and a significant increase in the likelihood of damage occurrence. Quantifying and mapping the percentage shifts in wind speed thresholds highlight the magnitude of this vulnerability, with deteriorated materials exhibiting reductions in wind speed thresholds across different EF scales and Degree of Damage categories. For example, the wind speed threshold previously associated with EF2 damage in pristine materials may now correspond to EF3 damage. The research found that deterioration-induced changes in material properties may directly influence material fragility, with deteriorated materials exhibiting heightened susceptibility to wind-induced damage, with implications for damage rating, EF scale ranking, disaster preparedness, and mitigation efforts.

5.2 Contributions

The findings of this research carry significant implications for theory, practice, and policy-making in the field of building resilience:

1. This research facilitates more targeted risk assessment and mitigation strategies by identifying the key components prioritized during Facility Condition Assessments (FCAs) and post-event storm surveys. The research underscores the importance of interdisciplinary collaboration between facility managers, meteorologists, policymakers, and researchers in post-event storm survey efforts. By integrating expertise from various domains, stakeholders can develop holistic strategies to enhance building resilience and mitigate the impacts of tornado events on communities. Facility managers can use this information to prioritize maintenance and repair efforts. Additionally, while building deterioration may not be explicitly mentioned in insurance policies, it can influence the assessment of claims following tornadic events. Insurers consider various factors, including pre-existing conditions, maintenance practices, and policyholder obligations, when evaluating claims and determining coverage. This research highlights the importance of property owners maintaining their buildings adequately and promptly addressing any signs of deterioration to avoid potential issues with insurance claims.
2. This research highlights the dynamic nature of material vulnerability to tornado events over time due to deterioration. By quantifying the shifts in EF ranking and DODs associated with material degradation, the research provides valuable insights into the evolving risk profiles of buildings and structures. The observed leftward

- shifts in fragility curves and changes in EF ranking and DOD wind speed thresholds underscore the inadequacy of existing evaluation protocols that do not account for material deterioration. Post-event storm surveys may now consider the impact of aging and degradation on building resilience to assess structural integrity and accurately prioritize repair and reconstruction efforts.
3. Storm survey crews may be encouraged to prioritize assessments in newer construction neighborhoods, defined as those constructed within the past 10 -15 years, where feasible. “Newer” in the context of this research may be defined as 10-15 years where the findings exhibit a significant leftward shift in the fragility curves.
 4. In addition to assessing immediate storm damage, future engineering reconnaissance efforts may consider incorporating evaluations for signs of material deterioration. By systematically benchmarking the condition of building materials during post-event surveys, valuable data can be collected to track degradation trajectories. This proactive approach to monitoring material conditions enhances our understanding of structural vulnerability and provides essential data for validating fragility models.
 5. The development of time-dependent deterioration models and fragility curves emphasizes the importance of proactive maintenance and repair interventions to address material aging and degradation. By quantifying the impact of deterioration on building vulnerability, the research highlights the need for regular inspections and timely repairs to maintain structural integrity over time.
 6. The result of this research may lead to educating the public about the potential risks associated with building deterioration during tornado events, which can empower

individuals to make informed decisions about their safety. While taking shelter remains paramount for personal safety during tornado events, understanding the relationship between building deterioration and structural vulnerability can enhance overall emergency preparedness and response efforts.

7. This research provides decision-makers with empirical evidence on the shifting wind speed thresholds and changes in material vulnerability over time. This information can inform policy decisions related to building codes, zoning regulations, and disaster preparedness planning, enabling more informed decision-making processes prioritizing public safety and resilience.

5.3 Future Research Recommendations

This research has advanced the understanding of tornado fragility and building resilience through a multifaceted analysis of material deterioration effects. The findings have laid the groundwork for informed decision-making, disaster preparedness, and risk mitigation strategies by revealing the interconnectedness between maintenance practices, material properties, and structural vulnerability. By integrating considerations of material deterioration into maintenance practices and resilience planning, practitioners and policymakers can enhance the resilience of built environments and minimize the potential impacts of extreme weather events.

Building on the findings, several avenues for future research merit exploration:

1. Conducting longitudinal studies to monitor material deterioration and building resilience over extended periods can provide deeper insights into time-based trends and dynamics. By tracking degradation patterns and assessing the effectiveness of maintenance interventions, researchers can refine existing models and develop more accurate building

performance predictions. Conducting comprehensive field studies can validate vulnerability models and evaluate the real-world performance of deteriorated building components under tornado conditions.

2. Exploring advanced modeling techniques like machine learning algorithms or agent-based modeling may enhance deterioration models' predictive power and scalability. Researchers can capture complex interactions between material properties, environmental factors, and maintenance practices by leveraging big data analytics and computational tools.
3. With more consistent data, other methods of deterioration prediction (such as the gamma process) and modeling of deterioration rates can be examined. These may capture the complex dynamics of tornado-induced damage and deterioration processes.
4. Future research may use real-world or experimental data to validate and verify the accuracy of the time-dependent deterioration fragility models for buildings to reduce uncertainties associated with probabilistic modeling.
5. Future research could focus on refining the time-dependent fragility model to account for additional factors influencing building vulnerability, such as structural design, construction materials, and environmental conditions. By incorporating these variables into vulnerability assessments, researchers can improve the accuracy and reliability of risk predictions and inform more effective disaster mitigation strategies.
6. Future research could investigate the combined effects of multiple insults, such as wind, floods, temperature variations, and other environmental factors, on the deterioration of built infrastructure. There is an opportunity to develop and validate fragility models that

account for the interactions between different hazards and their synergistic effects on structural vulnerability to tornadoes. Research efforts may focus on gathering comprehensive data on each hazard's frequency, intensity, duration, and spatial and temporal interactions. Advanced data analytics techniques can then be applied to analyze the combined impact of multiple insults on deterioration rates and structural fragilities.

7. While this research focuses on the fragility of individual building components' materials, the implications extend far beyond isolated material performance. Future studies may explore integrating time-dependent material-level fragility data with structural analysis tools to predict whole-building performance under tornado loading conditions. By extrapolating the findings to the holistic evaluation of entire buildings, researchers can envisage a comprehensive approach to tornado vulnerability evaluation.
8. Future research could integrate identified socioeconomic factors and community resilience measures into time-dependent deterioration tornado fragilities at the building or community level to develop all-inclusive risk management approaches. Integrating socioeconomic factors (e.g., housing tenure, income levels, etc.) and community resilience measures (e.g., infrastructure resilience, economic diversification, etc.) into time-dependent deterioration tornado fragilities can develop more comprehensive risk management strategies that address the multifaceted challenges of tornado hazards. This could be through the use of vulnerability indices (e.g., Social Vulnerability Index (SoVI), Community Resilience Index (CRI), etc.), which may help quantify the overall vulnerability of buildings or communities to tornado events by considering various socioeconomic, demographic, and environmental factors. This may allow researchers to

assess how variations in socioeconomic factors and community resilience affect the vulnerability of buildings to tornado events over time. By considering these factors, the fragility models can provide more comprehensive risk assessments that account for both structural vulnerabilities and societal vulnerabilities.

REFERENCES

- Alipour, A., Shafei, B., and Shinozuka, M. (2010). Performance Evaluation of Deteriorating Highway Bridges Located in High Seismic Areas. *Journal of Bridge Engineering*, 1(1), 117.
- Amini, M. O., and J. W. van de Lindt. (2014). Quantitative insight into rational tornado design wind speeds for residential wood-frame structures using fragility approach. *Journal of Structural Engineering*. 140 (7): 04014033. [https://doi.org/10.1061/\(ASCE\)ST.1943-541X.0000914](https://doi.org/10.1061/(ASCE)ST.1943-541X.0000914)
- American Meteorological Society (2013), "Meteorology Glossary," American Meteorological Society, retrieved from <http://glossary.ametsoc.org>
- Argyroudis, S. A., Mitoulis, S. A., Winter, M. G., & Kaynia, A. M. (2019). Fragility of transport assets exposed to multiple hazards: State-of-the-art review toward infrastructural resilience. *Reliability Engineering & System Safety*, 191, 106567–. <https://doi.org/10.1016/j.ress.2019.106567>
- American Society of Civil Engineers (ASCE), (2010), Minimum Design Loads for Buildings and Other Structures. *American Society of Civil Engineers Reston, VA*
- American Society of Civil Engineers (ASCE), (2016), Minimum Design Loads for Buildings and Other Structures. *American Society of Civil Engineers, Reston, VA.*
- American Society of Civil Engineers (ASCE), (2022), Minimum Design Loads for Buildings and Other Structures. *American Society of Civil Engineers, Reston, VA*
- Aktan, A. E., Farhey, D. N., Helmicki, A. J., Brown, D. L., Hunt, V. J., Lee, K. L., & Levi, A. (1997). Structural identification for condition assessment: experimental arts. *Journal of structural engineering*, 123(12), 1674-1684.
- Attary, N., J. W. van de Lindt, H. Mahmoud, and S. Smith. (2018). Hindcasting community-level damage to the interdependent buildings and electric power network after the 2011 Joplin, Missouri, Tornado. *Natural Hazards Review*. 20 (1): 04018027. [https://doi.org/10.1061/\(ASCE\)NH.1527-6996.0000317](https://doi.org/10.1061/(ASCE)NH.1527-6996.0000317).
- Attary, N., V. U. Unnikrishnan, J. W. van de Lindt, D. T. Cox, and A. R. Barbosa. (2017). Performance-based tsunami engineering methodology for risk assessment of structures. *Engineering Structures*. 141 (Jun): 676–686. <https://doi.org/10.1016/j.engstruct.2017.03.071>.
- Auld, H., Waller, J., Eng, S., Klaassen, J., Morris, R., Fernandez, S., ... & MacIver, D. (2010). 5.6 The changing climate and national building codes and standards.

- Bailey, B. and Galecka, C. (2008). Facility Decommissioning: A Look At Key SH&E Considerations. *Professional Safety*, 53(8).
- Baik, H. S., Jeong, H. S. & Abraham, D. M. (2006). Estimating Transition Probabilities in Markov Chain-Based Deterioration Models for Management of Wastewater Systems. *Journal of Water Resources Planning and Management ASCE*, 132(1), 15-24.
- Barbhuiya, S., & Das, B. B. (2023). Life Cycle Assessment of construction materials: Methodologies, applications and future directions for sustainable decision-making. *Case Studies in Construction Materials*, 19, e02326-. <https://doi.org/10.1016/j.cscm.2023.e02326>
- Boruff BJ, Easoz JA, Jones SD, Landry HR, Mitchem JD, Cutter SL (2003) Tornado hazards in the United States. *Climate Research*. 24:103–117
- Butt, A. A., Shahin, M.Y., Feighan, K.J. & Carpenter, S.H. (1987). Pavement performance prediction model using the Markov process (No. 1123).
- Charette, R. P., & Marshall, H. E. (1999). UNIFORMAT II elemental classification for building specifications, cost estimating, and cost analysis. U.S. Dept. of Commerce, National Institute of Science and Technology. NISTIR 6389, Gaithersburg, MD: National Institute of Standards and Technology, October.
- Choe, D.-E., Gardoni, Paolo, Rosowsky, D., and Haukaas, T. (2008). Probabilistic capacity models and seismic fragility estimates for RC columns subject to corrosion. *Reliability Engineering & System Safety*, 93(3), 383–393.
- Choe, D.-E., Gardoni, Paolo, Rosowsky, D., and Haukaas, T. (2009). Seismic fragility estimates for reinforced concrete bridges subject to corrosion. *Structural Safety*, 31(4), 275–283.
- Construction Specifications Institute (CSI) (2020) Building Product and Construction Material MasterFormat 2020 CSI Divisions. Retrieved from <https://www.csiresources.org/standards/masterformat>
- Cohen J. (1988). Statistical power analysis for behavioral sciences (2nd. Ed.). New York: Academic Press. (p.12)
- Dowdy, S., Wearden, S. & Chilko, D. (2011). *Statistics for Research*, Wiley - Interscience.
- Dziadosz, A., & Meszek, W. (2015). Selected aspects of determining of building facility deterioration for real estate valuation. *Procedia Engineering*, 122, 266-273.

Elhakeem, A. A. (2005). An asset management framework for educational buildings with life-cycle cost analysis. *Waterloo: University of Waterloo*.

Ellingwood, B. R., Rosowsky, D. V., Li, Y., & Kim, J. H. (2004). Fragility Assessment of Light-Frame Wood Construction Subjected to Wind and Earthquake Hazards. *Journal of Structural Engineering*, (December), 1921–1930.

Federal Emergency Management Agency (FEMA). (2011). National Disaster Recovery Framework: Strengthening Disaster Recovery for the Nation. <https://www.fema.gov/pdf/recoveryframework/ndrf.pdf>

Federal Emergency Management Agency (FEMA). (2015). “Safe rooms for tornadoes and hurricanes.” FEMA P-361, Washington, DC.

Federal Emergency Management Agency (FEMA). (2010). “HAZUS-MH MR5: Technical manual.” Washington, DC.

Gardner, A., K. C. Mehta, L. J. Tanner, Z. Zhou, M. Conder, R. Howard, M. S. Martinez, and S. Weinbeck. (2000). The tornadoes of Oklahoma City of May 3, 1999. Lubbock, TX: *Wind Science and Engineering Research Center, Texas Tech Univ.*

Gill, A., Genikomsou, A.S. & Balomenos, G.P. (2021). Fragility assessment of wood sheathing panels and roof-to-wall connections subjected to wind loading. *Frontiers of Structural and Civil Engineering* **15**, 867–876. <https://doi.org/10.1007/s11709-021-0745-5>

Ghosh, J., & Padgett, J. E. (2010). Aging Considerations in the Development of Time-Dependent Seismic Fragility Curves. *Journal of Structural Engineering (New York, N.Y.)*, *136*(12), 1497–1511. [https://doi.org/10.1061/\(ASCE\)ST.1943-541X.0000260](https://doi.org/10.1061/(ASCE)ST.1943-541X.0000260)

Haan, F., Jr., V. K. Balaramudu, and P. Sarkar. (2010). Tornado-induced wind loads on a low-rise building. *Journal of Structural Engineering*. *136* (1): 106–116. [https://doi.org/10.1061/\(ASCE\)ST.1943-541X.0000093](https://doi.org/10.1061/(ASCE)ST.1943-541X.0000093).

Ham, H. J., Lee, S., and Kim, H. S. (2009). Development of typhoon fragility for industrial buildings. Presented at the Seventh Asia-Pacific *Conference of Wind Engineering*. Taipei, Taiwan, Nov. 8–12.

Henley, J.E. & H., K. (1992). Probabilistic Risk Assessment. IEEE Press, Tokyo.

Houser, J.L., Bluestein, H. B., & Snyder, J. C. (2015). Rapid-Scan, Polarimetric, Doppler Radar Observations of Tornadogenesis and Tornado Dissipation in a Tornadic Supercell: The "El Reno,

Oklahoma" Storm of 24 May 2011. *Monthly Weather Review*, 143(7), 2685–2710.
<https://doi.org/10.1175/MWR-D-14-00253.1>

Hwang, B. H. H. M., and Jaw, J. (2007). Probabilistic Damage Analysis of Structures. *Journal Structural Engineering*. 116(7), pp. 1992–2007.

IPWEA - NAMS Condition Assessment & Asset Performance Guidelines. (2009).

Jain, A., Bhusar, A. A., Roueche, D. B., & Prevatt, D. O. (2020). Engineering-based tornado damage assessment: Numerical tool for assessing tornado vulnerability of residential structures. *Frontiers in Built Environment*, 6, 89.

Johnson, V.E., and Albert, J.H. (1992). Ordinal Data Modeling. Springer, Amsterdam.

Jordan, J. W. (2007). Tornado damage assessment for structural engineers. In *Forensic Engineering Conference. at Structures Congress*, 1–17. Reston, VA: ASCE.
[https://doi.org/10.1061/40943\(250\)2](https://doi.org/10.1061/40943(250)2).

Kliener, Y., and Rajani, B. (2001). Comprehensive review of structural deterioration of water Mayo, G., & Karanja, P. (2018). Building condition assessments—methods and metrics. *Journal of Facility Management Education and Research*, 2(1), 1-11. doi.org/10.22361/jfmer/91666

Koliou, M., Masoomi, H., & van de Lindt, J. W. Fragility assessment of buildings with rigid walls/flexible roof diaphragms subjected to earthquake and tornado. (2017). *16th World Conference on Earthquake, 16WCEE 2017*. Santiago, Chile, January 9th to 13th, 2017. Paper No. 2946.

Koliou, M., Filiatrault, A., Kelly, D. J., and Lawson, J. (2014). Numerical Framework for Seismic Collapse Assessment of Rigid Wall Flexible Diaphragm Structures. NCEE 2014—10th U.S. National Conference on Earthquake Engineering: *Frontiers of Earthquake Engineering*, Anchorage, AK, July 21–25.

Koliou, M., and J.W. van de Lindt. (2020). Development of building restoration functions for use in community recovery planning to tornadoes. *American Society of Civil Engineers*. 21 (2): 04020004. [https://doi.org/10.1061/\(ASCE\)NH.1527-6996.0000361](https://doi.org/10.1061/(ASCE)NH.1527-6996.0000361)

Koliou, M., Masoomi, H., & van de Lindt, J. W. (2017). Performance Assessment of Tilt-Up Big-Box Buildings Subjected to Extreme Hazards: Tornadoes and Earthquakes. *Journal of Performance of Constructed Facilities*, 31(5). [https://doi.org/10.1061/\(ASCE\)CF.1943-5509.0001059](https://doi.org/10.1061/(ASCE)CF.1943-5509.0001059)

Konarsewka, M and Konarsewka, A. (2006). Chosen Aspects of Defining Technical Wear of Buildings.: Technological and Economic Development of the Economy. *12*(3), 200–203. <https://doi.org/10.3846/13928619.2006.9637742>

Konior, J. (2021). Over durability and Technical Wear of Materials Used in the Construction of Old Buildings. *Materials* 14, no. 2: 378. <https://doi.org/10.3390/ma14020378>

Kuzin, S.A. & Adams, B.J. (2005). Probabilistic Approach to the Estimation of Urban Stormwater Pollution Loads in Receiving Waters. *World Water Congress 2005, ASCE*, pp. 143-156.

Jiang, Y., and Sinha, K.C. (1989). Bridge service life prediction model using the Markov chain. *Transportation Research Record*.

Lacasse, M A., Abhishek G, and Travis V. M. (2020). Durability and Climate Change—Implications for Service Life Prediction and the Maintainability of Buildings. *Buildings* 10, no. 3: 53. <https://doi.org/10.3390/buildings10030053>

LaFave, J.M., Gao, Z., Holder, D.E., Kuo, M.J., and Fahnestock L.A.. (2016). Commercial and residential building performance during May 20, 2013, tornado in Moore, Oklahoma. *Journal of Performance of Construction Facilities*. 30(s): 04014210. [https://doi.org/10.1061/\(ASCE\)CF.1943-5509.0000722](https://doi.org/10.1061/(ASCE)CF.1943-5509.0000722).

Laraia, M. (2018). Nuclear Decommissioning: Its History, Development, and Current Status (1st ed. 2018.). *Springer International Publishing*. <https://doi.org/10.1007/978-3-319-75916-6>

Lee, S., Ham, H.J., and Kim, H.J. (2013). “Fragility assessment for cladding of industrial buildings subjected to extreme wind.” *Journal of Asian Architecture and Building Engineering*. 12 (1): 65-72. doi:10.3130/jaabe.12.65

Lee, J., Lee, Y.J., Kim, H., and Sim S-H. (2016). A new methodology development for flood fragility curve derivation considering structural deterioration for bridges. *Smart Structures and Systems*, 17,(1), 149 – 165. <http://dx.doi.org/10.12989/sss.2016.17.1.149>

Lewis, B. T. and Payant, R. P. (2000). Facility Inspection Field Manual: A Complete Condition Assessment Guide, McGraw–Hill, New York, U.S.A

Li Y, Ellingwood B R. Hurricane damage to residential construction in the US: Importance of uncertainty modeling in risk assessment. *Engineering Structures*, 2006, 28(7): 1009–1018

- Liu, Z., Ishihara, T., He, X., & Niu, H. (2016). LES study on the turbulent flow fields over complex terrain covered by vegetation canopy. *Journal of Wind Engineering and Industrial Aerodynamics*, 155, 60-73.
- Lombardo, F. T., Wienhoff, Z. B., Rhee, D. M., Nevill, J. B., & Poole, C. A. (2023). An Approach for Assessing Misclassification of Tornado Characteristics Using Damage. *Journal of Applied Meteorology and Climatology*, 62(6), 781–799. <https://doi.org/10.1175/JAMC-D-22-0197.1>.
- Madanat, S., and Ibrahim, W. H. W. (1995). Poisson regression models of infrastructure transition probabilities. *Journal of Transportation Engineering*. 121(3), 267–272.
- Madanat, S., Mishanlani, R., and Ibrahim, W. H. W. (1995). Estimation of infrastructure transition probabilities from condition rating data. *Journal of Infrastructure Systems*, 1(2), 120–125.
- Marshall, T. P. (2002). Tornado damage survey at Moore, Oklahoma. *Weather Forecasting*. 17 (3): 582–598. [https://doi.org/10.1175/1520-0434\(2002\)017<0582:TDSAMO>2.0.CO;2](https://doi.org/10.1175/1520-0434(2002)017<0582:TDSAMO>2.0.CO;2).
- Mattinzioli, T., Lo Presti, D., & Jiménez del Barco Carrión, A. (2022). A critical review of life cycle assessment benchmarking methodologies for construction materials. *Sustainable Materials and Technologies*, 33, e00496-. <https://doi.org/10.1016/j.susmat.2022.e00496>
- Morcous, G., Rivard, H., and Hanna, A. M. (2002). Case-based reasoning system for modeling infrastructure deterioration. *Journal of Computing in Civil Engineering*. 10.1061/(ASCE)0887-3801(2002)16:2(104), 104–114.
- Masoomi, H., and J.W. van de Lindt. (2016). “Tornado fragility and risk assessment of an archetype masonry school building.” *Engineering Structures*. 128 (Dec): 26-43. <https://doi.org/10.1016/j.engstruct.2016.09.30>.
- Masoomi, H., and J.W. van de Lindt. (2017). “Restoration and functionality assessment of a community subjected to tornado hazard.” *Structural Infrastructure. Eng.* 14 (3): 275-291. <https://doi.org/10.1080/15732479.2017.1354030>.
- Masoomi, H., van de Lindt, J. W., and Peek, L. (2018). Quantifying socioeconomic impact of a tornado by estimating population outmigration as a resilience metric at the community level. *Journal of Structural Engineering*. 144 (5):04018034. [https://doi.org/10.1061/\(ASCE\)ST.1943-541X.0002019](https://doi.org/10.1061/(ASCE)ST.1943-541X.0002019).

Masoomi, H., Ameri, M. R., and van de Lindt, J. W. (2018). Wind Performance Enhancement Strategies for Residential Wood-Frame Buildings, *Journal of Performance of Constructed Facilities*. 32(3), pp. 1–13.

Masters, L.W. and Brandt, E. (1987). Prediction of service life of building materials and components, in CIB W80/RILEM 71-PSL-Final Report, RILEM Technical Committees

Mayo, G., & Karanja, P. (2018). Building condition assessments—methods and metrics. *Journal of Facility Management Education and Research*, 2(1), 1-11. doi.org/10.22361/jfmer/91666

Memari, M., Attary, N., Masoomi, H., Mahmoud, H., van de Lindt, J. W., Pilkington, S. F., & Ameri, M. R. (2018). Minimal Building Fragility Portfolio for Damage Assessment of Communities Subjected to Tornadoes. *Journal of Structural Engineering (New York, N.Y.)*, 144(7). [https://doi.org/10.1061/\(ASCE\)ST.1943-541X.0002047](https://doi.org/10.1061/(ASCE)ST.1943-541X.0002047)

Munich Re, 2005: Flooding and Insurance (1997). Munich Reinsurance Group, Munich, Germany.

Micevski, T., Kuczera, G., and Coombes, P. (2002). Markov model for stormwater pipe deterioration. *Journal of Infrastructure Systems*. 8(2), 49–56.

Moeller, C. 2012. *Basics of Engineering Statistics*, White Word Publications.

Montgomery, D. C., Runger, G. C. & Hubele, N. F. (2004). *Engineering Statistics*, New York, Wiley.

Mohseni, H., Setunge, S., Zhang, G., & Wakefield, R. (2017). Markov process for deterioration modeling and asset management of community buildings. *Journal of Construction Engineering and Management*, 143(6), 04017003.

Mohseni H., Setunge S., Zhang G., and Wakefield R. (2012). Probabilistic deterioration prediction and cost optimization for community buildings using Monte-Carlo simulation. *ICOMS Asset Management Conference. 2012. Hobart Australia: Asset Management Council Limited.*

National Institute of Science and Technology. (2014). Technical Investigation of the May 23, 2011 tornado in Joplin, Missouri. NIST NCSTAR 3. Gaithersburg, MD: US Dept of Commerce, NIST.

NOAA (National Oceanic and Atmospheric Administration). (2019). “U.S. Tornado Climatology. Accessed July 15, 2019. <https://www.ncdc.noaa.gov/climate-information/extreme-events/us-tornado-climatology>.

NOAA (National Oceanic and Atmospheric Administration). (2017). “Deadliest tornadoes.” Accessed October 9, 2017. <https://www.ncdc.noaa.gov/climate-information/extreme-events/us-tornado-climatology/deadliest> NOAA (National Oceanic and Atmospheric Administration). 2017. “Deadliest tornadoes.” Accessed October 9, 2017. <https://www.ncdc.noaa.gov/climate-information/extreme-events/us-tornado-climatology/deadliest>.

NIST/SEMATECH (2012). E-Handbook of Statistical Methods.

NWS (National Weather Service). (2014). The May 2013 Oklahoma tornadoes and flash flooding. National Weather Service. <https://www.weather.gov/oun/events-20130531>

Ortiz-Garcia, J., Costello, S. & Snaith, M. S. (2006). Derivation of transition probability matrices for pavement deterioration modeling. *Journal of Transportation Engineering*, 132.

Pan, K., P. Montpellier, and M. Zadeh. (2002). “Engineering observations of 3 May 1999 Oklahoma tornado damage.” *Weather Forecasting* 17 (3): 599–610. [https://doi.org/10.1175/1520-0434\(2002\)017<0599:EOMOT>2.0.CO;2](https://doi.org/10.1175/1520-0434(2002)017<0599:EOMOT>2.0.CO;2).

Pandey, M. D., & Yuan, X. X. (2006). A comparison of probabilistic models of deterioration for life cycle management of structures. In *Advances in Engineering Structures, Mechanics & Construction* (pp. 735-746). Springer Netherlands.

Peng, X., Roueche, D. B., Prevatt, D. O., & Gurley, K. R. (2016). An Engineering-Based Approach to Predict Tornado-Induced Damage. In *Multi-hazard Approaches to Civil Infrastructure Engineering* (pp. 311–335). Springer International Publishing. https://doi.org/10.1007/978-3-319-29713-2_15

Prevatt, D. O., J.W. van de Lindt, A. Graettinger, W. Coulbourne, R. Gupta, S. Pei, S. Hensen, and D. Grau. (2011). Damage study and future direction for structural design following the Tuscaloosa tornado of 2011, 1–56. Alexandria, VA: National Science Foundation.

Prevatt, D. O., D. B. Roueche, J. W. van de Lindt, S. Pei, T. Dao, W. Coulbourne, A. J. Graettinger, R. Gupta, and D. Grau. (2012). Building damage observations and EF classifications from the Tuscaloosa, AL, and Joplin, MO, Tornadoes. *Procurement*. Structures Congress 2012, 999–1010. Reston, VA: ASCE.

Refan, M., Romanic, D., Parvu, D., & Michel, G. (2020). Tornado loss model of Oklahoma and Kansas, United States, based on the historical tornado data and Monte Carlo simulation. *International Journal of Disaster Risk Reduction*, 43, 101369-. <https://doi.org/10.1016/j.ijdr.2019.101369>

- Roueché, D. B., and D. O. Prevatt. (2013). "Residential damage patterns following the 2011 Tuscaloosa, AL and Joplin, MO Tornadoes." *Journal of Disaster Resources*. 8 (6): 1061–1067. <https://doi.org/10.20965/jdr.2013.p1061>.
- Rosowsky, David V., & Ellingwood, B. R. (2002). Performance-Based Engineering of Wood Frame Housing: Fragility Analysis Methodology. *Journal of Structural Engineering*, 128(1), 32.
- Rugless, J. M. (1993). Condition assessment surveys. *AIPE FACILITIES*, 20, 11-11.
- Sabareesh, Geetha Rajasekharan, Masahiro Matsui, and Yukio Tamura. (2013). Ground roughness effects on internal pressure characteristics for buildings exposed to tornado-like flow. *Journal of Wind Engineering and Industrial Aerodynamics* 122 (2013): 113-117.
- Sharabah, A., Setunge, S. & Zeephongsekul, P. (2006). Use of Markov chain for deterioration modeling and risk management of infrastructure assets. *Information and Automation, 2006. ICIA 2006. International Conference on, 2006. IEEE*, 384-389.
- Sharabah, A., Setunge, S. & Zeephongsekul, P. (2007). A Reliability-Based Approach for Service Life Modeling of Council Owned Infrastructure Assets. *ICOMS Asset Management Conference*. Melbourne, Australia.
- Schoen, L. J. 2010. Preventive Maintenance Guidebook: Best Practices to Maintain Efficient and Sustainable Buildings. *Building Owners and Managers Association (BOMA) International*.
- Shafieezadeh, A., Onyewuchi, U. P., Begovic, M. M., & DesRoches, R. (2014). Age-Dependent Fragility Models of Utility Wood Poles in Power Distribution Networks Against Extreme Wind Hazards. *IEEE Transactions on Power Delivery*, 29(1), 131–139. <https://doi.org/10.1109/TPWRD.2013.2281265>
- Shafieezadeh, A. K. Ramanathan, J. E. Padgett, and R. DesRoches. (2011) Fractional order intensity measures for probabilistic seismic demand modeling applied to highway bridges. *Earthquake Engineering Structural Dynamics*. vol. 41, pp. 391–409, May 2011.
- Standohar-Alfano, C. D., J. W. van de Lindt, and B. R. Ellingwood. (2017). Vertical load path failure risk analysis of residential wood-frame construction in Tornadoes. *Journal of Structural Engineering*. 143 (7): 04017045. [https://doi.org/10.1061/\(ASCE\)ST.1943-541X.0001775](https://doi.org/10.1061/(ASCE)ST.1943-541X.0001775).
- Structural Extreme Events Reconnaissance (StEER). (2019). VAST Handbook: DE/QC - US Windstorm Building Resilience through Reconnaissance. Version 2.0 | Released August 23, 2019
- Swiss Re, (1997). Tropical Cyclones. Swiss Reinsurance Company. Zurich, Switzerland.

Texas Tech University. (2006). A Recommendation for an Enhanced Fujita Scale (EF-Scale): Submitted to the National Weather Service and Other Interested Users. Wind Science and Engineering Center.

The Home Quality Mark one, Technical Manual SD239, England, Scotland & Wales, published in 2018, (2018) - <https://www.homequalitymark.com/wp-content/uploads/2018/09/HQM-ONE-Technical-Manual-SD239-.pdf>

Unanwa, C. O., McDonald, J. R., Mehta, K. C., and Smith, D. A., (2000). The Development of Wind Damage Bands for Buildings. *Journal of Wind Engineering Industrial Aerodynamics*. 84(1), pp. 119–149.

Tran, H. D. (2007). Investigation of Deterioration Models for Storm Water Pipe Systems. PhD Thesis, Victoria University.

Unanwa, C. O., McDonald, J. R., Mehta, K. C., and Smith, D. A. (2000). The Development of Wind Damage Bands for Buildings. *Journal of Wind Engineering Industrial Aerodynamics*, 84(1), pp. 119–149.

Rosowsky, D. V., and Ellingwood, B. R. (2002). Performance-Based Engineering of Wood Frame Housing: Fragility Analysis Methodology. *Journal of Structural Engineering*. 128(1), pp. 32–38.

Simon, J., Bracci, J. M., and Gardoni, P. (2010). Seismic response and fragility of deteriorated reinforced concrete bridges. *Journal of Structural Engineering*. 136(10), 1273–1281.

Unanwa, C. O., McDonald, J. R., Mehta, K. C., and Smith, D. A. (2000) The Development of Wind Damage Bands for Buildings. *Journal of Wind Engineering Industrial Aerodynamics*, 84(1), pp. 119–149.

Uzarski, D.R. and L.A. Burley. (1997). Assessing Building Condition by the Use of Condition Indexes. Proceedings of the ASCE Specialty Conference Infrastructure Condition Assessment: Art, Science, Practice, pp.365-374.

Uzarski, D.R. and Grussing, M.N. (2008), Building condition assessment metrics: best practices in Amekudzi, A.A. and McNeil, S. (Eds), *Infrastructure Reporting and Asset Management. Best Practices and Opportunities*, American Society of Civil Engineers, Reston, VA. 147-152.

van de Lindt, J. W., M. O. Amini, C. Standohar-Alfano, and T. Dao. (2012). Systematic study of the failure of a light-frame wood roof in a tornado. *Buildings* 2 (4): 519–533. <https://doi.org/10.3390/buildings2040519>.

Waugaman, H., Alzarrad, M. A., & Bryce, J. (2022) Cost Estimate Risk Factors in U.S. Army Corps of Engineers Emergency Streambank Protection Projects. In *Construction Research Congress 2022* (pp. 381-390).

Wurman, J. Koshiba, K and P. Robinson. (2013) “In-situ, Doppler Radar, and Video Observations of the Interior Structure of a Tornado Wind-damage Relationship,” *Bulletin of the American Meteorological Society*. Vol.94, pp. 835-846. 2013.

Wurman, J L, Koshiba, K, Markowski, P. Richardson, Y, Doswell, D, and P. Robinson. P. (2010) Fine Scale Single and Dual Doppler Analysis of Tornado Intensification, Maintenance, and Dissipation in the Orleans, Nebraska Tornado Supercell. *Mon. Weather Review*. Vol.138, No.12, pp. 4439-4455

WSEC. (2006). A recommendation for an enhanced Fujita scale (EF-scale). Texas Tech University Wind Science and Engineering Center Rep., 95 pp. [Available online at www.depts.ttu.edu/weweb/pubs/fscale/efscale.pdf.]

Yang, L., K. R. Gurley, and D. O. Prevatt. (2013). Probabilistic modeling of wind pressure on low-rise buildings. *Journal of Wind Engineering Industrial Aerodynamics*. 114 (Mar): 18–26. <https://doi.org/10.1016/j.jweia.2012.12.014>.

Zhang, H., Cai, J., & Braun, J. E. (2023). A whole building life-cycle assessment methodology and its application for carbon footprint analysis of U.S. commercial buildings. *Journal of Building Performance Simulation*, 16(1), 38–56. <https://doi.org/10.1080/19401493.2022.2107071>

APPENDICES

7.1 APPENDIX A: DETERIORATION PREDICTION – TRANSITION MATRICES AND PROBABILITIES

Table 7.1: Transition matrices for doors, windows, and walls

Superstructure - Roof - Transition matrix					
Condition	1	2	3	4	5
1	0.43	0.15	0.29	0.12	0.01
2	0.00	0.45	0.54	0.00	0.01
3	0.00	0.00	0.93	0.07	0.00
4	0.00	0.00	0.00	1.00	0.00
5	0.00	0.00	0.00	0.00	1.00

Superstructure - External Walls - Transition matrix					
Condition	1	2	3	4	5
1	0.24	0.44	0.31	0.00	0.01
2	0.00	0.54	0.46	0.00	0.00
3	0.00	0.00	0.85	0.15	0.00
4	0.00	0.00	0.00	0.97	0.03
5	0.00	0.00	0.00	0.00	1.00

Superstructure - Windows - Transition matrix					
Condition	1	2	3	4	5
1	0.37	0.23	0.30	0.10	0.00
2	0.00	0.59	0.29	0.11	0.01
3	0.00	0.00	0.94	0.06	0.00
4	0.00	0.00	0.00	1.00	0.00
5	0.00	0.00	0.00	0.00	1.00

Superstructure - External Doors - Transition matrix					
Condition	1	2	3	4	5
1	0.60	0.10	0.27	0.02	0.01
2	0.00	0.51	0.00	0.49	0.00
3	0.00	0.00	0.93	0.06	0.01
4	0.00	0.00	0.00	0.99	0.01
5	0.00	0.00	0.00	0.00	1.00

Table 7.2: Condition State 1 Matric and Deterioration Trends for all Components

	Roof	Walls	Doors	Windows
0	1.00	1.00	1.00	1.00
10	0.43	0.24	0.60	0.37
15	0.18	0.06	0.36	0.13
20	0.08	0.01	0.22	0.05
25	0.03	0.00	0.13	0.02
30	0.01	0.00	0.08	0.01
35	0.01	0.00	0.05	0.00
40	0.00	0.00	0.03	0.00
45	0.00	0.00	0.02	0.00
50	0.00	0.00	0.01	0.00
55	0.00	0.00	0.01	0.00
60	0.00	0.00	0.00	0.00
65	0.00	0.00	0.00	0.00
70	0.00	0.00	0.00	0.00
75	0.00	0.00	0.00	0.00
80	0.00	0.00	0.00	0.00
85	0.00	0.00	0.00	0.00
90	0.00	0.00	0.00	0.00
95	0.00	0.00	0.00	0.00
100	0.00	0.00	0.00	0.00

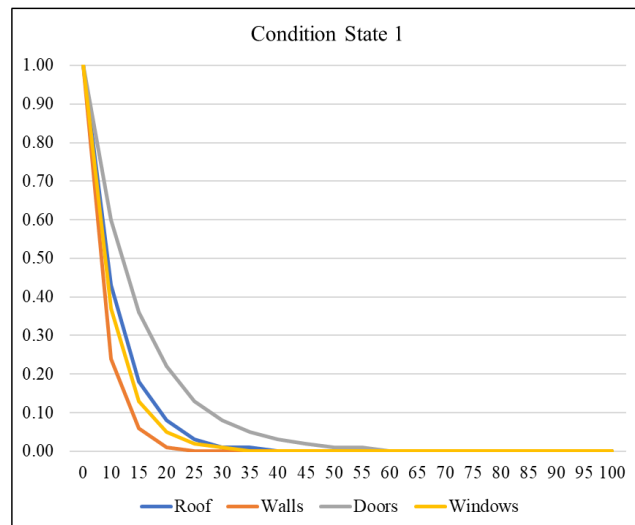


Table 7.3: Condition State 2 Matric and Deterioration Trends for all Components

	Roof	Walls	Doors	Windows
0	0.00	0.00	0.00	0.00
10	0.15	0.44	0.10	0.23
15	0.13	0.34	0.11	0.22
20	0.08	0.21	0.10	0.16
25	0.05	0.12	0.07	0.11
30	0.03	0.07	0.05	0.07
35	0.01	0.04	0.03	0.04
40	0.01	0.02	0.02	0.02
45	0.00	0.01	0.01	0.01
50	0.00	0.01	0.01	0.01
55	0.00	0.00	0.01	0.01
60	0.00	0.00	0.00	0.00
65	0.00	0.00	0.00	0.00
70	0.00	0.00	0.00	0.00
75	0.00	0.00	0.00	0.00
80	0.00	0.00	0.00	0.00
85	0.00	0.00	0.00	0.00
90	0.00	0.00	0.00	0.00
95	0.00	0.00	0.00	0.00
100	0.00	0.00	0.00	0.00

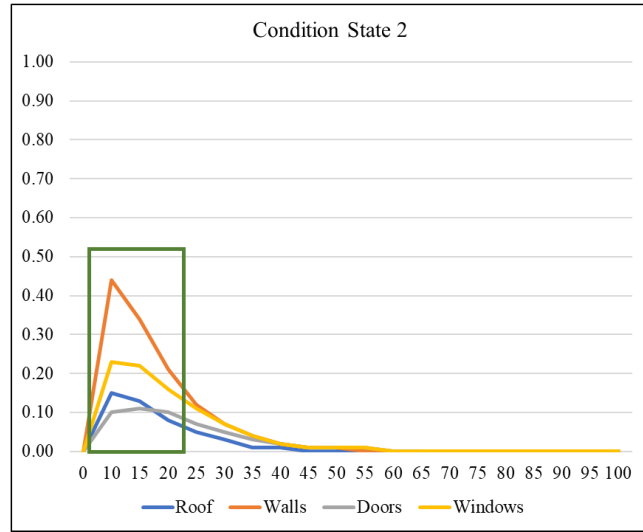


Table 7.4: Condition State 3 Matric and Deterioration Trends for all Components

	Roof	Walls	Doors	Windows
0	0.00	0.00	0.00	0.00
10	0.29	0.31	0.27	0.30
15	0.48	0.54	0.41	0.45
20	0.57	0.63	0.48	0.53
25	0.59	0.64	0.50	0.55
30	0.59	0.60	0.50	0.55
35	0.56	0.54	0.49	0.54
40	0.53	0.48	0.47	0.52
45	0.50	0.41	0.44	0.49
50	0.46	0.36	0.41	0.46
55	0.43	0.31	0.39	0.44
60	0.40	0.26	0.36	0.41
65	0.37	0.22	0.34	0.38
70	0.34	0.19	0.31	0.36
75	0.32	0.16	0.29	0.34
80	0.29	0.14	0.27	0.32
85	0.27	0.12	0.25	0.29
90	0.25	0.10	0.23	0.28
95	0.23	0.09	0.22	0.26
100	0.21	0.07	0.20	0.24

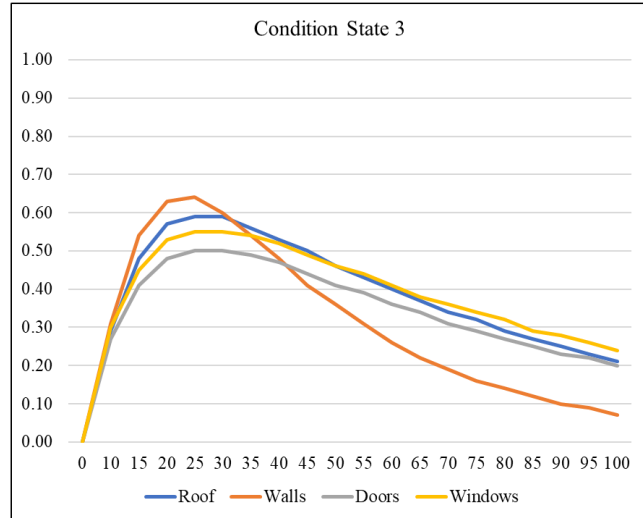


Table 7.5: Condition State 4 Matric and Deterioration Trends for all Components

	Roof	Walls	Doors	Windows
0	0.00	0.00	0.00	0.00
10	0.12	0.00	0.02	0.10
15	0.20	0.05	0.10	0.18
20	0.25	0.12	0.19	0.25
25	0.31	0.21	0.27	0.30
30	0.35	0.30	0.34	0.34
35	0.40	0.38	0.39	0.38
40	0.44	0.45	0.44	0.42
45	0.48	0.51	0.48	0.45
50	0.52	0.55	0.51	0.48
55	0.55	0.59	0.53	0.50
60	0.58	0.61	0.56	0.53
65	0.61	0.63	0.58	0.55
70	0.64	0.65	0.6	0.57
75	0.67	0.66	0.61	0.59
80	0.69	0.66	0.63	0.61
85	0.71	0.66	0.64	0.62
90	0.73	0.65	0.65	0.64
95	0.75	0.65	0.66	0.66
100	0.77	0.65	0.67	0.67

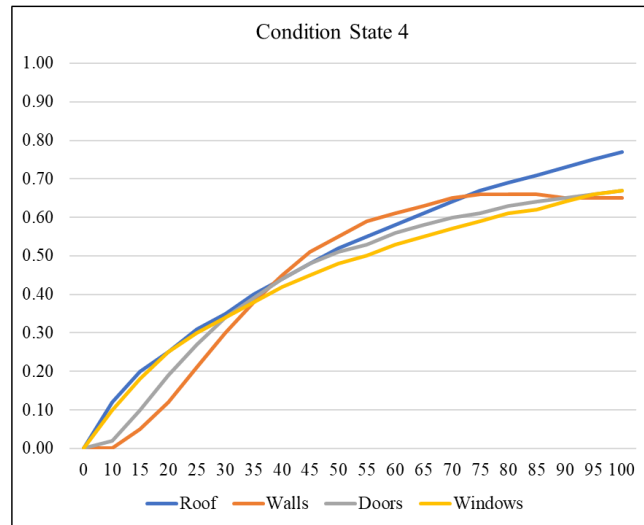
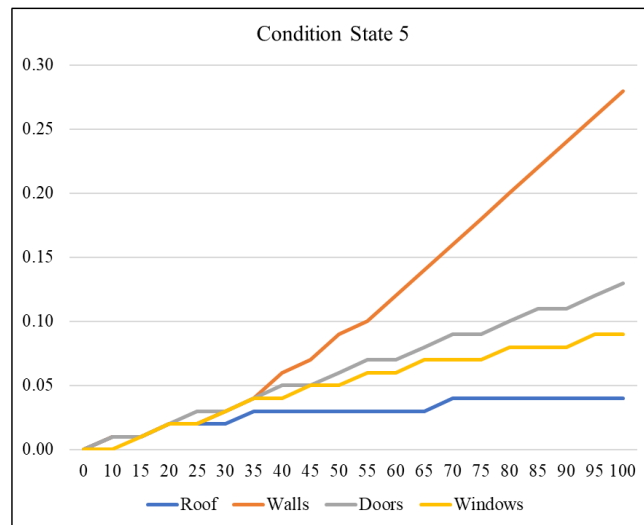


Table 7.6: Condition State 5 Matric and Deterioration Trends for all Components

	Roof	Walls	Doors	Windows
0	0.00	0.00	0.00	0.00
10	0.01	0.01	0.01	0.00
15	0.01	0.01	0.01	0.01
20	0.02	0.02	0.02	0.02
25	0.02	0.02	0.03	0.02
30	0.02	0.03	0.03	0.03
35	0.03	0.04	0.04	0.04
40	0.03	0.06	0.05	0.04
45	0.03	0.07	0.05	0.05
50	0.03	0.09	0.06	0.05
55	0.03	0.10	0.07	0.06
60	0.03	0.12	0.07	0.06
65	0.03	0.14	0.08	0.07
70	0.04	0.16	0.09	0.07
75	0.04	0.18	0.09	0.07
80	0.04	0.20	0.10	0.08
85	0.04	0.22	0.11	0.08
90	0.04	0.24	0.11	0.08
95	0.04	0.26	0.12	0.09
100	0.04	0.28	0.13	0.09



Superstructure no. of deteriorated elements vs. Age

Table 7.9: Expected Deterioration Data

Age/Condition	1	2	3	4	5
Average	13	0	0	0	0
10	10	1	2	0	0
15	7	2	3	1	0
20	5	2	4	2	1
25	4	2	4	2	1
30	3	1	5	3	1
35	2	1	5	4	2
40	2	1	4	5	2
45	2	1	4	5	2
50	1	0	4	6	2
55	1	0	3	6	3
60	1	0	3	7	3
65	0	0	2	8	3
85	0	0	2	8	4
Total	38	11	45	57	24

Table 7.10: Chi-Square Test Results

Attribute	$x^2 = \sum_{i=1}^k (O_i - E_i)^2 / E_i$	$x_{0.05,2}^2$
Regression	5.6	5.99

7.2 APPENDIX B: DETERIORATION RATES

Table 7.11: All Deterioration Rates across all Maintenance Conditions

Year	Poor Maintenance	Average Maintenance	Satisfactory Maintenance	Excellent Maintenance
Roofing - Metal, Clay, and Slate				
0	0.00	0.00	0.00	0.00
10	0.13	0.08	0.06	0.02
20	0.27	0.17	0.14	0.07
30	0.40	0.28	0.24	0.16
40	0.53	0.41	0.37	0.28
50	0.67	0.56	0.52	0.44
60	0.80	0.72	0.69	0.64
70	0.93	0.90	0.89	0.87
Roofing - Asphalt, BUR				
0	0.00	0.00	0.00	0.00
10	0.50	0.38	0.33	0.25
20	1.00	1.00	1.00	1.00
Walls - Poured Concrete Systems, Timber Frames				
0	0.00	0.00	0.00	0.00
10	0.13	0.07	0.05	0.02
20	0.25	0.16	0.13	0.06
30	0.38	0.26	0.22	0.14
40	0.50	0.38	0.33	0.25
50	0.63	0.51	0.47	0.39
60	0.75	0.66	0.63	0.56
70	0.88	0.82	0.80	0.77
80	1.00	1.00	1.00	1.00
Walls - Structural Insulated Panels				
0	0.00	0.00	0.00	0.00
10	0.13	0.08	0.06	0.02
20	0.27	0.17	0.14	0.07
30	0.40	0.28	0.24	0.16
40	0.53	0.41	0.37	0.28
50	0.67	0.56	0.52	0.44
60	0.80	0.72	0.69	0.64
70	0.93	0.90	0.89	0.87
Siding - Brick, Engineered Wood, Fiber Cement, Manufactured Stone, Vinyl				
0	0.00	0.00	0.00	0.00
10	0.10	0.06	0.04	0.01
20	0.20	0.12	0.09	0.04
30	0.30	0.20	0.16	0.09

Year	Poor Maintenance	Average Maintenance	Satisfactory Maintenance	Excellent Maintenance
Siding - Brick, Engineered Wood, Fiber Cement, Manufactured Stone, Vinyl				
40	0.40	0.28	0.24	0.16
50	0.50	0.38	0.33	0.25
60	0.60	0.48	0.44	0.36
70	0.70	0.60	0.56	0.49
80	0.80	0.72	0.69	0.64
90	0.90	0.86	0.84	0.81
100	1.00	1.00	1.00	1.00
Siding - Stucco, Metal Curtain Walling, Glass Curtain Walling				
0	0.00	0.00	0.00	0.00
10	0.20	0.12	0.09	0.04
20	0.40	0.28	0.24	0.16
30	0.60	0.48	0.44	0.36
40	0.80	0.72	0.69	0.64
Doors - Glass Personnel, Cedar				
0	0.00	0.00	0.00	0.00
10	0.25	0.16	0.13	0.06
20	0.50	0.38	0.33	0.25
30	0.75	0.66	0.63	0.56
40	1.00	1.00	1.00	1.00
Doors - Fiberglass, Steel (Fire Rated)				
0	0.00	0.00	0.00	0.00
10	0.10	0.06	0.04	0.01
20	0.20	0.12	0.09	0.04
30	0.30	0.20	0.16	0.09
40	0.40	0.28	0.24	0.16
50	0.50	0.38	0.33	0.25
60	0.60	0.48	0.44	0.36
70	0.70	0.60	0.56	0.49
80	0.80	0.72	0.69	0.64
90	0.90	0.86	0.84	0.81
Doors - Pine and Vinyl				
0	0.00	0.00	0.00	0.00
10	0.50	0.38	0.33	0.25
20	1.00	1.00	1.00	1.00

Year	Poor Maintenance	Average Maintenance	Satisfactory Maintenance	Excellent Maintenance
Doors - Mahogany				
0	0.00	0.00	0.00	0.00
10	0.17	0.10	0.07	0.03
20	0.33	0.22	0.19	0.11
30	0.50	0.38	0.33	0.25
40	0.67	0.56	0.52	0.44
50	0.83	0.76	0.74	0.69
60	1.00	1.00	1.00	1.00
Windows - Window Glazing				
0	0.00	0.00	0.00	0.00
10	1.00	1.00	1.00	1.00
0	0.00	0.00	0.00	0.00
10	0.50	0.38	0.33	0.25
20	1.00	1.00	1.00	1.00
Windows - Wood				
0	0.00	0.00	0.00	0.00
10	0.33	0.22	0.19	0.11
20	0.67	0.56	0.52	0.44
30	1.00	1.00	1.00	1.00

7.3 APPENDIX C: TIME-DEPENDENT FRAGILITY CURVES – PRISTINE VS DETERIORATING BUILDINGS

Time-dependent Fragility Curves - Asphalt Shingles

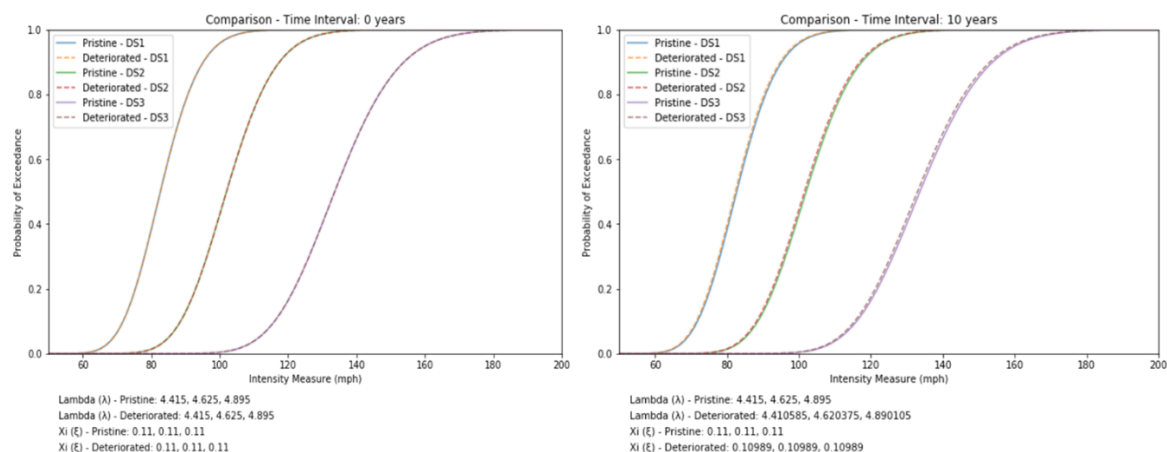


Figure 7.1: Lognormal best-fitted asphalt shingles fragilities at 0 and 10-year intervals

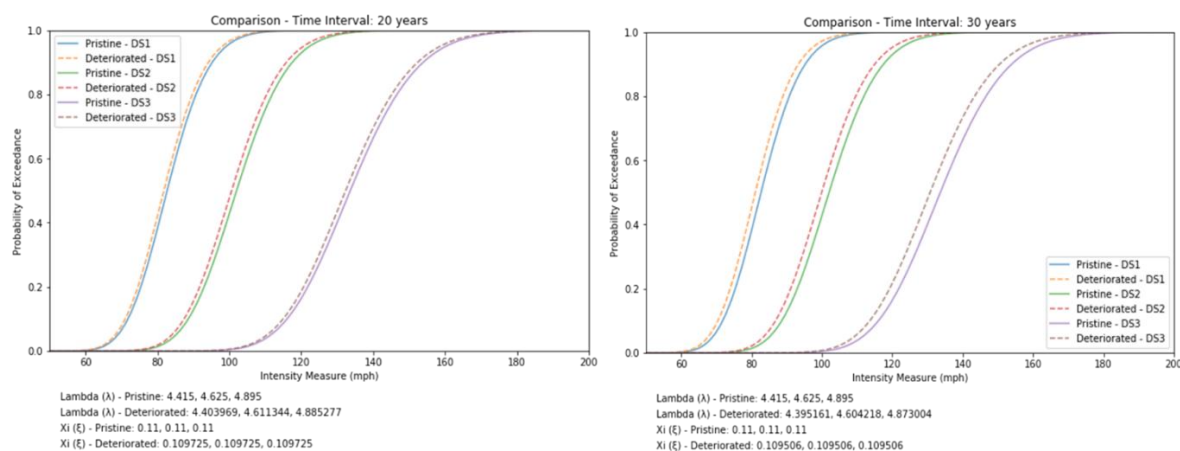


Figure 7.2: Lognormal best-fitted asphalt shingles fragilities at 20 and 30-year intervals

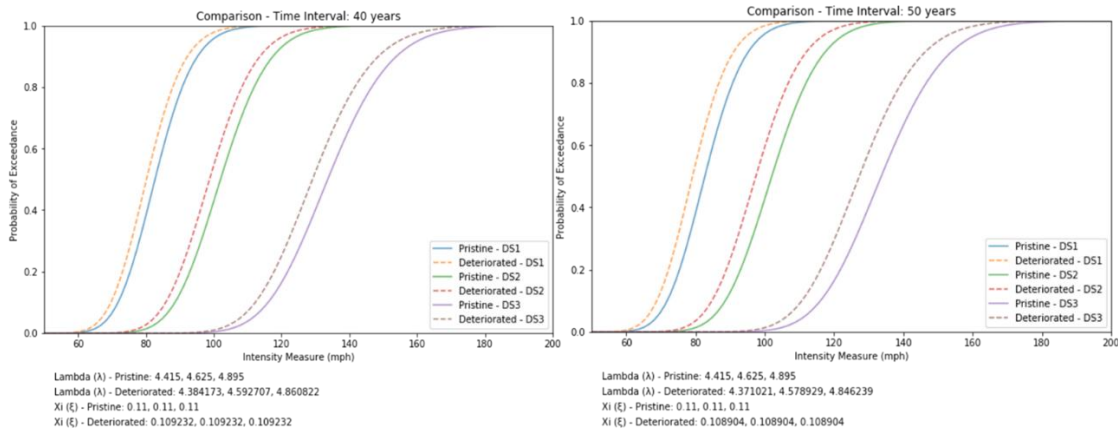


Figure 7.3: Lognormal best-fitted asphalt shingles fragilities at 40 and 50-year intervals

Time-dependent Modeling failure of structural components using fragilities - Clay Tiles

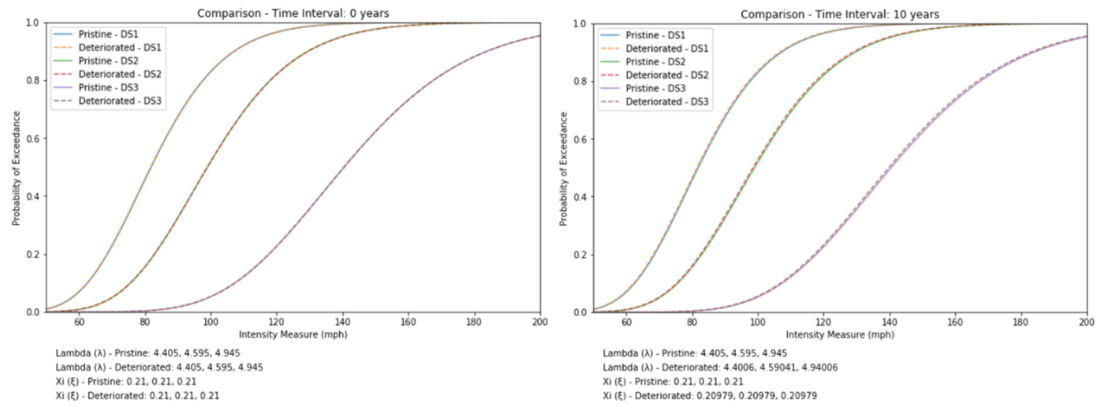


Figure 7.4: Lognormal best-fitted clay tile fragilities at 0 and 10-year intervals

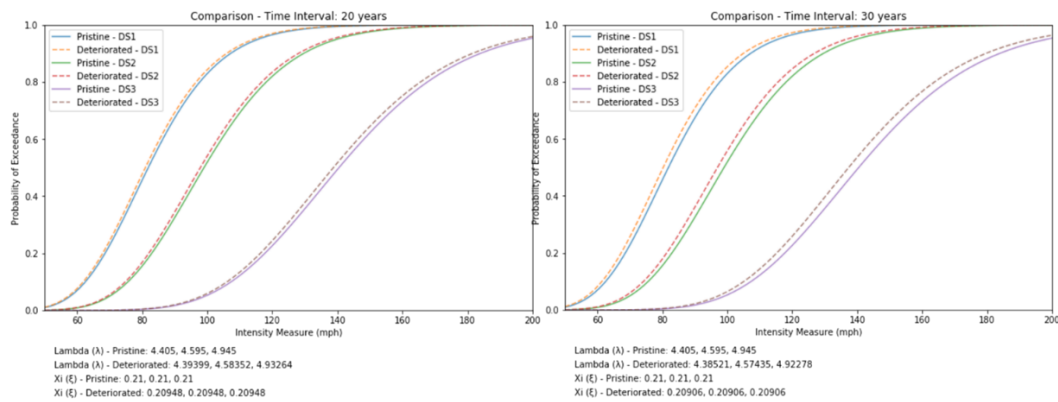


Figure 7.5: Lognormal best-fitted clay tiles fragilities at 20 and 30-year intervals

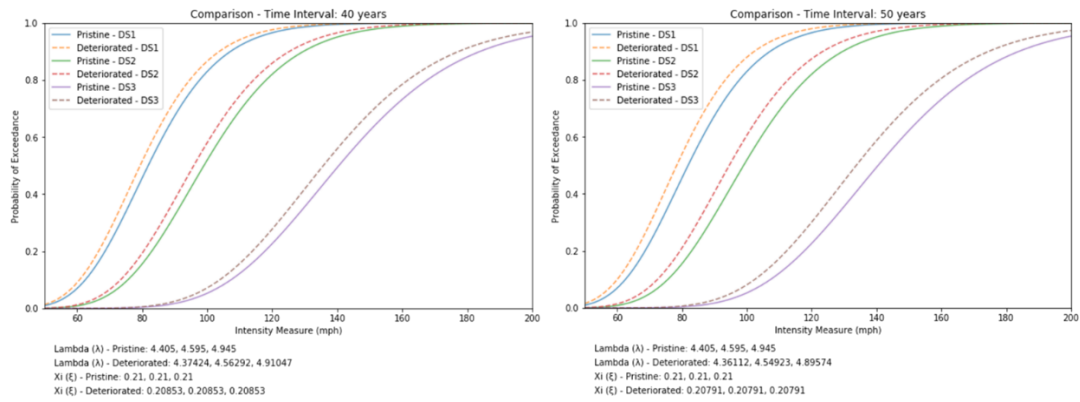


Figure 7.6: Lognormal best-fitted clay tiles fragilities at 40 and 50-year intervals

Time-dependent Modeling failure of structural components using fragilities – Walls

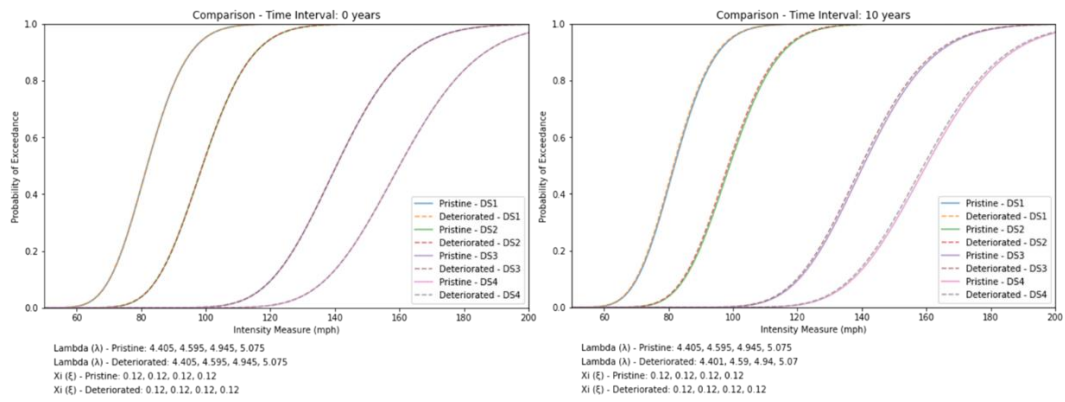


Figure 7.7: Lognormal best-fitted wall fragilities at 0 and 10-year intervals

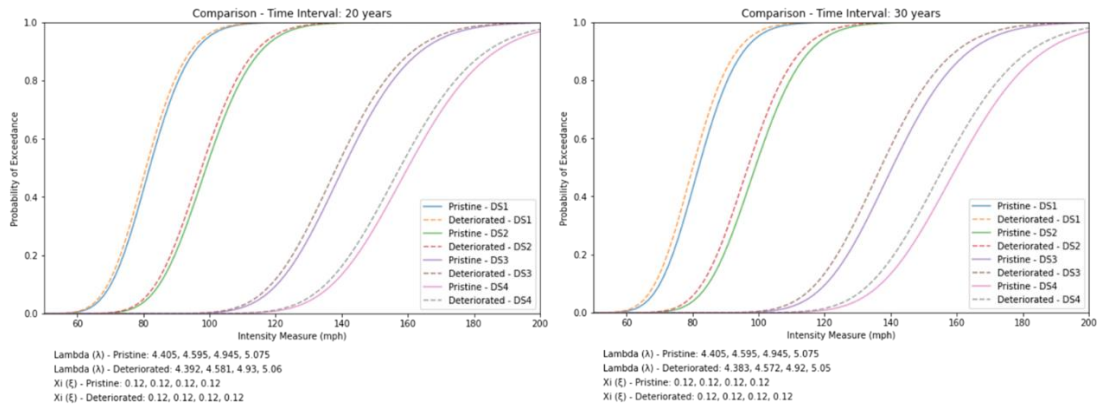


Figure 7.8: Lognormal best-fitted wall fragilities at 20 and 30-year intervals

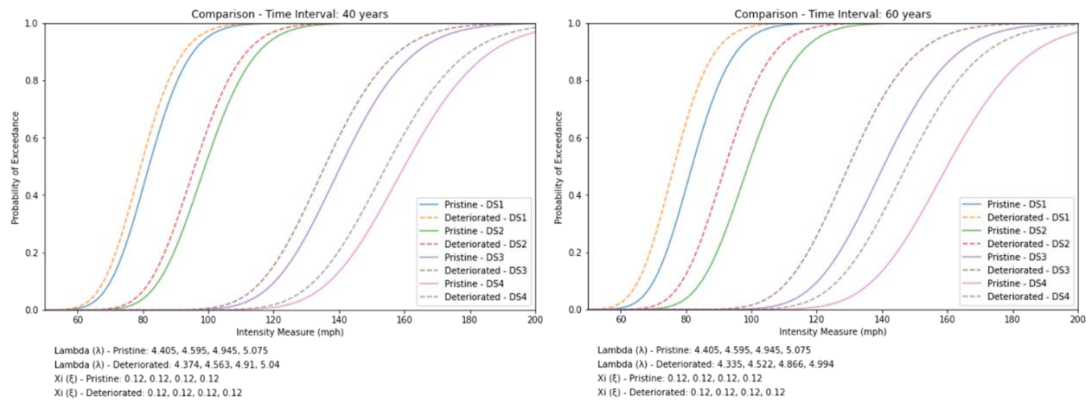


Figure 7.9: Lognormal best-fitted wall fragilities at 40 and 50-year intervals

Time-dependent Modeling failure of structural components using fragilities – Doors

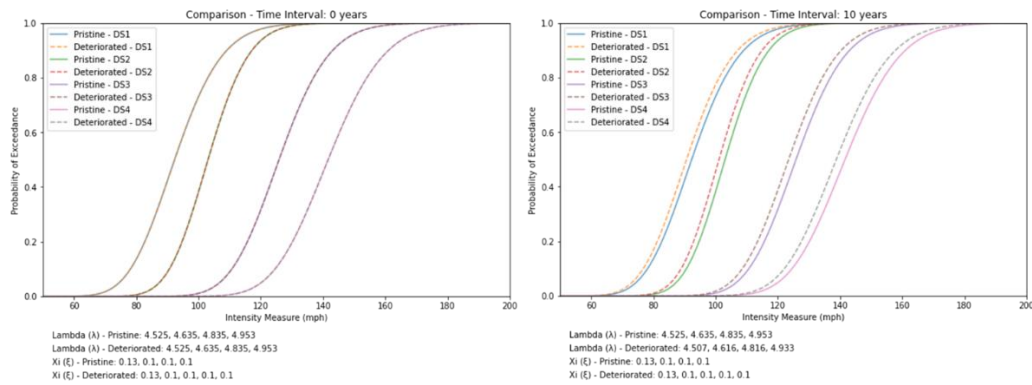


Figure 7.10: Lognormal best-fitted door fragilities at 0 and 10-year intervals

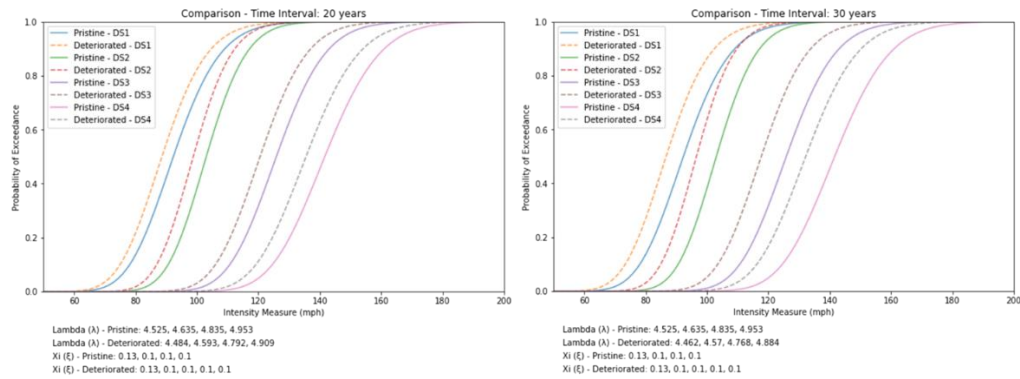


Figure 7.11: Lognormal best-fitted door fragilities at 20 and 30-year intervals

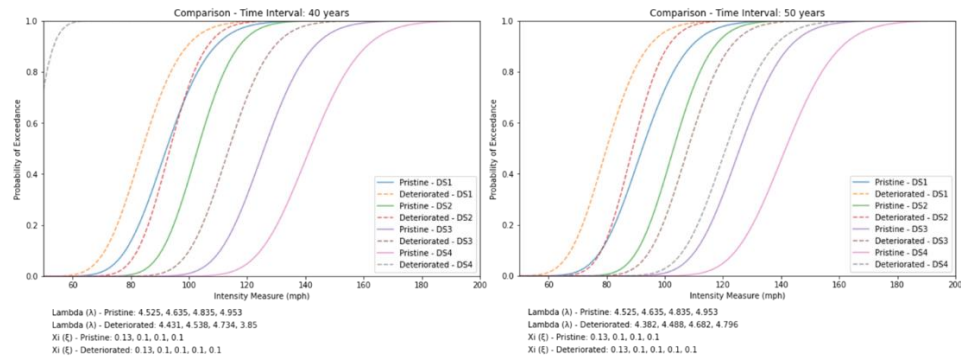


Figure 7.12: Lognormal best-fitted door fragilities at 40 and 50-year intervals

Time-dependent Modeling failure of structural components using fragilities – Windows

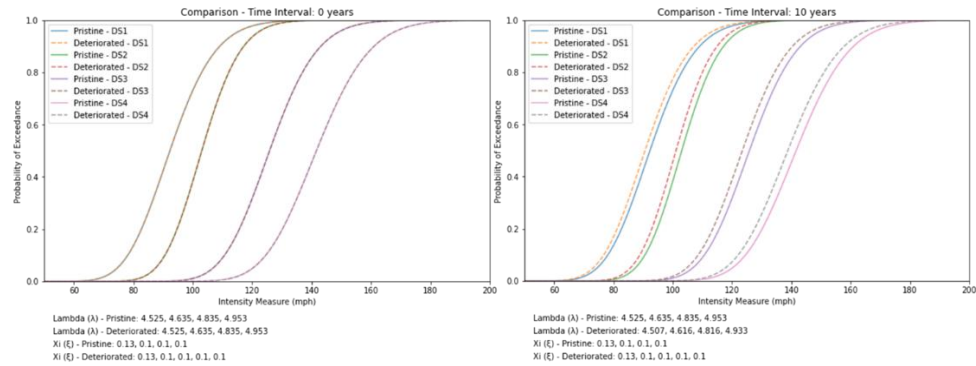


Figure 7.13: Lognormal best-fitted window fragilities at 0 and 10-year intervals

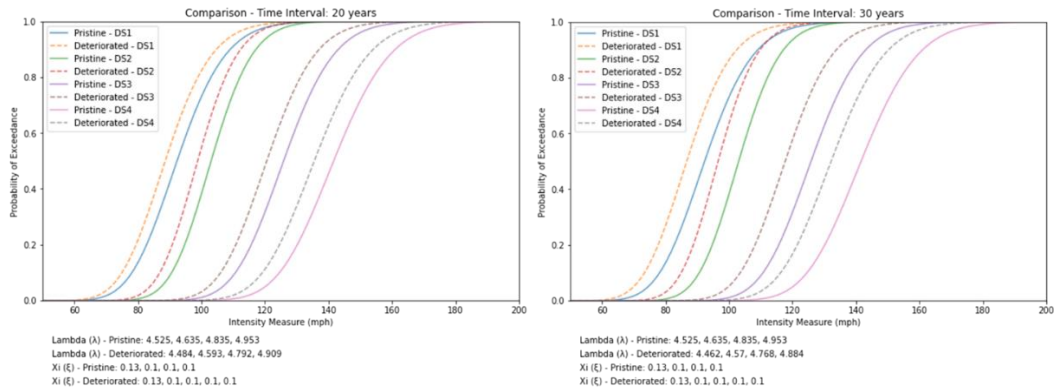


Figure 7.14: Lognormal best-fitted window fragilities at 20 and 30-year intervals

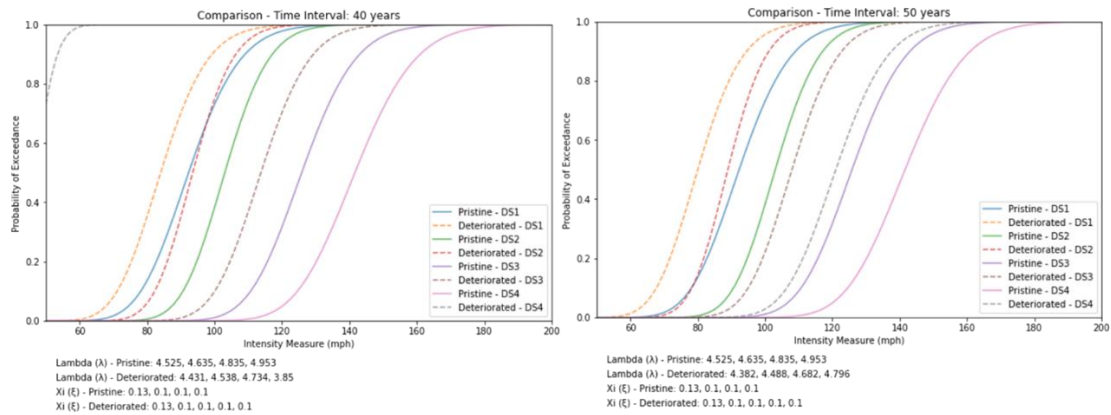


Figure 7.15: Lognormal best-fitted window fragilities at 40 and 50-year intervals

Time-dependent Modeling failure of structural components using fragilities - Aluminum Siding

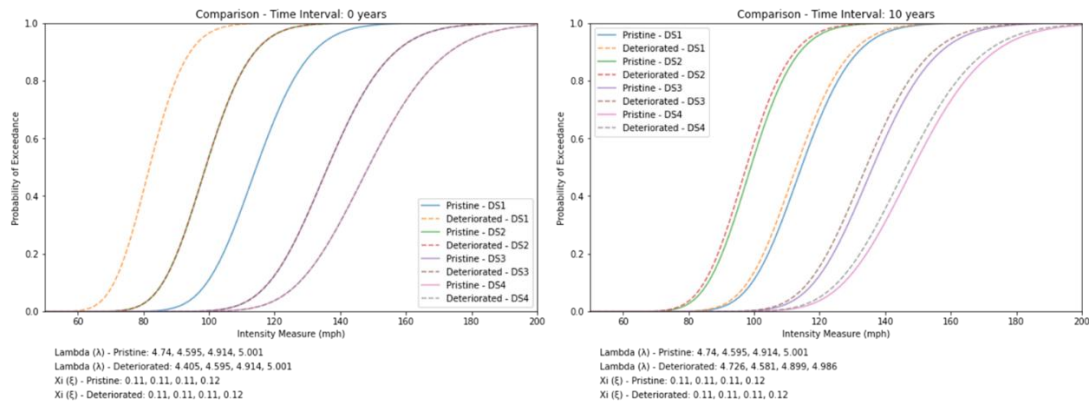


Figure 7.16: Lognormal best-fitted aluminum siding fragilities at 0 and 10-year intervals

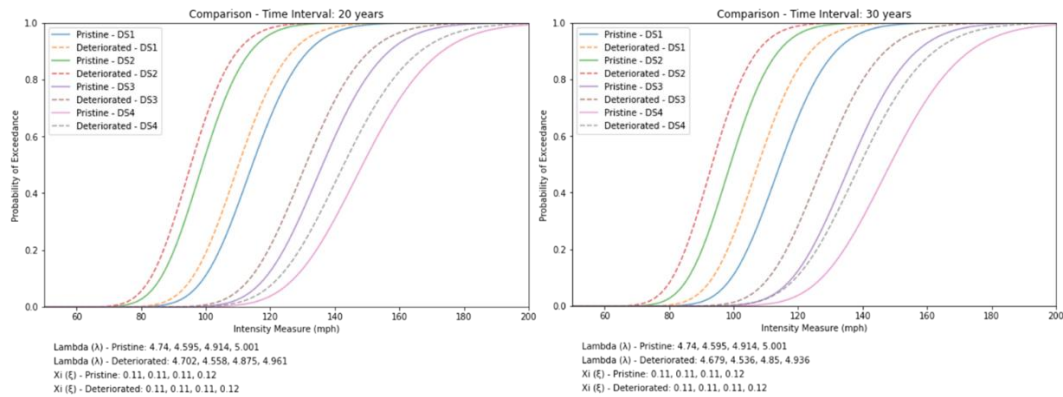


Figure 7.17: Lognormal best-fitted aluminum siding fragilities at 20 and 30-year intervals

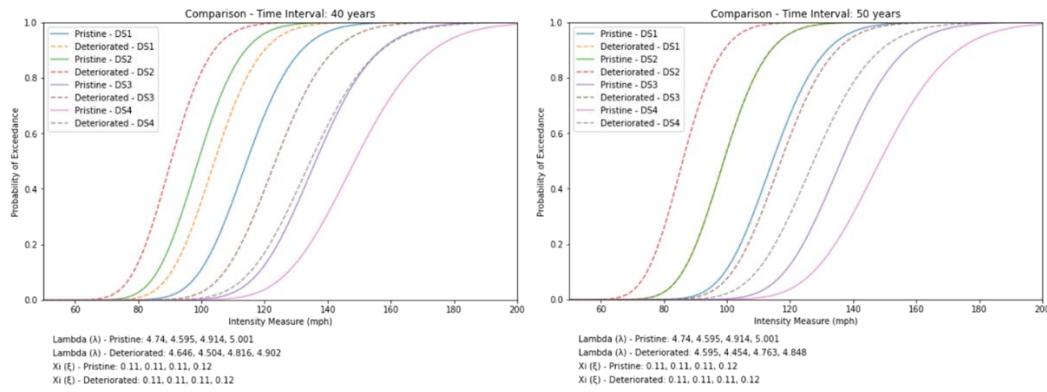


Figure 7.18: Lognormal best-fitted aluminum siding fragilities at 40 and 50-year intervals

Time-dependent Modeling failure of structural components using fragilities - Steel Roof Joists

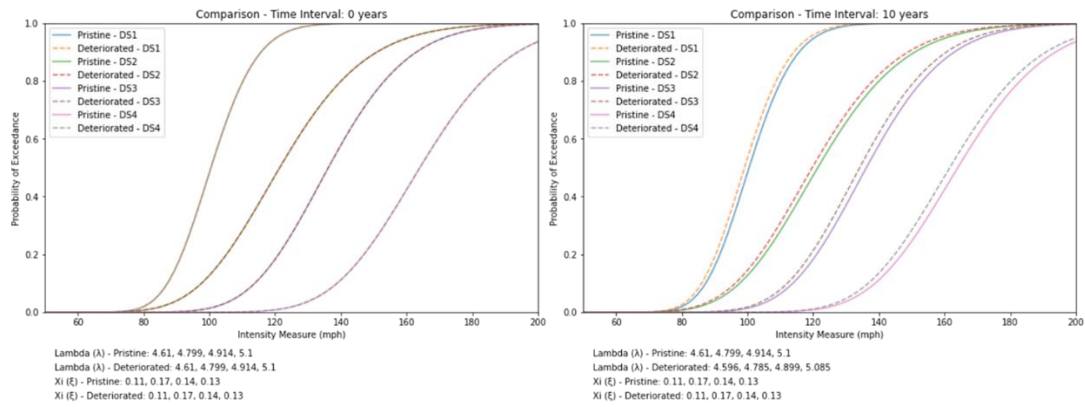


Figure 7.19: Lognormal best-fitted steel roof joists fragilities at 0 and 10-year intervals

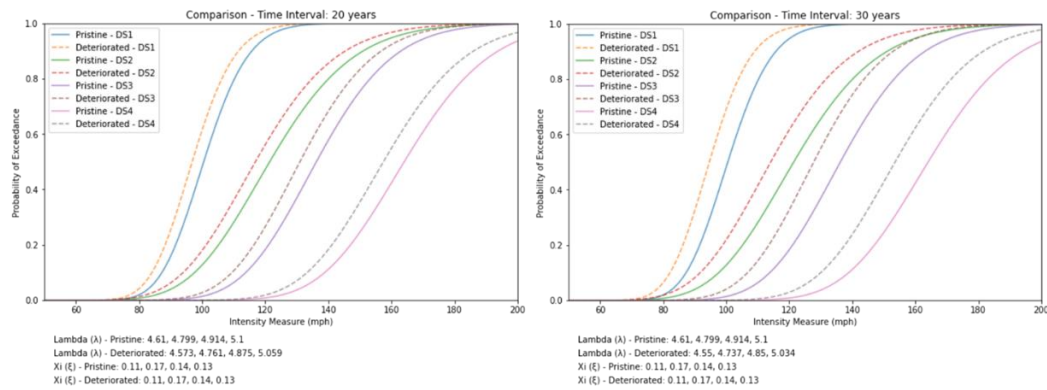


Figure 7.20: Lognormal best-fitted steel roof joists fragilities at 20 and 30-year intervals

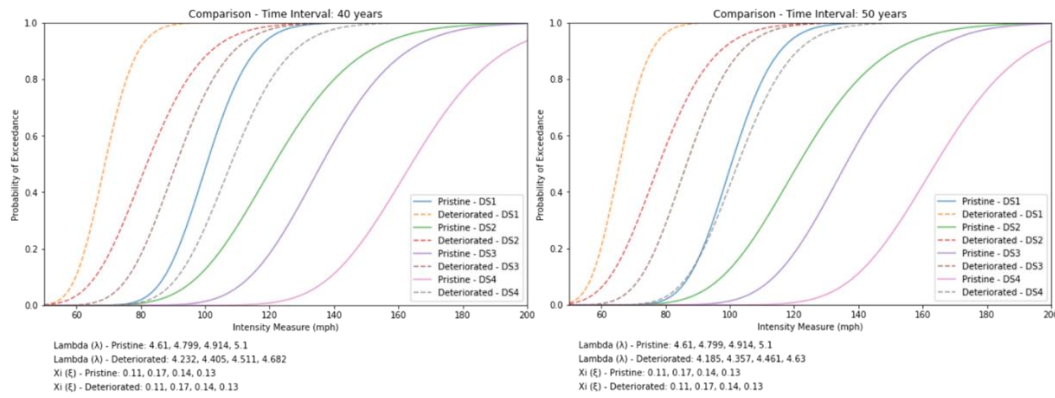


Figure 7.21: Lognormal best-fitted steel roof joists at 40 and 50-year intervals

Time-dependent Modeling failure of structural components using fragilities - Two 16d Toenails

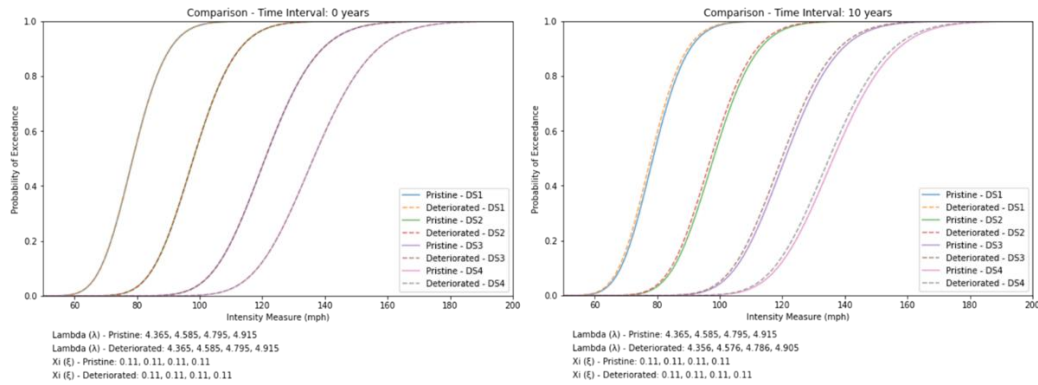


Figure 7.22: Lognormal best-fitted two 16d toenail fragilities at 0 and 10-year intervals

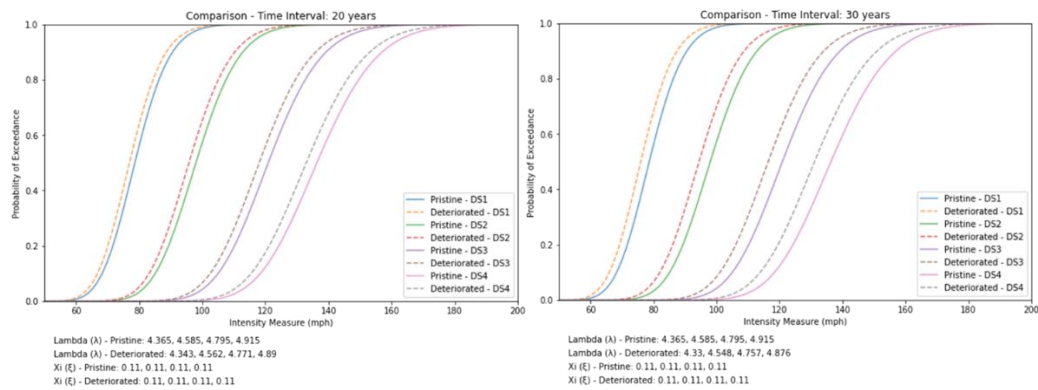


Figure 7.23: Lognormal best-fitted two 16d toenail fragilities at 20 and 30-year intervals

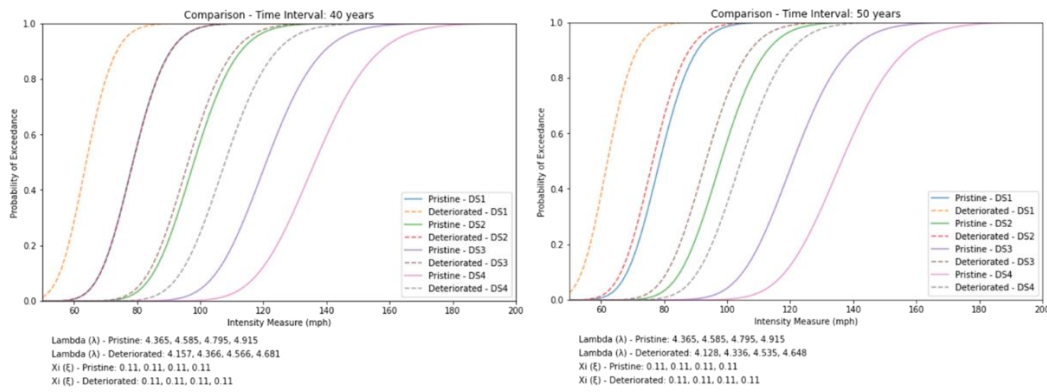


Figure 7.24: Lognormal best-fitted two 16d toenail fragilities at 40 and 50-year intervals

Time-dependent Modeling failure of structural components using fragilities - One H2.5 Clip

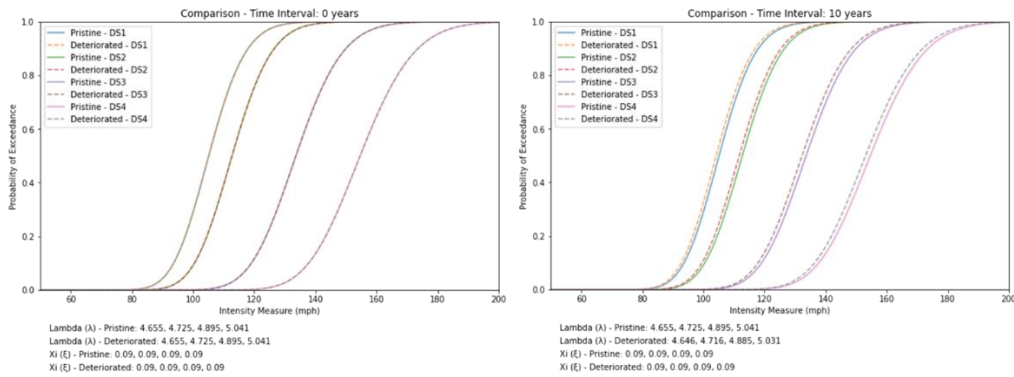


Figure 7.25: Lognormal best-fitted one H2.5 clip fragilities at 0 and 10-year intervals

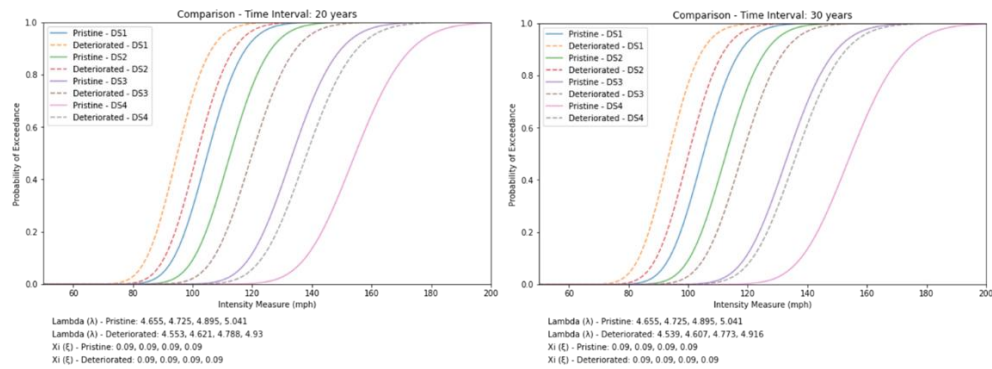


Figure 7.26: Lognormal best-fitted one H2.5 clip fragilities at 20 and 30-year intervals

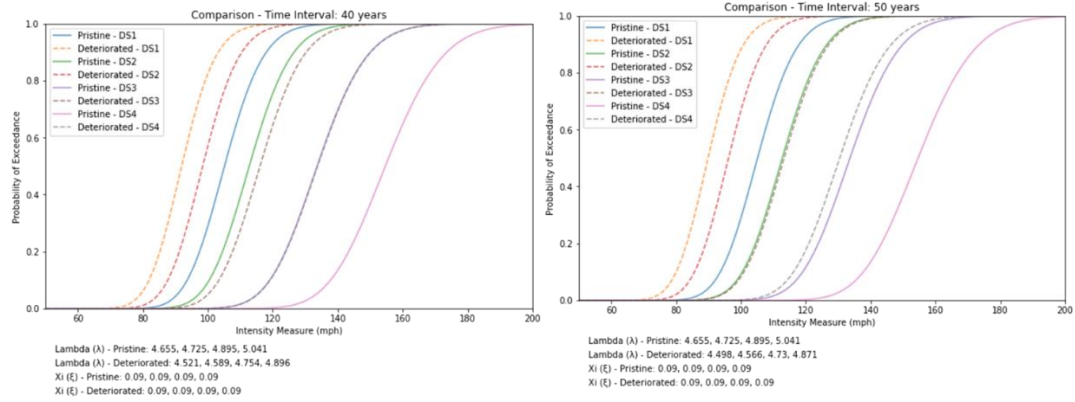


Figure 7.27: Lognormal best-fitted one H2.5 clip fragilities at 40 and 50-year intervals

Time-dependent Modeling failure of structural components using fragilities - Two H2.5 Clip

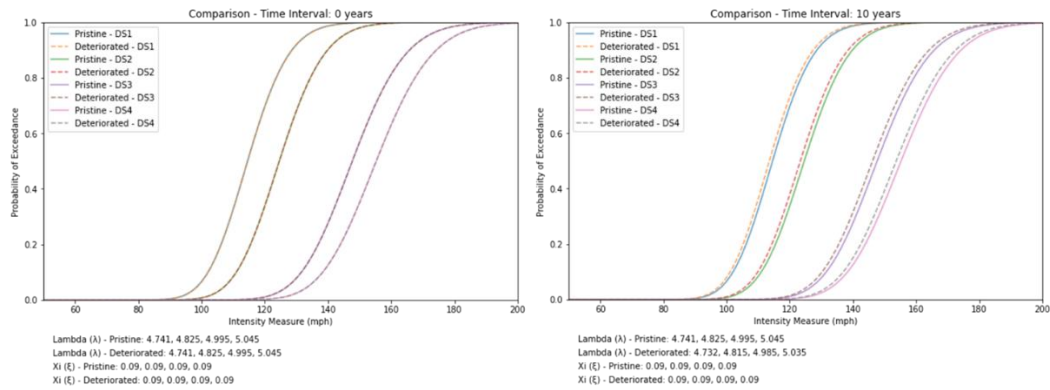


Figure 7.28: Lognormal best-fitted two H2.5 clip fragilities at 0 and 10-year intervals

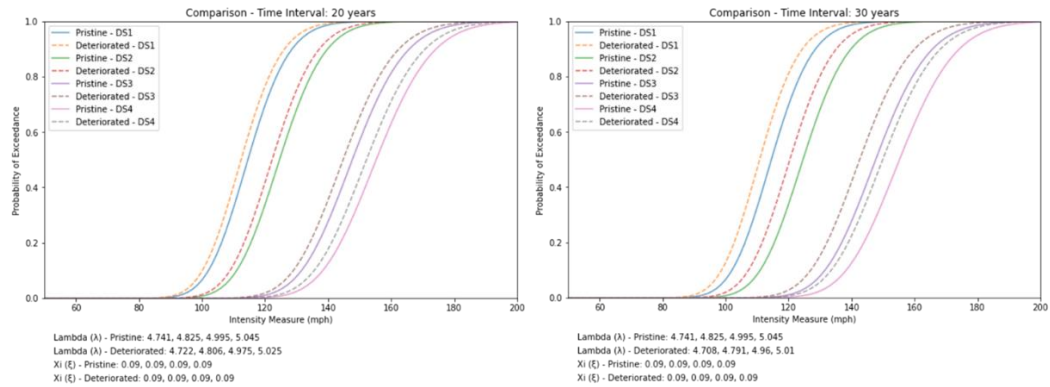


Figure 7.29: Lognormal best-fitted two H2.5 clip fragilities at 20 and 30-year intervals

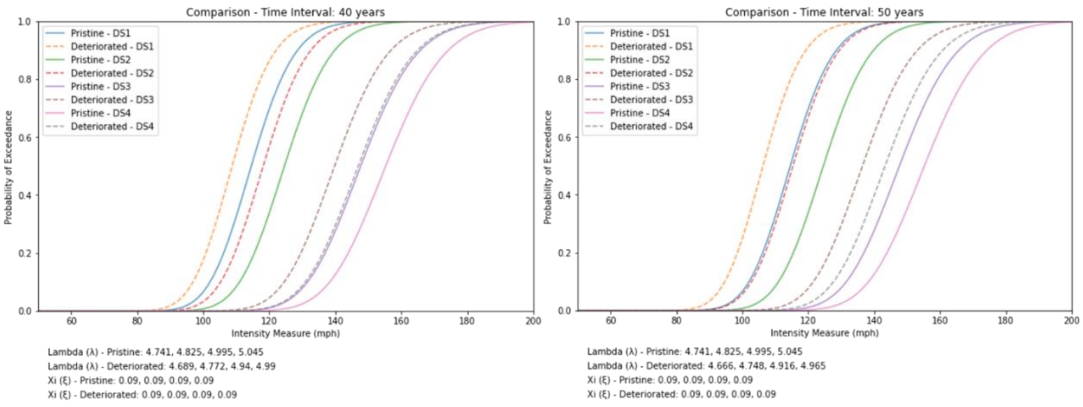


Figure 7.30: Lognormal best-fitted two H2.5 clip fragilities at 40 and 50-year intervals

7.4 APPENDIX D: TIME-DEPENDENT FRAGILITY CURVES – PRISTINE VS DETERIORATING BUILDINGS EF SCALE

Time-dependent Modeling failure of structural components using fragilities – Asphalt Shingles – EF Scale

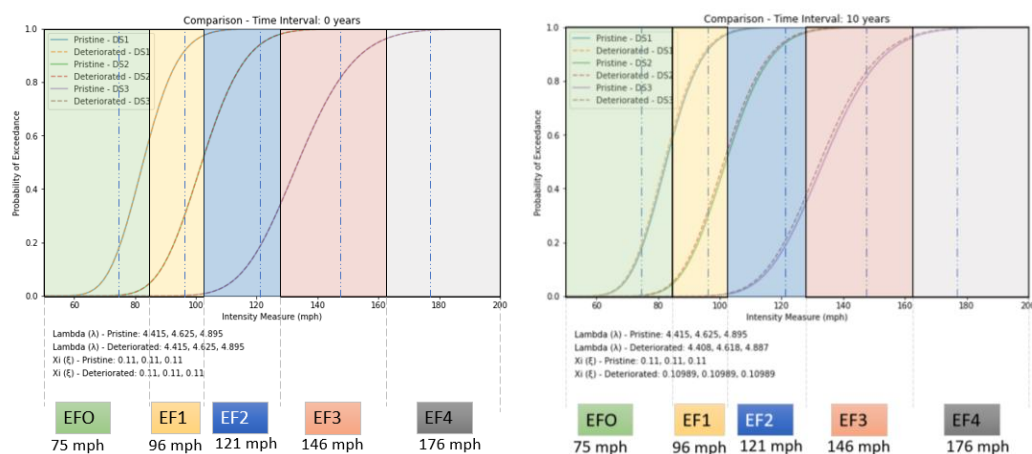


Figure 7.31: Time-dependent asphalt shingles fragilities with EF-Scale overlay at 0 and 10-year interval

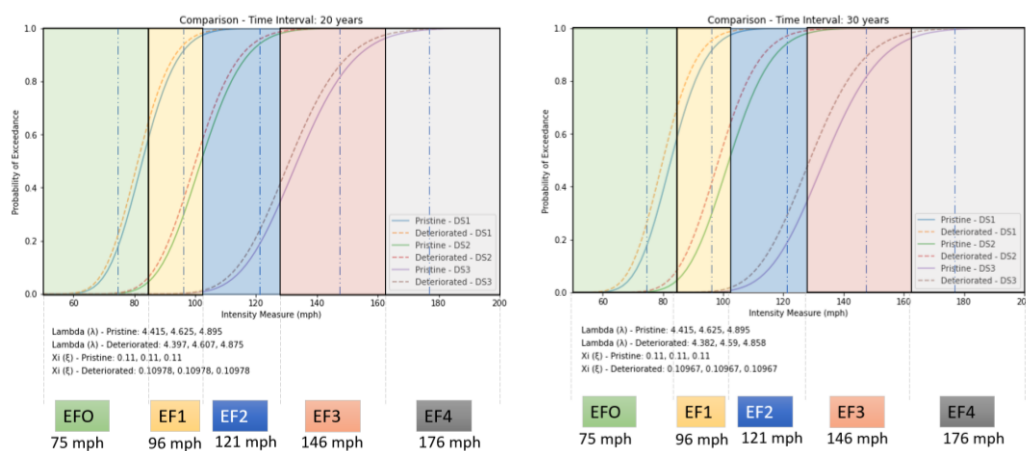


Figure 7.32: Time-dependent asphalt shingles fragilities with EF-Scale overlay at 20 and 30-year intervals

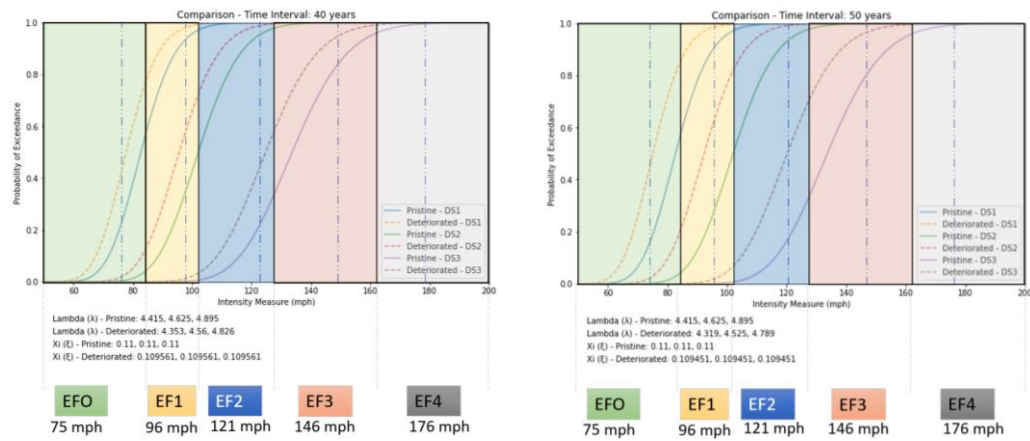


Figure 7.33: Time-dependent asphalt shingles fragilities with EF-Scale overlay at 40 and 50-year intervals

Time-dependent Modeling failure of structural components using fragilities - Clay Tiles – EF Scale

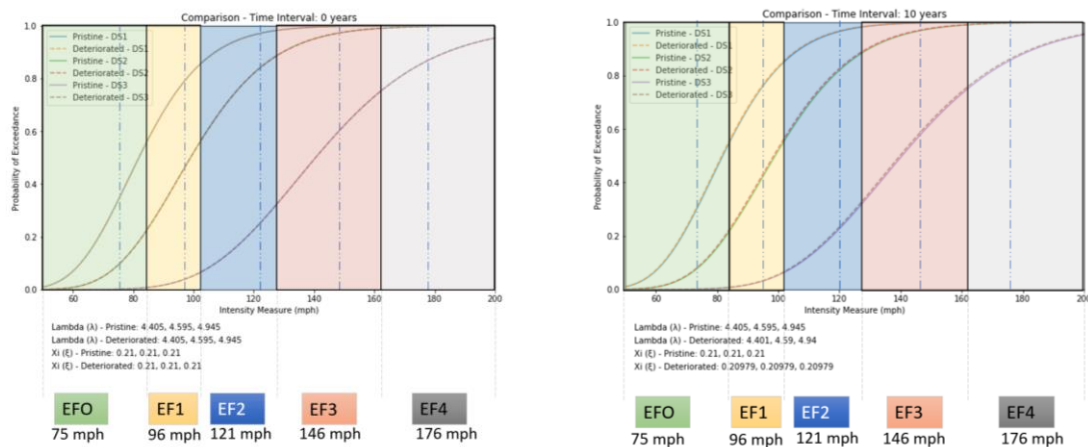


Figure 7.34: Time-dependent clay tile fragilities with EF-Scale overlay at 00 and 10-year intervals

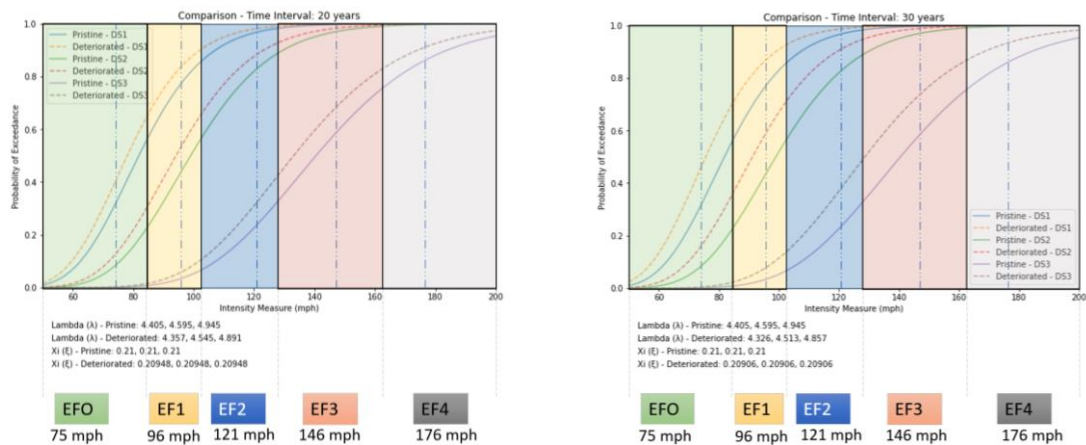


Figure 7.35: Time-dependent clay tile fragilities with EF-Scale overlay at 20 and 30-year intervals

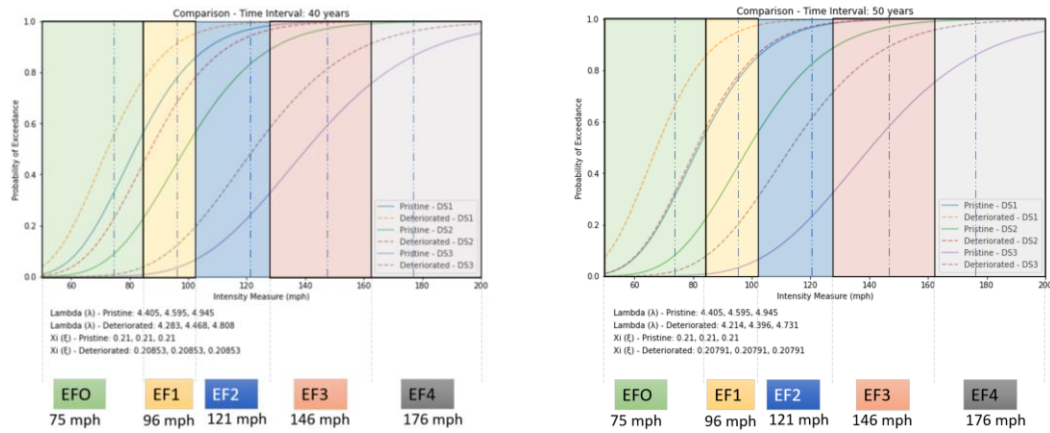


Figure 7.36: Time-dependent clay tile fragilities with EF-Scale overlay at 40 and 50-year intervals

Time-dependent Modeling failure of structural components using fragilities – Walls – EF Scale

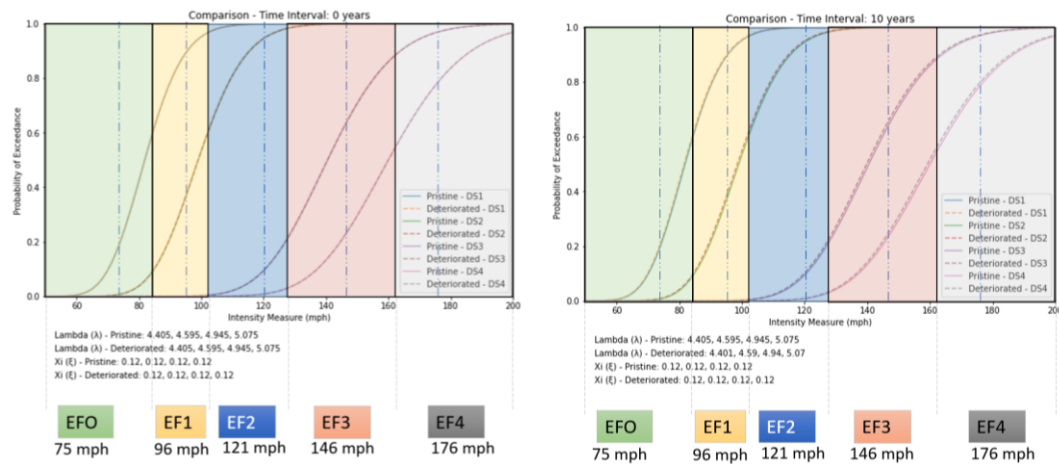


Figure 7.37: Time-dependent wall fragilities with EF-Scale overlay at 0 and 10-year intervals

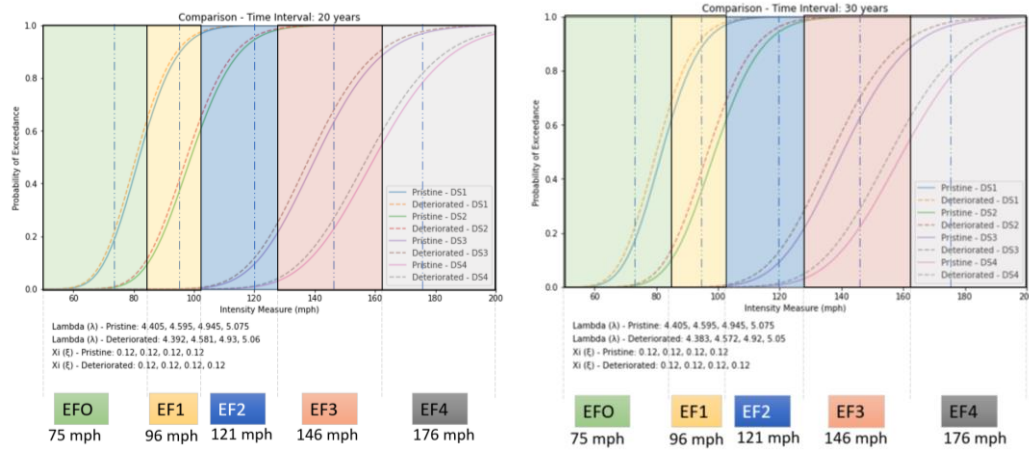


Figure 7.38: Time-dependent wall fragilities with EF-Scale overlay at 40 and 50-year intervals

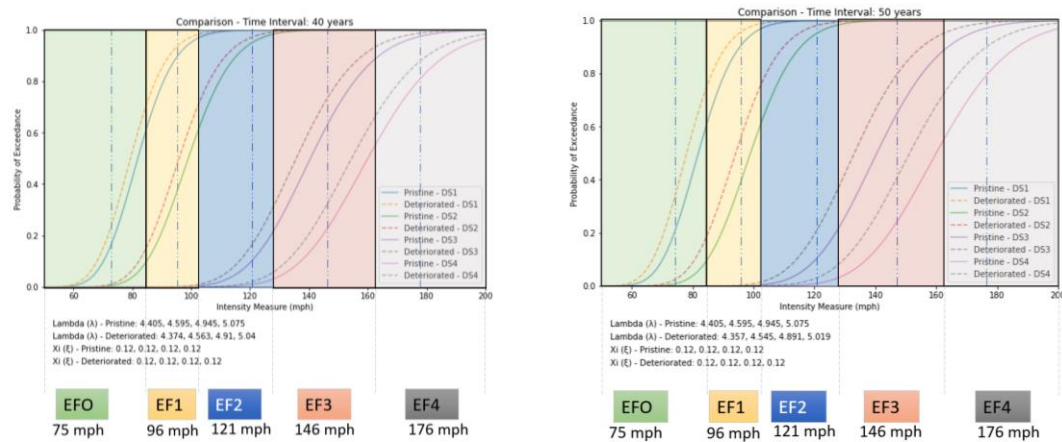


Figure 7.39: Time-dependent wall fragilities with EF-Scale overlay at 40 and 50-year intervals

Time-dependent Modeling failure of structural components using fragilities – Doors – EF Scale

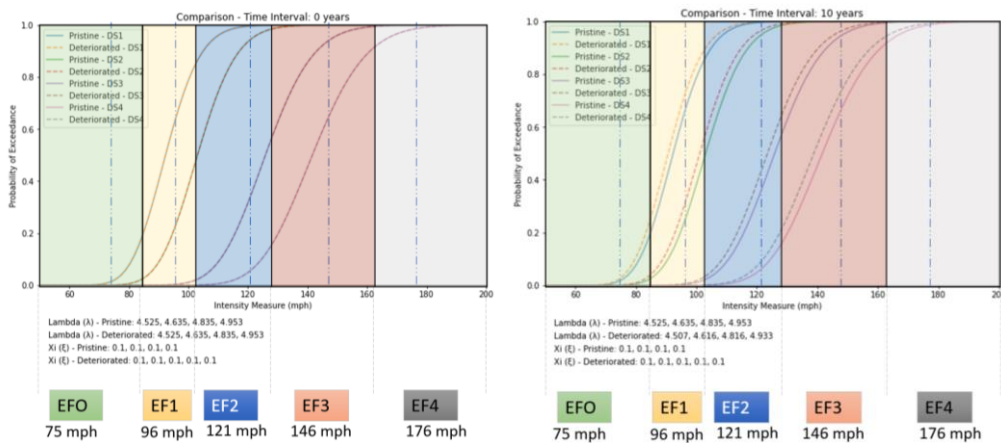


Figure 7.40: Time-dependent door fragilities with EF-Scale overlay at 0 and 10-year intervals

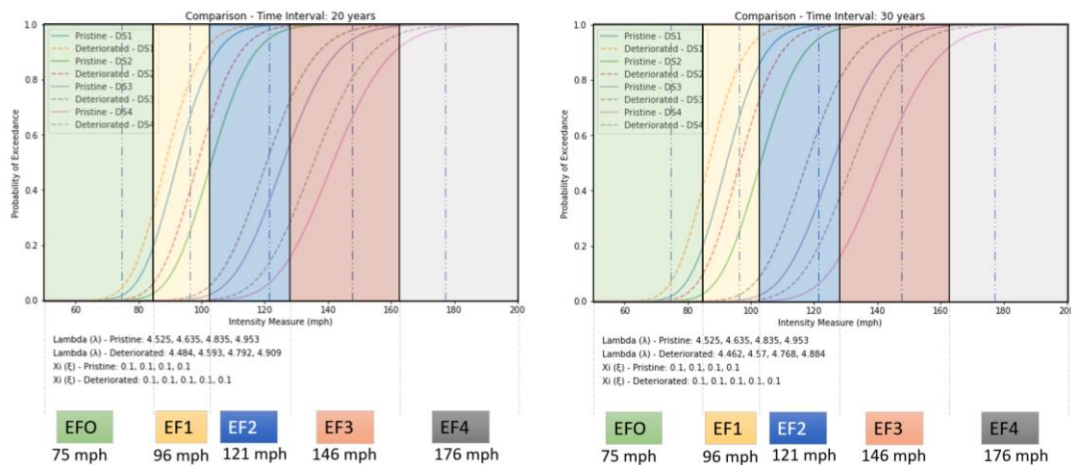


Figure 7.41: Time-dependent door fragilities with EF-Scale overlay at 20 and 30-year intervals

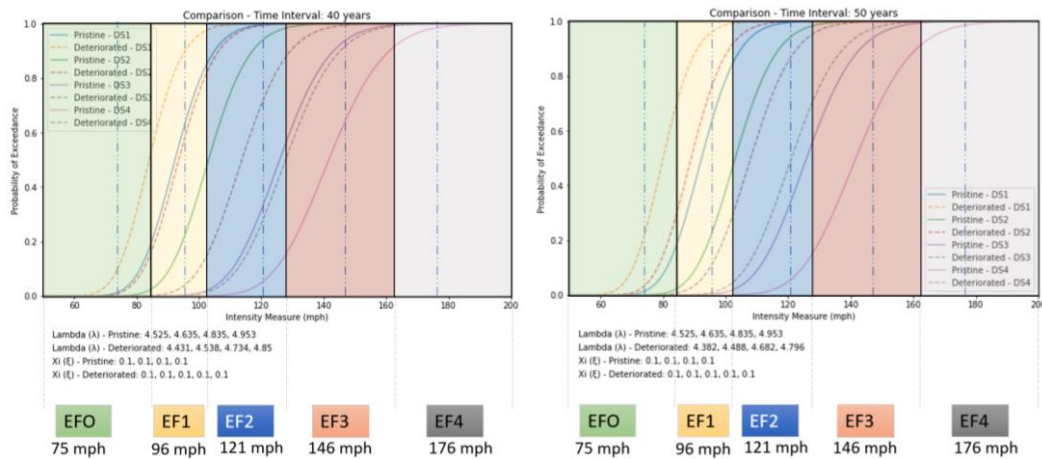


Figure 7.42: Time-dependent asphalt door with EF-Scale overlay at 40 and 50-year intervals

Time-dependent Modeling failure of structural components using fragilities – Windows – EF Scale

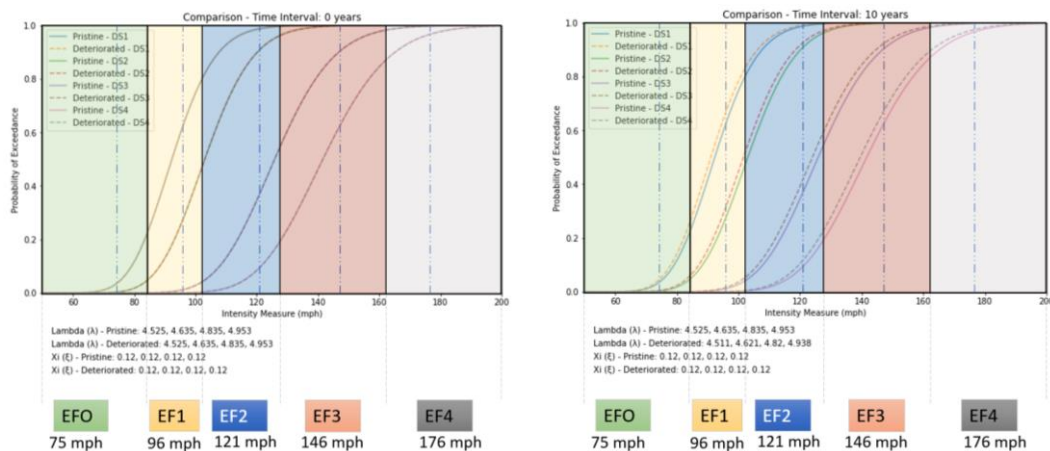


Figure 7.43: Time-dependent windows fragilities with EF-Scale overlay at 0 and 10-year intervals

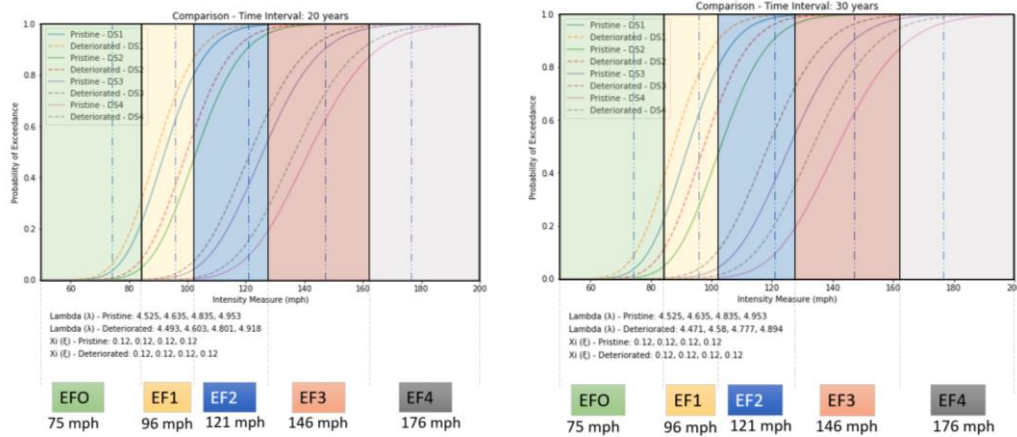


Figure 7.44: Time-dependent windows fragilities with EF-Scale overlay at 20 and 30-year intervals

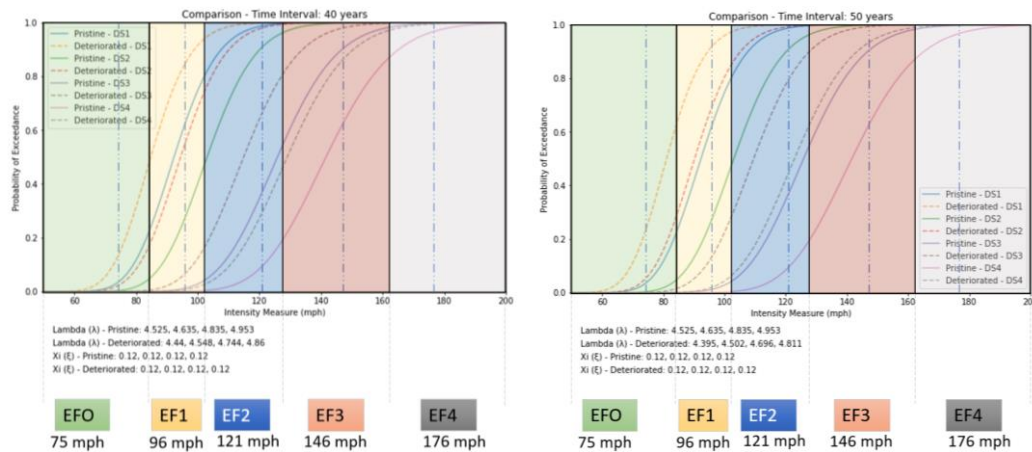


Figure 7.45: Time-dependent windows fragilities with EF-Scale overlay at 40 and 50-year intervals

Time-dependent Modeling failure of structural components using fragilities - Aluminum Siding – EF Scale

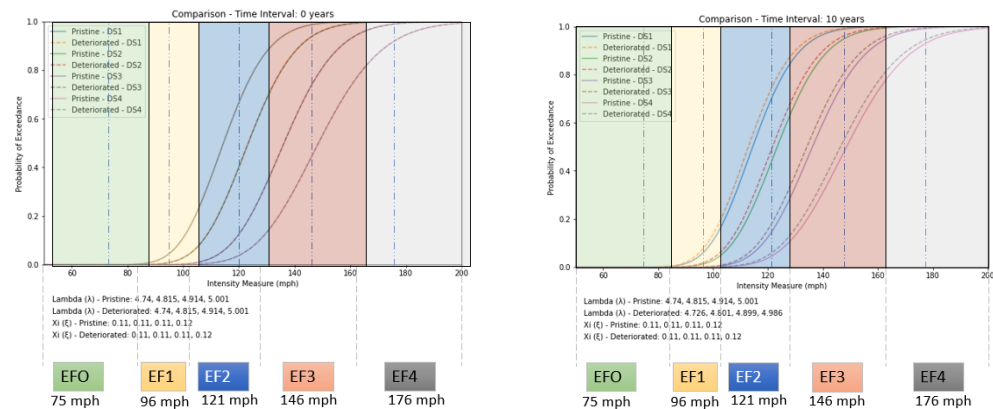


Figure 7.46: Time-dependent aluminum siding fragilities with EF-Scale overlay at 0 and 10-year intervals

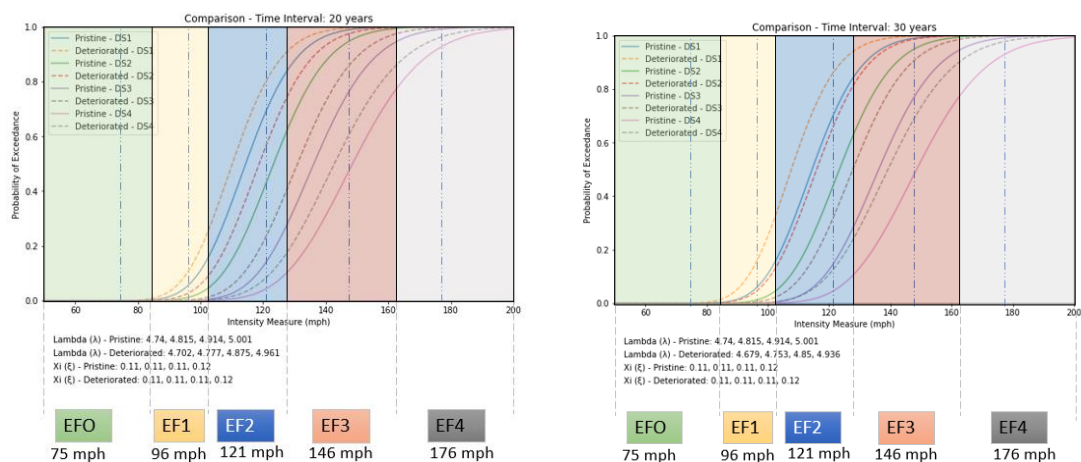


Figure 7.47: Time-dependent aluminum siding fragilities with EF-Scale overlay at 10 and 20-year intervals

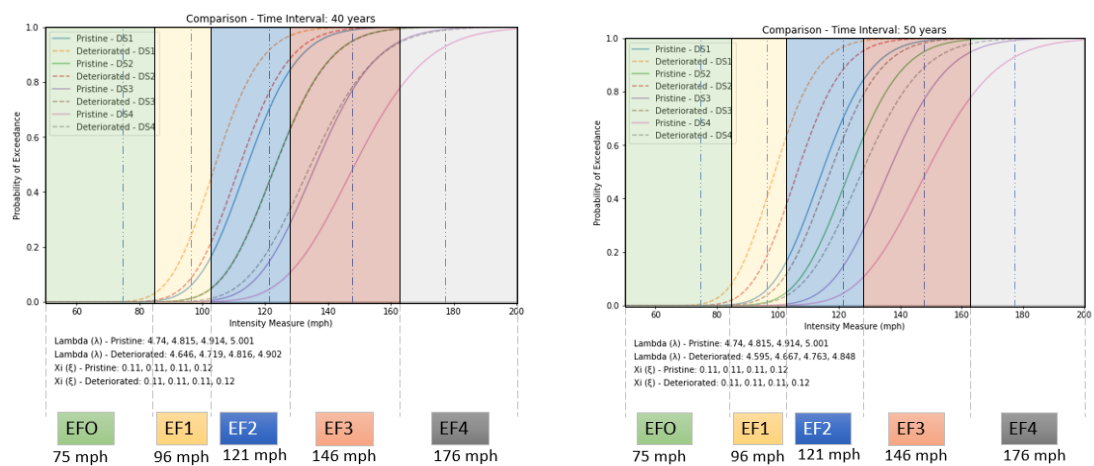


Figure 7.48: Time-dependent aluminum siding fragilities with EF-Scale overlay at 40 and 50-year intervals

Time-dependent Modeling failure of structural components using fragilities - Steel Roof Joists – EF Scale

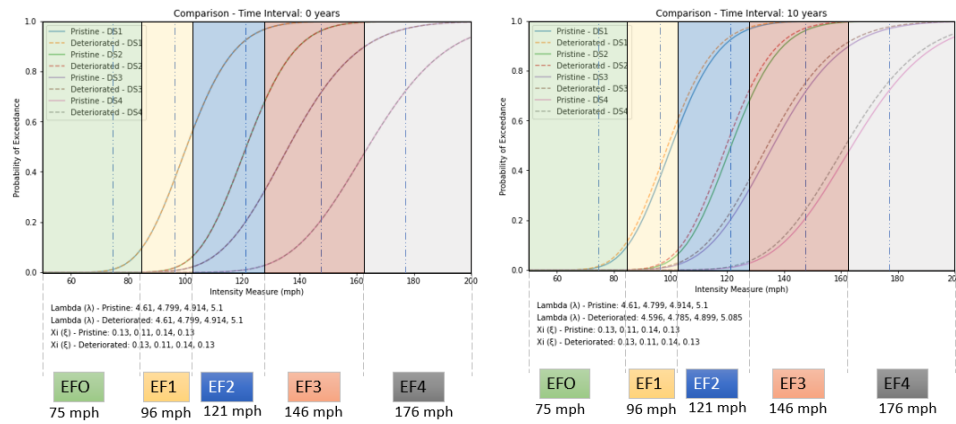


Figure 7.49: Time-dependent steel roof joists fragilities with EF-Scale overlay at 0 and 10-year intervals

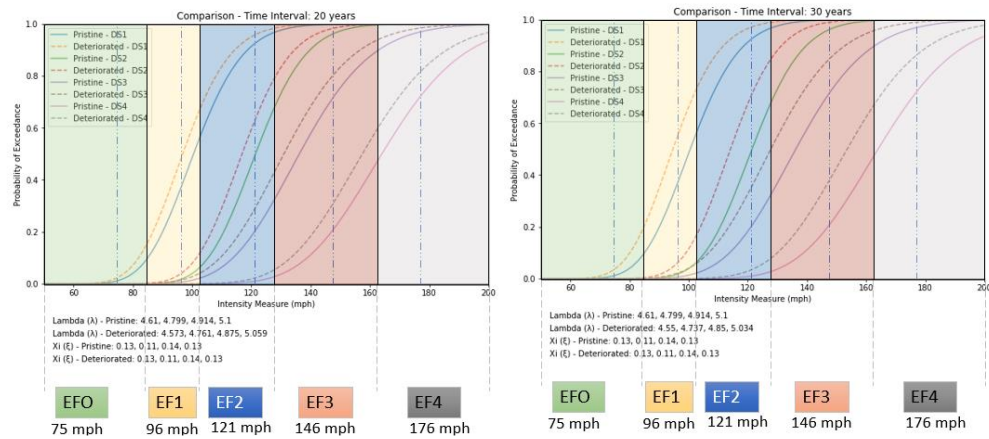


Figure 7.50: Time-dependent steel roof joists fragilities with EF-Scale overlay at 20 and 30-year intervals

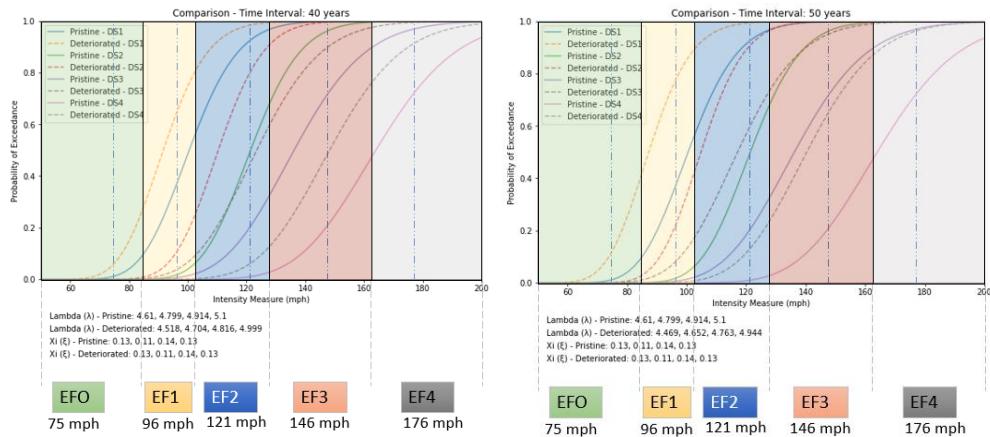


Figure 7.51: Time-dependent steel roof joists fragilities with EF-Scale overlay at 40 and 50-year intervals

Time-dependent Modeling failure of structural components using fragilities - 16d Toe Nails – EF Scale

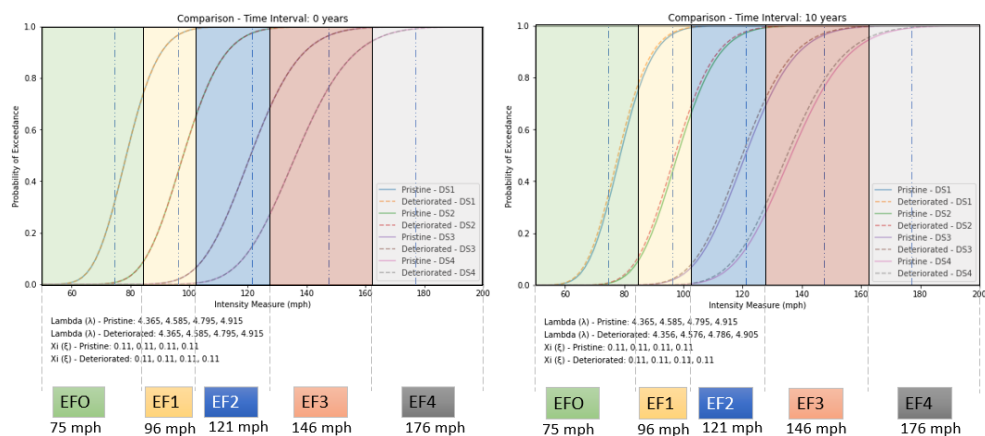


Figure 7.52: Time-dependent 16d toenail fragilities with EF-Scale overlay at 0 and 10-year intervals

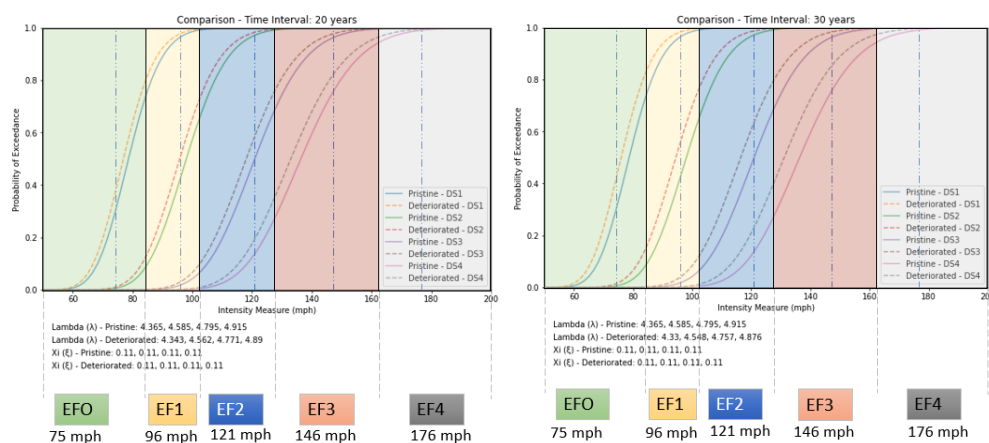


Figure 7.53: Time-dependent 16d toenail fragilities with EF-Scale overlay at 20 and 30-year intervals

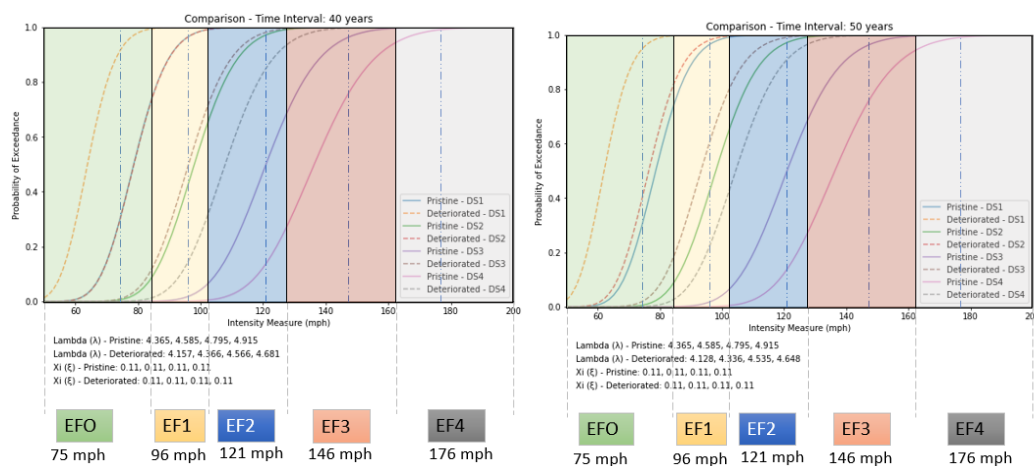


Figure 7.54: Time-dependent 16d toenail fragilities with EF-Scale overlay at 40 and 50-year intervals

Time-dependent Modeling failure of structural components using fragilities - One H2.5 Clip – EF Scale

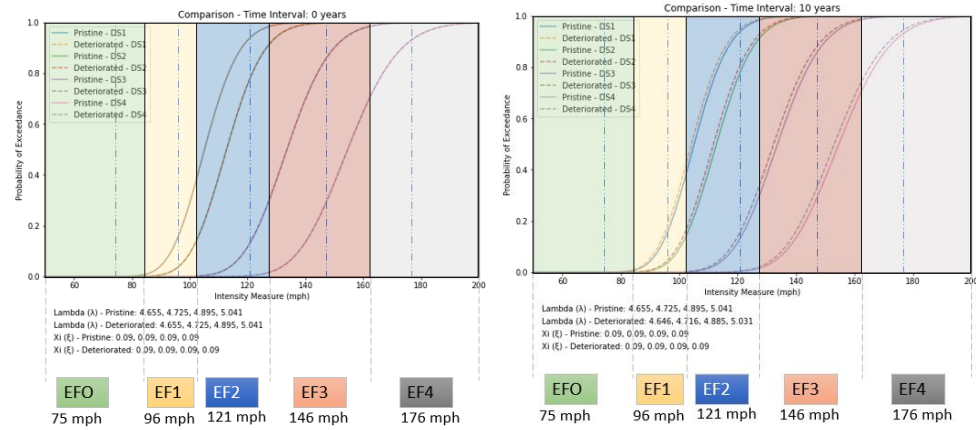


Figure 7.55: Time-dependent one H2.5 clip fragilities with EF-Scale overlay at 0 and 10-year intervals

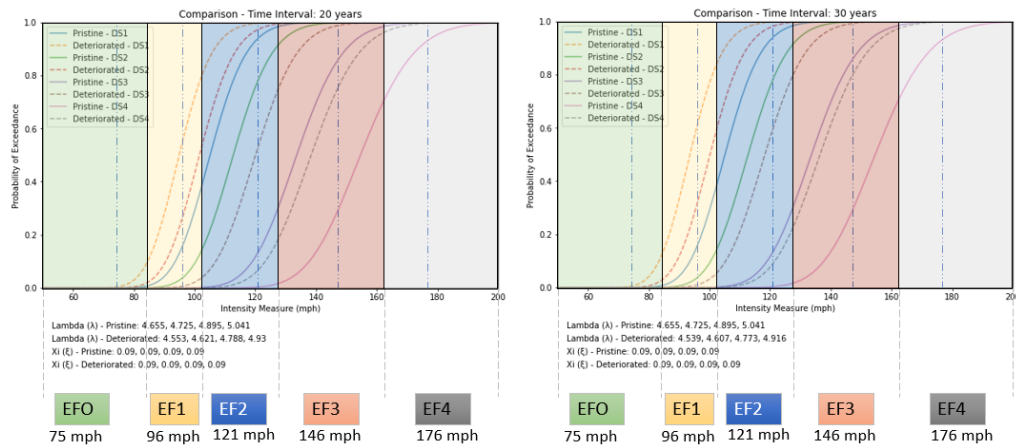


Figure 7.56: Time-dependent one H2.5 clip fragilities with EF-Scale overlay at 20 and 30-year intervals

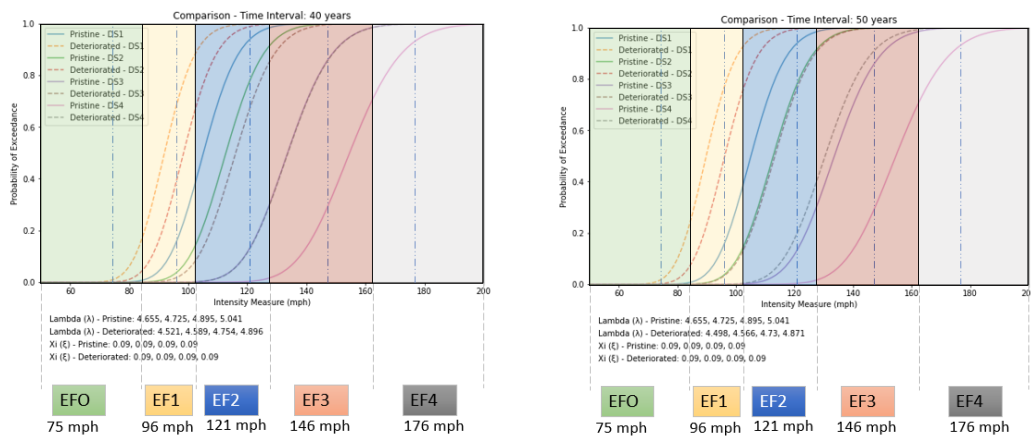


Figure 7.57: Time-dependent one H2.5 clip fragilities with EF-Scale overlay at 40 and 50-year intervals

Time-dependent Modeling failure of structural components using fragilities - Two H2.5 Clips – EF Scale

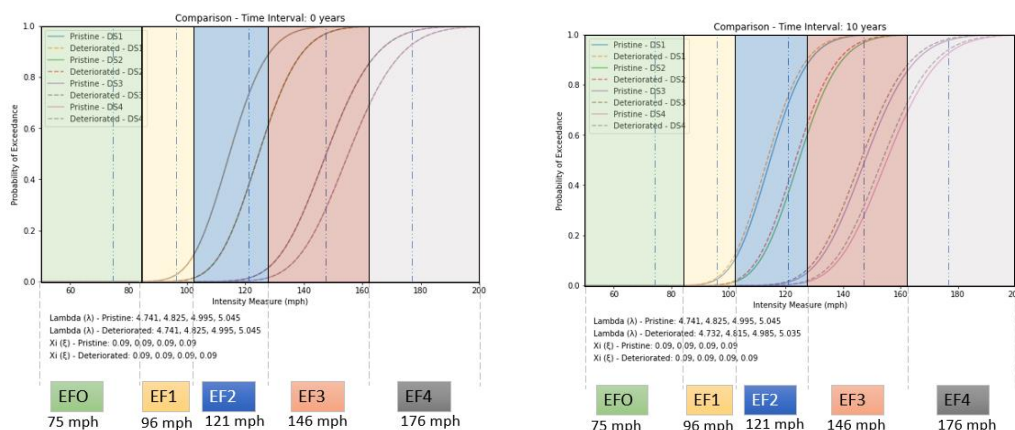


Figure 7.58: Time-dependent two H2.5 clip fragilities with EF-Scale overlay at 0 and 10-year intervals

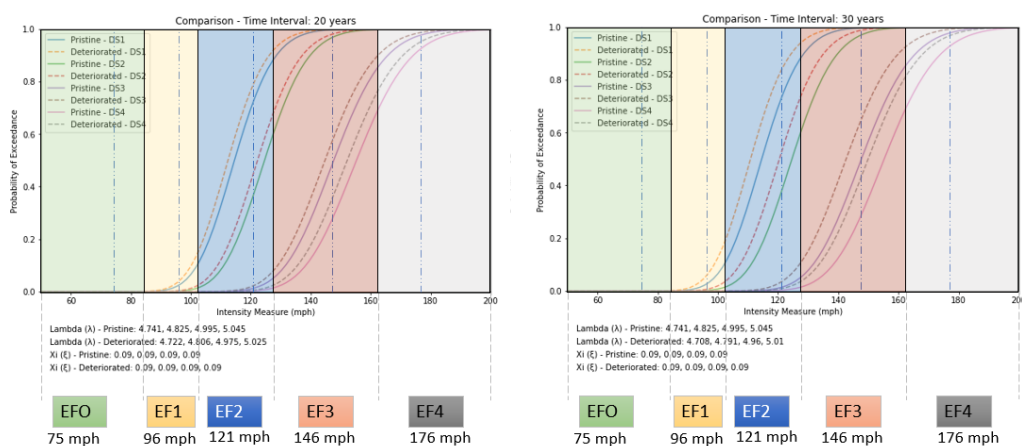


Figure 7.59: Time-dependent two H2.5 clip fragilities with EF-Scale overlay at 20 and 30-year intervals

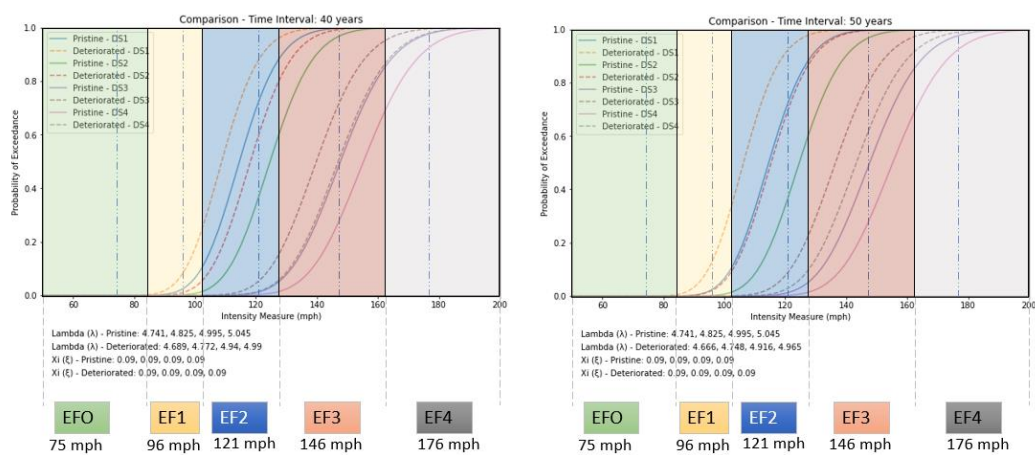


Figure 7.60: Time-dependent two H2.5 clip fragilities with EF-Scale overlay at 40 and 50-year intervals